Wissenschaftszentrum Weihenstephan

Lehrstuhl für Molekulare Ernährungsmedizin

Experimental strategies to evaluate the gut microbiota-host-diet interaction in the regulation of energy balance

Raphaela Kübeck

Vollständiger Abdruck der von der Fakultät Wissenschaftszentrum Weihenstephan für Ernährung, Landnutzung und Umwelt der Technischen Universität München zur Erlangung des akademischen Grades eines

Doktors der Naturwissenschaften

genehmigten Dissertation.

Vorsitzender: Univ.-Prof. Dr. D. Haller

Prüfer der Dissertation:

1. Univ.-Prof. Dr. M. Klingenspor
2. Univ.-Prof. Dr. M. Schemann

Die Dissertation wurde am 16.11.2015 bei der Technischen Universität München eingereicht und durch die Fakultät Wissenschaftszentrum Weihenstephan für Ernährung, Landnutzung und Umwelt am 14.03.2016 angenommen.

TABLE OF CONTENTS

1 INTRODUCTION

Obesity and associated comorbidities are major health concerns caused by skewed energy balance in Western societies. Although the role of gut microorganisms in host energy metabolism has been known for decades (Wostmann, 1981; Wostmann et al., 1983), recent studies have shown that the gut microbiota is an integral part of the pathogenicity of metabolic disorders such as obesity, and point at the urgent need to understand molecular mechanisms (Le Roy et al., 2013; Nieuwdorp et al., 2014).

1.1 Characterization of gut microbiota

Within these microorganisms archaea, eukaryotes and bacteria represent most abundant communities within the gut (Leser and Molbak, 2009). Yielding a biomass that approximates the size of a liver, the gut microbiota may be considered as a multicellular organ (Karlsson et al., 2013; Leser and Molbak, 2009). A total of 10^{14} bacteria thereby account for 90 % of total cells within the mammalian organism resulting in 10-times more bacterial than eukaryotic cells (Arslan, 2014; Bianconi et al., 2013). So far, around 1,000 species have been estimated to colonize the mammalian intestine (Karlsson et al., 2013). Among them, members of the bacterial phyla *Bacteroidetes* and *Firmicutes* are major representatives whilst *Proteobacteria*, *Verrucomicrobia* and *Actinobacteria* are found at lower abundances (Leser and Molbak, 2009).

Despite its high inter-individual variability, the mammalian gut has a core microbial genome (Turnbaugh et al., 2009). Moreover, the microbiome encodes 300-fold more genes than the mammalian genome. There is a consensus on microbiota effects on digestion of complex molecules, production of hormones and essential amino acids and vitamins. Additionally, bacteria are implicated in the normal development and homeostasis of the enteric immune system and defense against pathogens (Hooper et al., 2012; Karlsson et al., 2013; Smith et al., 2007). Gut microorganisms detoxify xenobiotic compounds and thus, affect drug metabolism (Backhed, 2011; Jia et al., 2008), as well as

influence the enterohepatic cycle of bile acids via deconjugation and dehydroxylation (Fukuda and Ohno, 2014). Thus, the gut microbiota mainly represented by the phyla *Bacteroidetes* and *Firmicutes* hava tremendous effects on host metabolism.

1.2 Gut microbiota-host-diet interaction in obesity

A link between an imbalanced host energy metabolism leading to obesity and the gut microbiota was first described by animal studies (Backhed et al., 2004). However, obesity accompanied by a lowered ratio of *Bacteroidetes* to *Firmicutes* was found in mice (Fleissner et al., 2010; Ley et al., 2005; Turnbaugh et al., 2006), but not in humans (Armougom et al., 2009; Duncan et al., 2008; Furet et al., 2010; Santacruz et al., 2010; Schwiertz et al., 2010; Turnbaugh et al., 2009). Nevertheless, features of gut microbiota related to obesity in humans are reduced microbial diversity, increased pathogen counts, and decreased number of anti-inflammatory bacteria (Festi et al., 2014; Le Chatelier et al., 2013). Hence, heterogeneous findings within species may be based on different study designs and microbiota-profiling methodologies.

1.2.1 Experimental strategies to evaluate gut microbiota-host interaction

Studies designed to evaluate the interaction of the gut microbiota and host metabolism are not uniform, i.e. fecal transplantations and cohousing, and may contribute to inconsistent results. Even 1,000 years ago, fecal transplantations from healthy donors were performed by Chinese medical doctors to cure patients from food poisoning or severe diarrhea (Zoetendal and de Vos, 2014). So far, fecal transplantation has been successfully applied in *Clostridium difficile* infections and the treatment of colitis (Bakken, 2009; Damman et al., 2012; Gough et al., 2011). In humans, the benefit of fecal transplantation with metabolic syndrome is scarcely investigated, although, microbiota transfer has been shown to increase insulin sensitivity (Vrieze et al., 2012).

In mice, transmissibility of obesity was first described by oral transplantation of complex cecal microbes originating from genetically- (ob/ob) or diet-induced (Western diet) obese donors into germfree (GF) C57BL/6J recipients (Backhed et al., 2007; Turnbaugh et al., 2006). Moreover, associations with particular bacteria indicated that microbes are a cause rather than a consequence for metabolic dysbalance (Fei and Zhao, 2013). However, studies on fecal transplantation into GF animals are hardly an optimal model for the complex microbiota of a patient's intestine. Therefore, microbiota transfer into conventional (CV) mice may better reflect the clinical situation (Damman et al., 2012). Nevertheless, there are some constraints to fecal transplants: Given that donor feces is rarely purified nor enriched in bacteria, stool transplantations mainly contain any kind of particles including microorganisms, fibres, mucus, proteins, fat and bile acids (de Vos, 2013). Viability of the donor microbiota is further undefined as samples are difficult to process under strict anaerobic conditions. It is therefore assumed that the majority of the transplanted microbes are dead and that other fecal compounds contribute to the transplantation success (de Vos, 2013). Thus, cohousing represents a natural approach to induce bacterial transfer by coprophagy (Vijay-Kumar and Gewirtz, 2012).

Cohousing studies related to energy metabolism are scarce, however, a central role of the gut bacteria in the progression of metabolic disorders has been proposed (Henao-Mejia et al., 2012). Obese individuals are characterized by low microbial diversity and are therefore more susceptible to colonization by foreign microbes and phenotypic changes than lean ones (Henao-Mejia et al., 2012; Seedorf et al., 2014; Stecher et al., 2010). Interactions of diet and gut microbiota were identified in mice harboring a microbiota from either obese or lean twins. Cohousing of these mice induced weight loss in obese but not lean cage mates when provided with a diet enriched in fruits and vegetables, and low in saturated fat (Ridaura et al., 2013). Thus, these models set the basis to clarify mechanisms of bacterial invasion impacted by diet composition and to unravel dietary components affecting microbial and host metabolism.

1.2.2 Dietary effects on gut microbiota

Published research is inconsistent with respect to the nomenclature describing diets high in fat and sugar, which leads to conflicting results in the ability of GF mice to develop obesity or the role of diet in inducing shifts in bacterial community structure in mice harboring a complex microbiota (Backhed et al., 2005; Fleissner et al., 2010; Parks et al., 2013; Rabot et al., 2010; Scott et al., 2013; Zhang et al., 2012). Generic terms such as ‘Western diet’ or ‘high-fat diet’ refer to experimental diets that markedly differ in total energy content, amount and composition of macronutrients, and detailed information is often not provided in a transparent manner.

Changes in the human gut microbiota are congruent for obesity and high dietary fat intake. In this respect, the type (saturated/unsaturated) and quantity of the dietary fat impacts gut microbial composition and activity including higher *Firmicutes* levels associated with increased fat oxidation rates, increased energy harvest, and a decreased number of total bacteria in high-fat, high-calorie diets. Additionally, an increased short-chain fatty acid (SCFA) excretion was found in diets high in saturated fat (Fava et al., 2013; Jumpertz et al., 2011; Kelder et al., 2014). Moreover, plant- compared to animal-derived diets indicated marked differences in microbial diversity such as lower amounts of bile-tolerant bacteria as well as increased levels of *Bacteroidetes* and plant polysaccharides fermenting *Firmicutes* accompanied with enhanced SCFA excretion (David et al., 2014; De Filippo et al., 2010; Kabeerdoss et al., 2012; Zimmer et al., 2012). Overall, these studies highlight diet-induced alterations of gut microbiota related to functional and metabolic changes beyond inter-individual variances.

Interestingly, mouse phenotype and microbial composition have recently been related to the type of saturated fat. Thus, palm oil compared to olive or safflower oil induced body mass gain, lowered microbial diversity and increased *Firmicutes* to *Bacteroidetes* ratio (de Wit et al., 2012). Additionally, lard rather than fish oil aggravated white adipose tissue inflammation and promoted a higher degree of

obesity which was partly attributed to different microbiota composition (Caesar et al., 2015). However, underlying mechanisms are still unknown.

In a screen of 100 inbred mouse strains, exposure to a high-fat, high-sugar diet revealed substantial differences in body mass gain and microbial composition indicating a possible association between metabolic and microbial changes due to diet and mouse strain (Parks et al., 2013). However, several investigations highlighted the high sensitivity of the gut microbiota to high-fat diet (HFD) irrespective of the phenotypic outcome questioning the role of gut microbiota on obesity development (de Wit et al., 2012; Hildebrandt et al., 2009; Murphy et al., 2010; Zhang et al., 2012). And despite shifts in the diversity of highly abundant bacteria that occurred due to HFD, chemical fingerprints were mainly affected by diet rather than by microbial composition (Daniel et al., 2014).

In summary, there is a clear relationship between dietary and microbial composition in mice and humans, although the microbiota-triggered mechanisms toward obesity development remain elusive.

1.2.3 Microbial effects contributing to obesity

Despite major breakthroughs proposing that microbial communities are related to changes in gut morphology, physiology and biochemistry (Backhed, 2011), the exact energetic contribution of the gut microbiota for the host is still unknown.

Microbes ferment polysaccharides and proteins, produce vitamins and metabolize bile acids, thereby affecting enterohepatic circulation and nutrient absorption (Fukuda and Ohno, 2014; Tremaroli and Backhed, 2012). The enterohepatic circulation involves the passage of metabolites through the intestinal tract, the absorption, transport and conversion within the liver, excretion into the bile and the transport via the blood stream into the gut for recycling or elimination, respectively. Hence, once entering the digestive tract, metabolites that undergo enterohepatic circulation such as sterols (i.e. cholesterol), bile acids and steroid hormones remain either untransformed or underlie extensive conformation by gut microbes (Groh, 1993).

Being part of the enterohepatic circulation, cholesterol metabolism is highly regulated by the intestine and liver. In the intestine, cholesterol levels are built up by animal-based diets, bile and mucosal secretion (Grundy, 1978). In addition to passive cholesterol diffusion into enterocytes, recent findings suggest additional protein-mediated apical cholesterol uptake (Hui et al., 2008). Since obesity is associated with increased cholesterol levels (Subramanian et al., 2008; Van Rooyen et al., 2011; Zhang et al., 2007), plant sterols, specifically β-sitosterol, have been proposed to target intestinal cholesterol absorption (Plosch et al., 2006). Plant sterols are taken up by the enterocyte, however, they do not reach circulation as they underlie protein-mediated re-transport into the intestinal lumen and excretion via the feces. Once entering the hepatocyte by lipoprotein receptors, cholesterol is secreted at the canalicular membrane by the ATP-binding cassette sub-family G member 5 and 8 proteins (ABCG5/8) to reach the bile, used as precursor for hepatic bile acid synthesis, or transported to peripheral tissues. In the liver, endogenous cholesterol biosynthesis is mediated by the key enzyme β-hydroxyl-β-methyl glutarate Coenzyme A (HMG-CoA) reductase (HMGCR), although there is now growing evidence for further rate-limiting enzymes (Grundy, 1978; Sharpe and Brown, 2013) (Figure 1). Endogenous cholesterol levels are held constant due to negative feedback inhibition by high cholesterol concentrations as well as oxygenated cholesterol. Cholesterol that escapes the intestinal absorption is converted into coprostanol by bacteria mainly belonging to the genus *Eubacterium*. Compared to cholesterol, coprostanol is less well absorbed and eliminated via the feces suggesting cholesterol-to-coprostanol conversion as a potential cholesterol lowering mechanism (Veiga et al., 2005). In the GF animal, lacking bacterial dehydrogenation of cholesterol into coprostanol contributes to improved cholesterol uptake and reduced excretion of neutral sterols (Wostmann, 1981). Thus, the fecal amount of free steroids is lower in GF compared to CV animals highlighting microbial cleaving capacity of conjugated metabolites (Eriksson and Gustafsson, 1970; Eriksson et al., 1969; Gustafsson, 1968). As a compensatory mechanism, HMGCR gene expression is down-regulated due to increased circulating cholesterol levels (Wostmann, 1981). In summary, cholesterol is a precursor for steroid hormone and bile-acid biosynthesis associated with obesity and underlies intestinal and hepatic regulation as it is part of the enterohepatic circulation.

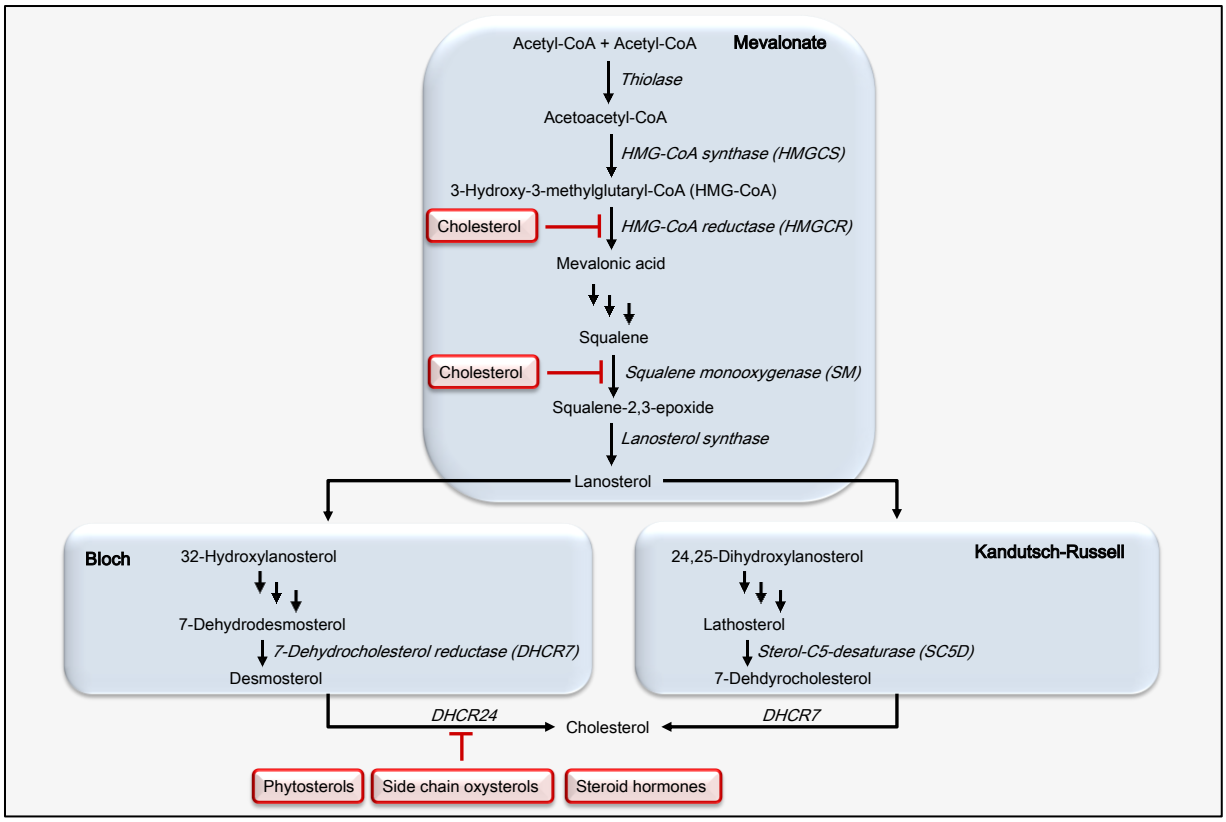

FIGURE 1 CHOLESTEROL BIOSYNTHESIS PATHWAY. Cholesterol originates from acetyl-CoA of the mevalonate pathway. Enzymatic reactions including HMG-CoA synthase (HMGCS), HMG-CoA reductase (HMGCR) and squalene monnooxygenase (SM) as well as lanosterol synthase direct lanosterol synthesis. Lanosterol is then diverted into the Bloch or the Kandutsch-Russell pathway. Both pathways lead to cholesterol synthesis either due to 24-dehydrocholesterol reductase (DHCR24)-driven desmosterol or 7-dehydrocholesterol reductase (DHCR7)-driven 7-dehydrocholesterol transformation, respectively. Cholesterol itself negatively feedbacks its own biosynthesis by suppressing HMGCR as well as SM. Steroid hormones, phytosterols as well as side chain oxysterols target DHCR24 activity thereby inhibiting final cholesterol formation. Modified according to Sharpe and Brown (Sharpe and Brown, 2013).

Steroid hormones such as corticosteroids (C_{21}), progestational hormones (C_{21}), androgens (C_{19}), and estrogens (C_{18}) are derived from cholesterol conversion (Figure 2). Synthesis was detected in adrenal glands, primary lymphoid organs, skin, brain, heart, but also in the intestine (Black, 1988; Taves et al., 2011). Once formed, steroid hormones enter the blood circulation, translocate to target tissues and mediate effects by passing through the plasma membrane, bind to intracellular receptors and thus, interact with Hormone Response Elements of the DNA to regulate gene transcription (Aranda and Pascual, 2001). The functions of steroid hormones are manifold and tissue-specific. With respect to obesity, a special role has been attributed to the action of 11β-hydroxysteroid dehydrogenase 1 (11β-

HSD1), which increases the glucocorticoid action within hepatocytes, stimulates gluconeogenesis and inhibits β-oxidation of fats. The efficiency to counteract metabolic disorders by enzymatic inhibition is, however, less clear for the liver than the adipose tissue (Chapman et al., 2013). On the other hand, estrogens as well as testosterone have beneficial effects on insulin sensitivity and obesity in liver, adipose tissue as well as in muscle (Louet et al., 2004; Yu et al., 2014). Before elimination, steroid hormones are extensively metabolized in the liver by sulfate and glucuronide conjugations. Bacterial-derived enzymatic deconjugations as well as intestinal glucuronidase activity, however, ensure ileal and cecal reabsorption (Groh, 1993). Thus, the rate of fecal excretion and the implication in obesity development differ among steroid hormones classes.

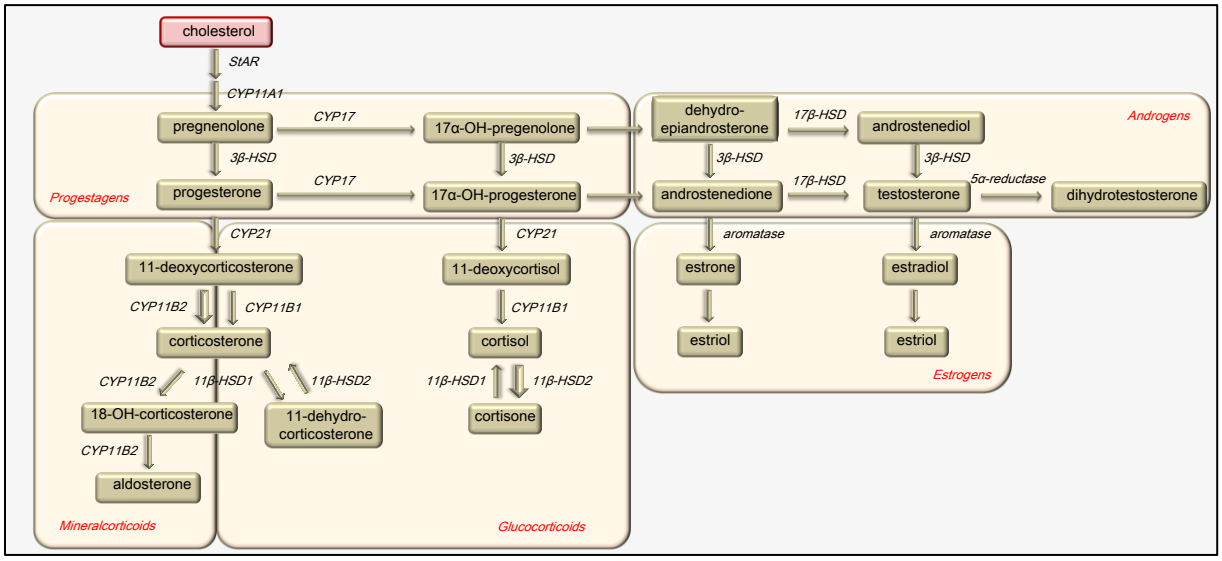

FIGURE 2 STEROID HORMONE BIOSYNTHESIS. Cholesterol is the precursor of steroid hormone biosynthesis and is translocated via the steroidogenic acute regulatory protein (StAR) into the inner mitochondrial membrane. Cyp11a1 is the key enzyme mediating progestagen biosynthesis. Following enzymatic reactions mineralcorticoids, glucocorticoids, estrogens as well as androgens evolve. Cyp11a1 – cholesterol monooxygenase. Cyp11b1 – 11β-hydroxylase. Cyp11b2 – aldosterone synthase. Cyp17 – 17α-hydroxylase. Cyp21 – 21-hydroxylase. 3β-HSD – 3β-hydroxysteroid dehydrogenase. 11β-HSD1/2 – 11β-hydroxysteroid dehydrogenase 1/2. 17β-HSD – 17β-hydroxysteroid dehydrogenase.

Bile acids which also derive from cholesterol and are part of the enterohepatic circulation act as signaling molecules in diverse metabolic pathways such as lipoprotein, glucose, drug and energy metabolism (Sayin et al., 2013). In this respect, bile acids not only facilitate intestinal fat and cholesterol uptake, but have also been associated with increased energy expenditure and DIO resistance in mice (Watanabe et al., 2011; Watanabe et al., 2006).

Bile acid synthesis is triggered by the cholesterol 7α-hydroxylase (Cyp7a1) representing the rate-limiting step. This enzyme is highly controlled at the transcriptional level (Kir et al., 2012; Martinez-Augustin and Sanchez de Medina, 2008) (Figure 3), which includes bile acid-mediated positive and negative feedback mechanisms involving the coordinated control by the transcription factors Farnesoid X receptor (FXR) and Liver X receptor (LXR) (Figure 3). Upon hepatic biosynthesis, the primary bile acids cholic acid (CA) and chenodeoxycholic acid (CDCA) found in humans and additionally, α- and β-muricholic acids (MCA) in mice, are conjugated with taurine and glycine before release into the bile. In mice unlike humans, conjugation is mainly attributed to taurine (Sayin et al., 2013). Within the gut, bacterial enzymes are capable of deconjugating and dehydroxylating primary bile acids into the secondary bile acids, deoxycholic acid (DCA) and lithocholic acid (LCA) as well as mouse-derived Ω-MCA. Secondary rather than primary bile acids predominate in fecal excretions, although, DCA and LCA have a low hydrophobicity and are also part of the enterohepatic circulation facing hepatic sulfatation (Ridlon et al., 2006). Around 95 % of bile acids are reabsorbed actively in the ileum or by passive diffusion in the colon (Martinez-Augustin and Sanchez de Medina, 2008). Being devoid of the bacterial capacity to deconjugate and dehydroxylate bile acids, only primary taurine-conjugated bile acids are represented in the GF gut. Bile acids were, thus, reported to be reabsorbed at an efficiency of 99 % which in consequence imply increased bile acid-mediated cholesterol absorption and increased endogenous cholesterol pools (Wostmann, 1981). Moreover, hepatic expression and activity of Cyp7a1 is stimulated in GF mice by tauro-β-MCA (β-TMCA) that antagonizes ileal FXR signaling. Decreased FXR levels, thus, entail less activation of ileal fibroblast growth factor 15 (Fgf15) which then lead to a reduced inhibition of hepatic Cyp7a1 expression and hence, increased bile acid levels

(Sayin et al., 2013). Taken together, bile acids are cholesterol-derived metabolites associated with DIO resistance in mice. Bile acid concentrations are highly controlled on the level of enzymatic gene expression and by the gut microbiota.

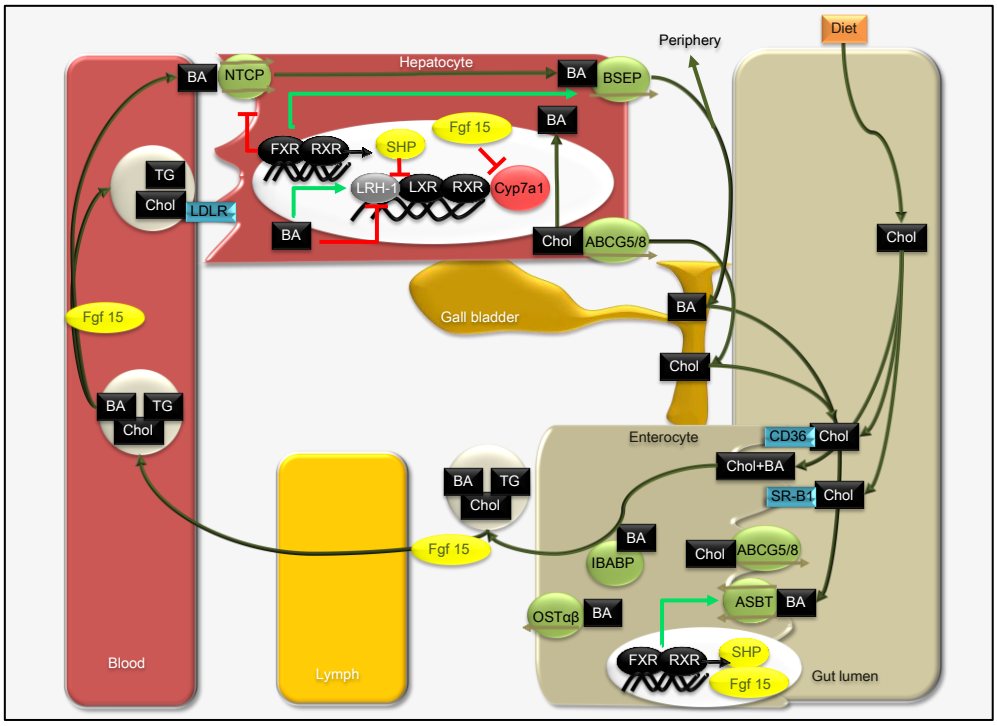

FIGURE 3 ENTEROHEPATIC CIRCULATION AND METABOLISM OF CHOLESTEROL AND BILE ACIDS. Dietary cholesterol (Chol) is taken up either passively via mixed micelles including bile acids (BA) or actively via scavenger receptor class B1 (SR-B1) or CD36 on the apical side of the enterocyte. BA can further be transported by the apical sodium-dependent bile acid transporter (ASBT), delivered to the ileal bile acid protein (IBABP) and released via the organic solute and steroid transporter (OST) αβ on the basolateral side of the enterocyte. Reverse Chol transport out of the enterocyte into the gut lumen to balance Chol concentrations are a matter of the apically located ATP-binding cassette sub-family G member 5 and 8 proteins (ABCG5/8). Chylomicrons containing BA, Chol and triglycerides (TG) pass the lymph and circulate through the blood to reach the liver. Chol either taken up into the hepatocyte by the low-density lipoprotein receptor (LDLR) or synthesized endogenously further underlies Cyp7a1-driven BA synthesis or ABCG5/8 dependent release and storage in the gall bladder. BA are absorbed via the Na^+/taurocholate cotransporting polypeptide transporter (NTCP) into the hepatocyte and delivered by the bile-salt export pump (BSEP) to the gall bladder for storage and re-circulation. Liver X receptor (LXR) α and β as well as Liver Receptor Homolog-1 (LRH-1) dependent transcription of the cholesterol 7α-hydroxylase (Cyp7a1) is negatively regulated by Farnesoid X receptor α (FXRα)-mediated small heterodimer partner (SHP) protein levels. FXRα further lowers hepatic BA levels by inhibition of NTCP, reinforcing BSEP transcription and triggering transcription of the ileal-derived fibroblast growth factor 15 (Fgf15) which then hinders Cyp7a1 transcription (Houten et al., 2006).

Metabolites such as bile acids or SCFA have been attributed to protect or mediate DIO, respectively, however, the resolution of published energy balance measurements is often relatively low and the real implication of gut bacteria on host energy homeostasis remains elusive (Backhed et al., 2004; Wostmann et al., 1982). Data on energy expenditure are often computed as percentages or size-specific indices to account for body mass effects, which renders comparison challenging and can also lead to spurious data interpretation (Packard and Boardman, 1999; Tschöp et al., 2012). Energy expenditure corrected by body mass does also not take into account differences in body composition since lean mass is metabolically more active than fat mass (Even and Nadkarni, 2012). Analysis of covariances (ANCOVA) is therefore needed to account for confounders (Packard and Boardman, 1999; Tschöp et al., 2012). Hence, there is urgent need for more precise measurement of host energy balance when investigating the influence of diets, metabolites and the host microbiome on obesity development.

Obesity that originates from an imbalanced energy homeostasis has recently been discussed to involve disturbed gut permeability (Lau et al., 2015; van Olden et al., 2015). Commensal gut bacteria located at the mucosal surface contribute to barrier integrity by hindering pathogen colonization. However, derangement of the gut microbial composition by Western diet feeding reinforced bacterial-derived lipopolysaccharide release and induced low-grade inflammation via increased gut permeability, hence, triggering metabolic endotoxaemia (Cani et al., 2007; Cani et al., 2008; Everard et al., 2011; Muccioli et al., 2010). Reduced transepithelial resistance and mRNA expression of the tight junction protein zonula occludens 1, together with increased mRNA levels of TNFα were further attributed to gut barrier dysfunction and obesity (Lam et al., 2012). However, there are also data providing no evidence for increased intestinal inflammation related to gut barrier dysfunction and obesity in mice and in humans (Brignardello et al., 2010; Kless et al., 2015; Woting et al., 2014). Thus, data on gut barrier integrity in obesity caused by gut microbiota are not consistent.

Overall, gut microbes affect enterohepatic circulation of metabolites by extensive transformation. Metabolites such as cholesterol, steroid hormones and bile acids are known to play a special role in

obesity and there is evidence for alterations by gut microbes. However, presentation and interpretation of data related to energy balance is often vague and the real implication of gut microbes to disturbed gut barrier remains also unclear. In summary, gut microbiota exerts effects on host metabolism, although the underlying mechanisms are still scarce.

2 AIM OF THE PRESENT STUDY

The **overall aim** of the present study was **to elucidate the impact of gut microbiota-host-diet interaction in obesity**. This aim was achieved **by evaluating the microbial impact on body mass development by using diet- and genetically-induced obesity mouse models combined with different treatment strategies. Additionally, dietary compounds interacting with bacteria and host in the presence of high-fat diet (HFD) were investigated**.

The first objective was based on **oral transplantations of complex cecal microbes** originating from genetically- or diet-induced obese donor mice **into germfree (GF) recipients that demonstrated transmissibility of obesity** (Turnbaugh et al., 2006). However, microbiota transfer into conventional (CV) mice may better reflect the clinical situation, and oral transplantations are discussed to include the transfer of dead microorganisms and unknown cecal or fecal compounds. In this respect, **the present study aimed to investigate treatment strategies on gut microbiota and obesity development in CV mice with genetic- or diet-induced obesity (DIO).** Thus, **cage swap and fecal transplantations** of male mice either **prone (AKR/J) or resistant (SWR/J) to DIO**, but also **cohousing of genetically obese Mc4r-deficient Mc4r^{W16X}/C57BL/6J with wildtype mice** were investigated to **clarify the bacterial impact on phenotypes**.

Secondly, **published research on DIO is inconsistent** with respect to dietary energy content, amount and composition of macronutrients which leads to **discrepancies in the ability of GF mice to develop obesity** (Backhed et al., 2007; Fleissner et al., 2010). Recently, the **type of dietary fat appeared to be of particular interest** in this interplay (Caesar et al., 2015). **Thus, the present study also aimed to examine the role of plant- and animal-based HFD in GF mice on obesity onset and to clarify mechanisms related to DIO resistance.** In that matter, male GF and CV C57BL6/N mice were fed a HFD either based on **palm oil or lard** that only differed in few candidate ingredients.

The exact role of gut microbiota on host energy homeostasis is still scant since the resolution of published energy balance measurements is relatively low. Hence, **expenditure, intake as well as excretion of energy were evaluated to phenotypically characterize and explain the effect of bacteria on body mass gain of mice**. Data on jejunal electrophysiology, cecal metabolomics as well as cecal and fecal 16S rRNA sequencing were generated in cooperation with the group of Prof. Hannelore Daniel (Chair of Nutritional Physiology, ZIEL, TUM), Prof. Philippe Schmitt-Kopplin (Research Unit Analytical BioGeoChemistry, German Research Center for Environmental Health, Munich) and Thomas Clavel, PhD (ZIEL Junior Group Intestinal Microbiome, TUM), respectively. **These methods together with hepatic gene expression provided unique depth in the gut microbiota-host-diet interplay and even supported a model on how dietary fat quality may control DIO resistance.**

Overall, feeding and microbial transfer experiments on genetically- and diet-induced obesity mouse models aimed to clarify the impact of the gut microbiota on obesity onset.

3 METHODS

3.1 Animal experiments and diets

3.1.1 Animals

Studies were performed on male conventional (CV) C57BL/6N, AKR/J, SWR/J, Mc4r^{W16X}/C57BL/6J knockin (ki) and wildtype (wt) as well as on germfree (GF) C57BL/6N mice housed at 22 ± 1 °C and 50-60 % relative humidity with a 12 hour light-dark cycle. Mice were bred in-house and had free access to food and water. CV mice were kept in individually ventilated cages (Greenline, IVC, 501 cm², Tecniplast) under specific pathogen-free conditions. GF mice were housed in open cages (M2: 360 cm² or M3: 540 cm², Harlan) within flexible film isolators (Harlan) ventilated via HEPA-filtered air. Sterility was checked by cultivation of feces in LB and WCA broth (OXOID) and by microscopic observation of gram stained fecal smears every 10 – 14 days and at sampling. A mold-trap was used to indicate the presence of mold. No contaminations were observed during the experiments. In both facilities, the absence of pathogens was approved by regular sentinel monitoring according to the FELASA guidelines. Animal experimentation and procedures were approved at the district government (approval no. 55.2-1-54-2532-103-2014).

3.1.2 Diets

Mice received an autoclaved standard chow diet until the start of the experiments (V1124-000) and were then switched to γ-irradiated purified and chemically-defined control diet (CD; S5745-E702), palm oil-based high-fat diet (pHFD; S5745-E712), or lard-based high-fat diet (lHFD; S5745-E730) (Table 1 - Table 3). All diets were supplied by Ssniff Spezialdiäten GmbH (Soest, Germany).

TABLE 1 COMPOSITION OF THE CHEMICALLY-DEFINED DIETS USED IN THE PRESENT STUDY. Major differences between pHFD and lHFD are highlighted in bold.

	CD	pHFD	lHFD
		wt-%	
Casein	24.0	24.0	24.0
Corn starch	45.9	26.7	26.7
Sucrose	5.0	5.0	5.0
Maltodextrin	5.6	5.6	5.6
Soy oil	5.0	5.0	5.0
Palm oil	**-**	**20.0**	**-**
Lard	**-**	**-**	**20.0**
Cellulose	5.0	5.0	5.0
Mineral mixture	6.0	6.0	6.0
Vitamin mixture	1.2	1.2	1.2
		kJ-%	
Protein	23.0	18.0	18.0
Fat	12.0	48.0	48.0
Carbohydrates	65.0	34.0	34.0
Energy content [kJ*g^{-1}][1]	15.5	22.7	22.7

[1]gross caloric value according to bomb calorimetry

TABLE 2 FATTY ACID COMPOSITION OF THE CHEMICALLY-DEFINED DIETS. Major differences between pHFD and lHFD are highlighted in bold.

	CD	pHFD	lHFD
		wt-%	
C12:0	0.01	0.01	0.05
C14:0	0.02	0.22	0.29
C16:0	**0.58**	**8.87**	**5.37**
C16:1	**0.01**	**0.13**	**0.60**
C18:0	**0.18**	**1.19**	**2.88**
C18:1	**1.29**	**8.75**	**9.64**
C18:2	2.65	4.67	4.55
C18:3	0.29	0.43	0.49
C20:0	0.02	0.10	0.08
Total fatty acids	5.05	24.87	23.91

TABLE 3 STEROL CONTENT OF THE CHEMICALLY-DEFINED DIETS. Major differences between pHFD and lHFD are highlighted in bold.

	CD	pHFD	lHFD
		*mg*100g^{-1}*	
Cholesterol	**0.51**	**0.73**	**7.10**
Campesterol	**1.02**	**3.98**	**1.00**
Stigmasterol	**2.00**	**3.04**	**1.20**
Sitosterol	**3.34**	**11.02**	**3.00**
Δ^5Avenasterol	0.19	0.70	0.30
Sitostanol	1.11	0.90	0.70
24-Methylene cyclocartenol	0.22	0.30	0.10
Cyclocartenol	-	0.61	-
Campestanol	0.52	0.22	0.20
Total sterols	8.80	21.48	13.60

3.1.3 Mouse models for diet-induced obesity

The role of the gut microbiota in energy balance regulation was investigated in 2 CV inbred mouse strains chosen by their different susceptibility to diet-induced obesity (DIO) (AKR/J > SWR/J).

Cage swap of SWR/J and AKR/J mice

4-week-old male AKR/J and SWR/J were weight-matched and arranged in groups of 3 mice per cage. 4 independent cohorts were evaluated in the experiment (n = 12 mice per strain in total). Twice weekly, CV AKR/J and SWR/J were exposed to foreign mouse bedding via cage swap to allow inter-strain microbiota transfer (Figure 4). At the age of 8 weeks, mice were adapted to CD for 4 weeks before being exposed to pHFD for another 4 weeks. Every second week, body mass, body composition (NMR spectroscopy, Bruker), and rectal temperature (Almemo 2490, Ahlborn) were evaluated and fresh feces was sampled. At the end of the experiment animals were analyzed for their individual food intake and feces production, as well as energy expenditure in the indirect calorimetry. Animals were euthanized with carbon dioxide ahead of organ sampling and cecal preparations to determine bacterial density.

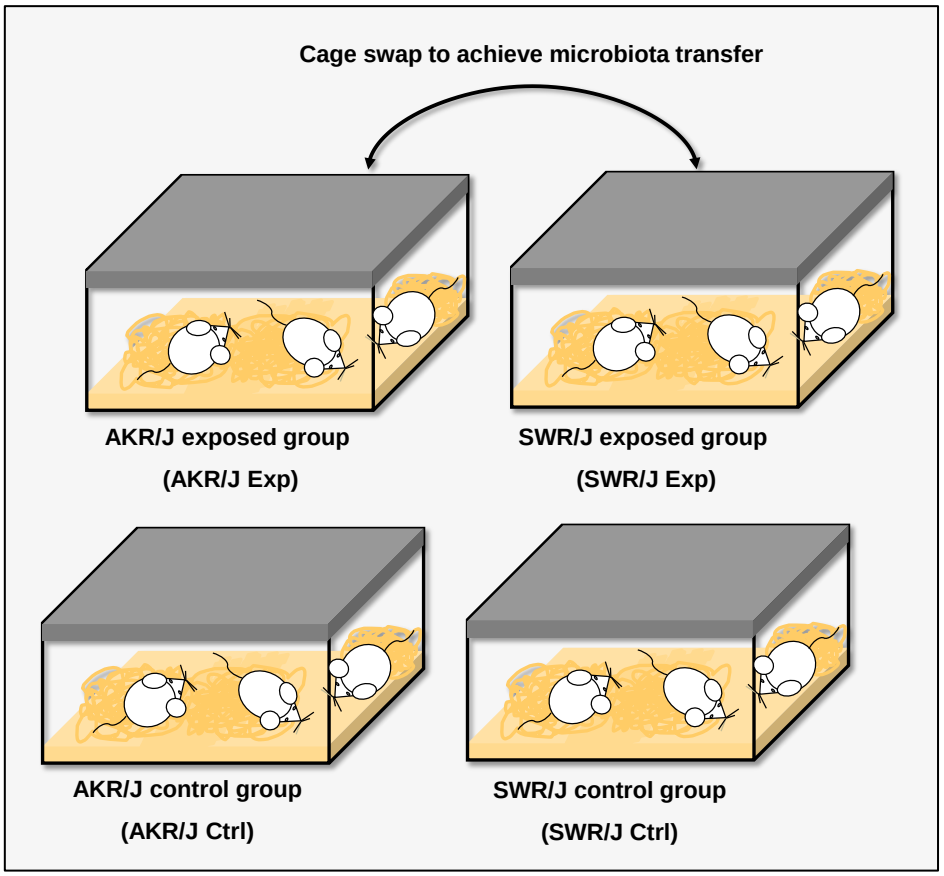

FIGURE 4 CAGE SWAP TO ACHIEVE MICROBIOTA TRANSFER BETWEEN AKR/J AND SWR/J MICE.

Fecal microbiota transplantation between SWR/J and AKR/J mice

8-week-old male mice were adapted to CD for 4 weeks. Until 10 weeks of age, mice were housed in groups of 4 to guarantee similar microbiota profile at the beginning of the experiment. Then, mice were weight-matched and assembled into groups of 2 animals per cage either classified as ‘recipient’ or ‘control’. Each donor mouse was assigned to one recipient cage. 2 – 5 days prior to the pHFD onset, mice received their first out of 5 microbiota transplantations which were performed once weekly (Figure 5, A). Body mass and body composition (NMR spectroscopy, Bruker) were monitored once weekly or every second week, respectively, but always 2 days before microbial transplantations.

For microbiota transplantations 2 pieces of fresh donor feces were collected and subsequently supplied with 1,000 µl of phosphate-buffered saline (PBS)/peptone cysteine (PC), vortexed until suspension and centrifuged for 1 min at 500 *g* to get rid of the debris. The supernatant was transferred into a new tube and centrifuged for 5 min at 8,000 *g*. The bacterial pellet was homogenized in 1,000 µl

PBS and 800 µl were used for microbiota transplantation. The remaining 200 µl were further centrifuged for 5 min at 8,000 *g* and the pellet was dissolved in 200 µl DNA stool stabilizer (Stratec) and stored at -80 °C for potential sequencing.

Immediately before fecal transplantations, the rectum of receiver mice was flushed 3 times with PBS using a disposable plastic pipette (VWR) to guarantee rectal entrance with the feeding needle (20 gauge, 30 mm length, Fine Science Tools). After 15 min PBS was blown off and 150 µl of fresh fecal homogenates or PBS were applied by oral gavage and rectal inoculation, respectively.

Mice were classified as ‘allogenic recipients’ or ‘autologous recipients’, either receiving fecal transplants of the foreign or the same mouse strain, respectively, or were assigned as ‘PBS controls’ (PBS Ctrl). Donor mice investigated at the same time were labeled as ‘untreated controls’ (untreated Ctrl) (Figure 5, B).

At the end of the experiment, food intake, feces production and energy expenditure were measured in the indirect calorimetry and fresh feces were collected to determine changes of bacterial diversity and composition between groups. Mice were euthanized with carbon dioxide and cecal samples were stored for further analysis of cecal bacterial diversity and composition.

Donors underwent the same feeding scheme as recipient mice, but were exposed to pHFD 5 weeks before the first fecal transplantation to assure a stable high-fat diet (HFD)-driven gut microbiota. Fecal transplantations started when donors were around 17 weeks of age (Figure 5, A).

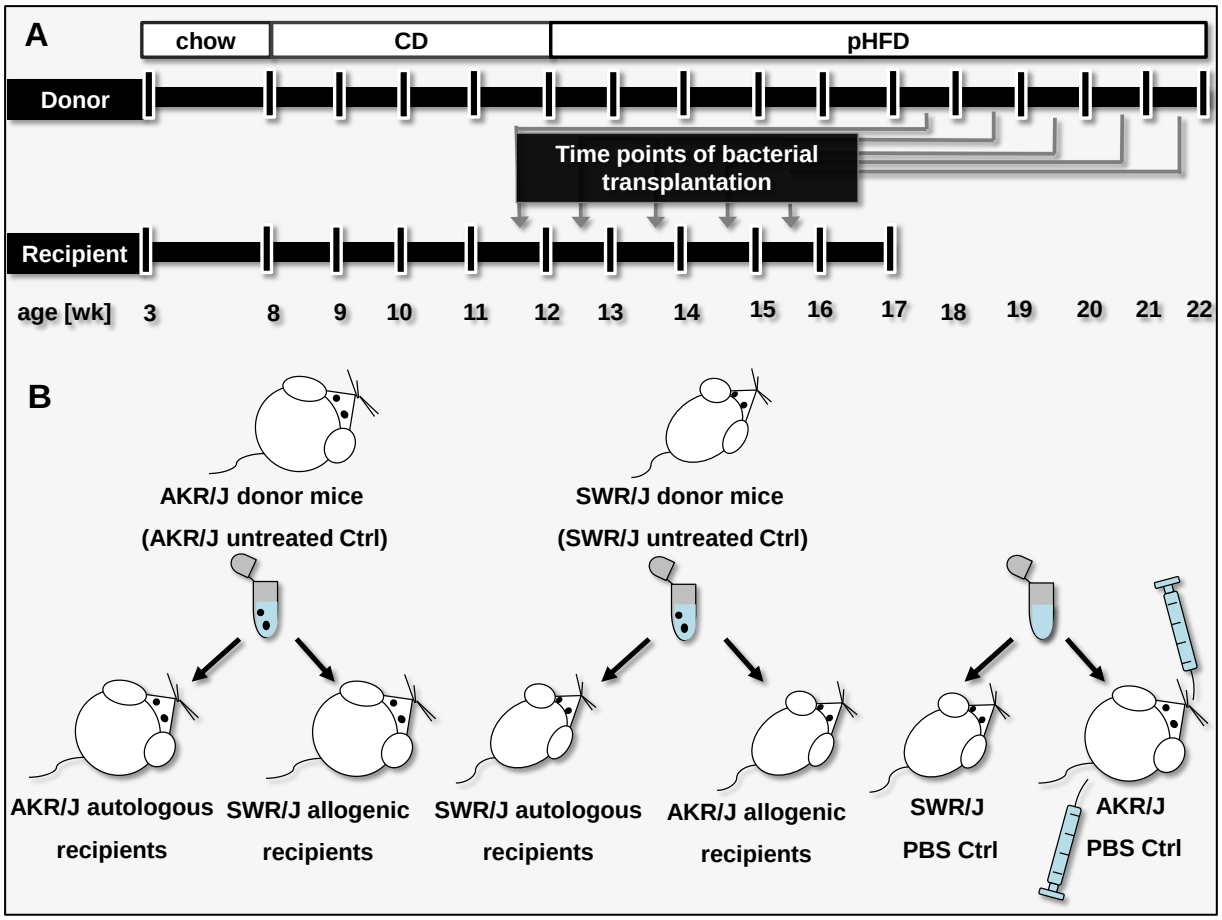

FIGURE 5 SCHEMATIC OVERVIEW OF FECAL MICROBIOTA TRANSPLANTATION PERFORMED WITH AKR/J AND SWR/J MICE. (A) Time course of the feeding and fecal microbiota transplantation strategy. (B) Group announcement following oral and rectal transplantations of fecal donor suspensions. The corpulence of the mice reflects the assumed body mass following high-fat diet feeding and bacterial transplantation success. CD – control diet; Ctrl – control; pHFD – palm oil-based high-fat diet.

Phosphate buffered saline solution supplemented with peptone and cysteine (PBS/PC): 8.60 g/l NaCl, 0.87 g/l Na2HPO4, 0.40 g/l KH2PO4, 0.2 g/l peptone from meat and 0.5 g/l L-cysteine (pH 7.2). The PBS/PC was sterilized by filtration.

3.1.4 Mouse model for genetically-caused obesity

The melanocortin-4 receptor (Mc4r) has a central role in hypothalamic regulation of energy homeostasis. Deletion of the Mc4r gene in knockout mice was associated with increased energy intake, growth and disturbed glucose metabolism (Huszar et al., 1997). Mc4r^{W16X}/C57BL/6J knockin (ki) and wildtype (wt) mice represent an in-house mouse model that was chosen to evaluate diet-independent effects of gut microbiota on obesity. This mouse line was established in cooperation with the German Research Center Munich and carries the stop mutation W16X that is positively associated with obesity in humans (Bolze et al., 2011). Based on homologous recombination in embryonic stem cells this mutation was integrated into the mouse genome. The mutation was crossed back into C57BL/6J mice and is maintained by mating of heterozygous mice.

Genotyping

Mc4r^{W16X}/C57BL/6J mice were genotyped at 3 weeks of age. Around 2 mm of cut tail tips were incubated with 195 µl tail buffer and 5 µl Proteinase K (Fermentas) for at least 4 hours at 65 °C and 1,000 rpm. Proteinase K was inactivated for 10 min at 95 °C. 1 µl of tail tip DNA was amplified during PCR using gene-specific primers. PCR products were visualized by agarose gelelectrophoresis (1.5 % gel, 45 min, 100 V) to distinguish wt mice (lane: 132 bp), ki mice (lane: 278 bp) and heterozygous mice (lane: 132 bp and 278 bp).

TABLE 4 PCR REACTION MIXTURE FOR GENOTYPING OF MC4R^{W16X} MICE.

	Volume per reaction [µl]
2x ImmoMix (Bioline)	10.0
Primer forward (10 µM)	1.0
Primer reverse (10 µM)	1.0
Nuclease-free water	7.0
Tail buffer	1.0
Total	20.0

TABLE 5 PCR PROGRAM FOR GENOTYPING OF MC4R^{W16X} MICE.

Step	Temperature [°C]	Time [s]	Cycles
Initialization	95	420	
Denaturation	95	10	35
Annealing	60	20	
Elongation	72	30	
Final elongation	72	180	

Forward primer: 5‘-CTACAGGCATACAGACTGGGAG-3‘

Reverse primer: 5‘-GTACATGGGTGAGTGCAGGTTC-3‘

Tail buffer: 243.3 mg TRIS, 160 ml H_2O bidest. pH 8.3, 745 mg KCl (50 mM), 900 µl Nonidet P40, 900 µl Tween 20 (0.45 %), 20 mg gelatine.

Cohousing of Mc4r^{W16X} ki mice with wt mice

Cohousing of male Mc4r^{W16X} /C57BL/6J ki and wt mice was performed to investigate diet independent microbiota effects on phenotypic outcomes. All animals were fed with *ad-libitum* chow (V1124-000) throughout the experiment. Mice were cohoused in groups of 4 per cage including a ki:wt ratio of 1:3 (ki 1+3) or 3:1 (wt 1+3) resulting either in a dominating ki or wt environment, respectively (Figure 6). Control mice were housed separately to the foreign genotype since they were 4 weeks of age. In total, 6 cohorts were evaluated. Every second week, body mass, body composition (NMR spectroscopy, Bruker), and rectal temperature (Almemo 2490, Ahlborn) were measured. At 12 weeks of age mice were single-housed in the indirect calorimetry for 2 – 4 days to examine individual energy expenditure, food intake and feces production. 1 week later, mice were euthanized with carbon dioxide and organs were stored for further analysis.

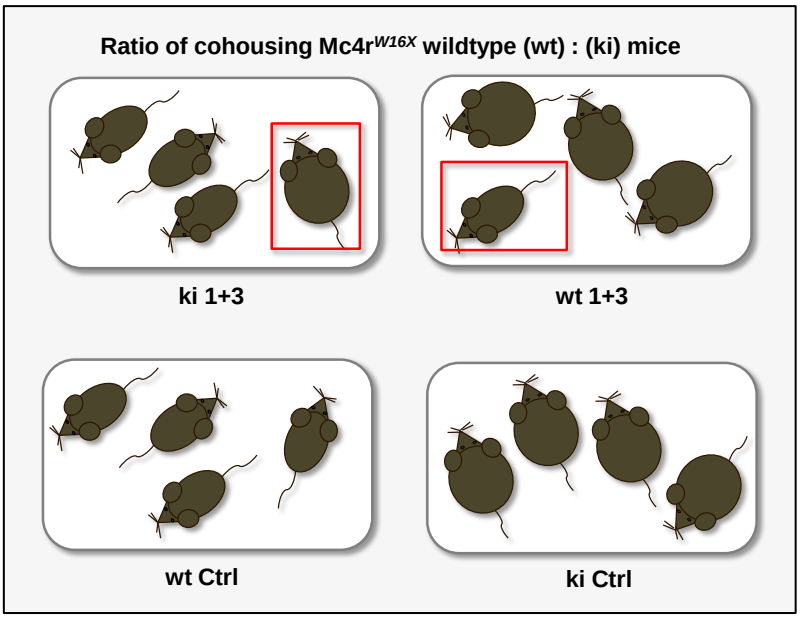

FIGURE 6 SCHEMATIC OVERVIEW OF A COHORT OF COHOUSED MC4R^{W16X} KNOCKIN (KI) AND WILDTYPE (WT) MICE.

3.1.5 High-fat diet challenge of germfree and conventional mice

8-week-old male GF and CV C57BL/6N mice were adapted to CD for 4 weeks. At 12 weeks of age mice were weight-matched and assembled into 3 groups that either stayed on CD, received pHFD or lHFD for another 4 weeks. Body mass was examined weekly, and body composition (NMR spectroscopy, Bruker) as well as rectal temperature (Almemo 2490, Ahlborn) were measured in the mornings of dissection. Within the first and the fourth week after the diet switch, food intake and feces production were monitored. 2 days before dissection, energy expenditure was investigated by indirect calorimetry. Mice were dissected in the *ad-libitum* fed state in the mornings or fasted for at least 6 hours at 30 ± 0.5 °C due to basal metabolic rate recordings and sacrificed in the afternoon. The GF status of mice was evaluated by cultivation and gram staining before transfer into the indirect calorimetry and at dissection. Mice were euthanized with carbon dioxide, blood of the ventricle and the portal vein as well as organs were sampled and stored for further analysis. Jejunum samples were used to determine transepithelial resistance using Ussing chambers (chapter 3.4).

3.2 Analysis of energy balance

3.2.1 Energy expenditure

Oxygen consumption (Δvol-% O_2) and carbon dioxide production (Δvol-% CO_2) were analysed by indirect calorimetry in a ventilated, open-circuit system using the LabMaster system from TSE Systems (Bad Homburg, Germany). Up to 8 mice were kept single-housed in gas-tight home cages (Greenline, IVC, 501 cm², Tecniplast) through which fresh air was passed with a constant flow rate of 0.7 l*min^{-1}.

For GF mice, ports for efflux and influx of air were provided with sterile filters (0.2 µm PTFE, 25 mm, X200 Fil. Seringue, Novo direct, 0.2 µm PTFE, 50 mm, Pleomax) fixed on top of metal adaptors (Luer Lock Connector, VBM Miscellaneous), and caps for water bottles were tightened by a flexible tube to avoid any contamination during the measurement. Cages including filters, lids, water bottles, food racks and bedding were autoclaved in separate plastic bags. GF mice, food and water were transferred into sterile cages under laminar air flow. Before the transfer and after the indirect calorimetry, the GF status of mice was evaluated by cultivation and gram staining of feces. Recordings were taken in up to 9 minute intervals over a time span of 2 – 4 days excluding the first day as adaption for analysis (except experiment 3.1.5, here, the first day was also taken into account). Animals had free access to food and water at 21.5 ± 0.5 °C. In the morning of the last measurement day, mice were food-deprived for 6 hours and ambient temperature was set at 30 ± 0.5 °C representing thermoneutrality. All measurements were performed in a temperature-controlled climate-chamber (Feutron®).

The respiratory exchange ratio (RER) is a measure of substrate oxidation whereby complete oxidation of glucose, proteins and lipids corresponds to values of 1.0, 0.81 and 0.7, respectively.

Heat production (HP) at 22 °C in the *ad-libitum* fed state was based on the sum of the hourly means of $\dot{V}O_2$ for 24 hours and the daily mean of RER. Basal metabolism measured for 6 hours in the

postabsorptive state was determined within the last 3 hours neglecting the first 3 hours as adaptation phase. The minimal $\dot{V}O_2$ with a coefficient of variation below 5 % computed over 27 min intervals and the corresponding RER were selected for calculations according to the following equation:

$$HP\ [mW] = (4.44 + 1.43 * RER) * \dot{V}O_2\ [ml*h^{-1}] \text{ (Heldmaier, 1975)} \qquad \text{[Equation 1]}$$

The variation in HP due to individual differences in lean mass and fat mass measured at the end of the indirect calorimetry was adjusted by ANCOVA using the S+ software (TIBCO Spotfire).

3.2.2 Energy contents of food and feces

Bomb calorimetry

Energy contents of food and feces were determined by bomb calorimetry. Feces were dried at 55 °C for 1 week, weighed, homogenized using a TissueLyser (Retsch) and pelletized. Dried food and feces pellets of about 1 g were completely burned under high pressure (30 bar) of oxygen.

Factors to define the caloric value of a sample imply the energy equivalence value of the respective bomb calorimeter (EE), the increase in temperature by combustion (ΔT), the energy released by the ignition thread (E_{thread} = 20 kJ), the weight and the energy released by the combustion aid if required ($E_{combustion\ aid}$ = 26.45 kJ/g), and the weight of the sample.

$$\text{Caloric value}\ [J*g^{-1}] = \frac{(EE*\Delta T)-E_{thread}-(E_{combustion\ aid}*m_{combustion\ aid})}{m_{sample}} \qquad \text{[Equation 2]}$$

Energy intake (E_{in}) and energy excretion (E_{out}) were calculated based on food intake or feces production and the caloric value of the sample (E_{food}, E_{feces}). Food intake and feces production were recorded simultaneously to determine energy resorption (E_{res}) and the efficiency of energy resorbed in the body, respectively.

$$E_{in}\ [kJ] = \text{Food intake } [g] * E_{food}\ [kJ*g^{-1}] \quad \text{[Equation 3]}$$

$$E_{out}\ [kJ] = \text{Feces production } [g] * E_{feces}\ [kJ*g^{-1}] \quad \text{[Equation 4]}$$

$$E_{res}\ [kJ] = E_{in}\ [kJ] - E_{out}\ [kJ] \quad \text{[Equation 5]}$$

$$\text{Resorption efficiency } [\%] = \frac{E_{res}\ [kJ]}{E_{in}\ [kJ]} * 100 \quad \text{[Equation 6]}$$

Energy excretion was adjusted for dietary energy intake, whereas energy resorption was adjusted for body composition (experiment 4.1 – 4.3) or body mass gain (experiment 4.4) using the S+ software (TIBCO Spotfire).

Fourier transform-infrared spectrometry

Fourier transform-infrared spectrometry (FT-IR) was performed to evaluate the amount of energy and fat in dried (55 °C, 1 week) and grinded fecal samples of group-housed CD-, pHFD- or lHFD-fed GF and CV mice. FT-IR measures the absorption of infrared radiation by the samples. IR absorption spectra are characteristic for particular molecular components and structures. The analysis was based on diffuse reflexion using a 96-well plate and a Tensor 27 HTS/XT Microplate Reader (Bruker). Fecal samples (10 mg) were measured in triplicate with a resolution of 4 cm^{-1} ranging from 600 – 7000 cm^{-1} covering the near to medium infrared range within 60 scans. The triplicate measurements mean spectra were analyzed using the QuantAnalysis (Bruker). Fecal fat and energy contents of mice were quantified by a standard curve that is based on validated fecal samples of three CV mouse strains (C57BL/6J, TallyHo/JngJ, C3HeB/FeJ) fed standard chow diet, HFD, or a diet with no or high amounts of carbohydrates.

Fecal energy and fat contents were adjusted for daily feces production and dietary intake of energy or fat, respectively, using the S+ software (TIBCO Spotfire).

3.3 Tissue dissection

Animals were sacrificed with carbon dioxide at the end of the feeding period. Body length was determined and blood was taken out of the ventricle. Organs were removed, weighed, snap frozen in liquid nitrogen and stored at -80 °C for further analysis. Cecum samples were divided into 2 parts including part A for 16S rRNA sequencing and part B for metabolome analysis or determination of bacterial density, respectively (Figure 7).

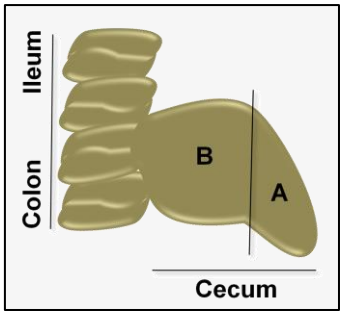

FIGURE 7 PARTS OF THE CECUM USED FOR 16S RRNA SEQUENCING (A) OR METABOLOME ANALYSIS AND DETERMINATION OF BACTERIAL DENSITY (B), RESPECTIVELY.

3.4 Ussing chambers for assessment of gut permeability

Ussing chamber measurements were carried out by Veronika Maria Müller from the group of Prof. Hannelore Daniel, Chair of Nutritional Physiology, ZIEL, TUM, as described recently (Kless et al., 2015). Briefly, jejunal samples were directly mounted in Ussing chambers (Warner Instruments) after dissection and continuously flushed on the luminal and serosal planes with carbogen-gassed Krebs buffer at 37 °C. Equilibration of tissues passed for 45 min with 125 µM fluorescein on the luminal side and transepithelial resistance (TER) of tissue responses was subsequently computed in the current clamp configuration. Complete barrier breakdown was induced by 12.5 µM EGTA applied after another 60 min.

Krebs buffer: 114 mM NaCl, 21 mM $NaHCO_3$, 5.4 mM KCl, 2.4 mM Na_2HPO_4, 1.2 mM $CaCl_2$, 1.2 mM $MgCl_2$, 0.6 mM Nh_2PO_4, 10 mM glucose, pH 7.4

3.5 Molecular biology

3.5.1 RNA isolation from liver tissue

Mice were dissected in the fed state. The lobus sinister lateralis of mouse livers was homogenized in TRIsure (Bioline) and RNA was purified using chlorophorm and the SV Total RNA Isolation System (Promega). RNA was eluted in 50 µl nuclease-free water and concentration was measured spectrophotometrically with the Infinite® 200 NanoQuant (Tecan). RNA Integrity was confirmed via agarose gel electrophoresis or by the RNA 6000 Nano chip system (Agilent).

3.5.2 Quantitative real-time polymerase chain reaction

500 ng of RNA were reverse transcribed into complementary DNA (cDNA) according to the QuantiTect® Reverse Transcription Kit (Qiagen). Gene expression was recorded on a 384-well format (Roche Light Cycler® 480) using Sensimix SYBR NoRox (Bioline) and quantified by a 2^n standard curve representing a cDNA pool of all samples. The standard curve was applied in duplicate and samples were measured in triplicate. The mean of the replicate target gene expression was normalized to the replicate mean of the 4 reference genes beta-actin (Actb), eukaryotic elongation factor 2 (Eef2), heat shock protein 90 (Hsp90) and hypoxanthine guanine phosphoribosyl transferase (Hprt1). Primers for quantitative real time-polymerase chain reaction (qPT-PCR) were designed with the Primer3 algorithm (SDSC Biology Workbench) (Untergasser et al., 2012) (Table S 1).

TABLE 6 QRT-PCR REACTION MIXTURE FOR ANALYSIS OF GENE EXPRESSION.

	Volume per reaction [µl]
Sensimix SYBR NoRox (Bioline)	6.25
Primer forward (final concentration)	1.00 (5 pmol/l)
Primer reverse (final concentration)	1.00 (5 pmol/l)
Nuclease-free water	3.25
cDNA	1.00
Total	12.50

TABLE 7 QRT-PCR PROGRAM FOR ANALYSIS OF GENE EXPRESSION.

Step	Temperature [°C]	Time [s]	Cycles
Initialization	95	420	
Denaturation	97	10	45
Annealing	52	15	
Elongation	72	20	
Melting curve	60 to 95	1,200	

3.6 Microbiology

3.6.1 Bacterial density

Cecal samples (part B, Figure 7) were weighed in sterile tubes (2 ml, Eppendorf) prefilled with glass beads (1 mm, Roth), diluted 1:10 w/v with PBS, vortexed, homogenized and centrifuged (1,000 *g*, 1 min). Supernatants were used to prepare a dilution series in duplicate of 1:10, 1:100 and 1:200 using PBS. Samples were frozen at -80 °C until analysis. Cells were counted within the 4 diagonal squares of the Thoma chamber (Roth) using the 200 x magnification of the microscope (Leica). Bacterial density was determined by the total cell counts (S), the chamber factor (K, $1.25 * 10^6$) and the sample dilution (V) according to the following formula:

$$\text{Bacterial density [cell counts * g cecal content}^{-1}\text{]} = S * K * V\,[v/v] * V\,[w/v] \quad \text{[Equation 7]}$$

3.6.2 Cultivation of bacteria and gram staining

Sterility was examined in GF mice before indirect calorimetry and at dissection. Fresh fecal and colon suspensions were cultivated under aerobic and anaerobic conditions for 2 – 3 weeks. Hungate-type tubes were gassed with nitrogen, closed with a flange type non-toxic butyl rubber stopper and a screw cap with 9 mm opening (16 x 125 mm, Dunnlab). Tubes were prefilled with sterile Wilkens-Chalgren anaerobe broth (WCA) (OXOID) for anaerobic cultivation at 37 °C and 0 % O_2. Aerobic cultivation was carried out in 15 ml falcon tubes (Sarstedt) filled with sterile lysogeny broth (LB) medium (Roth) and incubated at 37 °C in an orbital shaker (420, Thermo Forma). Samples were evaluated against a positive and negative control. Subcultures as well as gram staining were performed for ambiguous and positive samples.

For gram staining, fecal and colon contents were homogenized with sterile PBS, heat-fixed onto microscopic slides (ECN 631-1551, VWK) and assessed according to the Gram Staining Kit (Roth). Slides were microscopically evaluated with a 100 x magnification using the microscope (Leica).

3.6.3 High-throughput sequencing

Cecal and fecal DNA processing

Samples were processed and analyzed as described previously (Lagkouvardos et al., 2015). Metagenomic DNA from cecum and feces was purified using either the QIAamp DNA Stool Mini Kit (Qiagen) (experiment 3.1.3 feces) or the NucleoSpin® gDNA Clean-up kit (Macherey-Nagel) (3.1.3 fecal transplantation, 3.1.5) after mechanical lysis and RNAse treatment.

The V4 (3.1.3 cage swap) or the V3/V4 region (3.1.3 fecal transplantation, 3.1.5) of 16S rRNA genes were amplified in 2 steps using 50 ng (3.1.3 cage swap) or 12 ng (3.1.3 fecal transplantation, 3.1.5) of DNA (Table 8 – Table 10). Primer sequences are given in Table S 2. PCR was performed on a RealPlex Cycler (Eppendorf).

TABLE 8 PCR REACTION MIXTURE OF THE FIRST STEP OF THE 2-STEP PCR.

	Volume per reaction [µl]
5x Phusion® High-Fidelity (HF) Buffer	4.000
515/341 HTS forward primer (20 µM)[1]	0.125
806/785 HTS reverse primer (20 µM)[1]	0.125
Phusion® HF DNA Polymerase Hotstart	0.100
d'NTPs (Bioline) (20 µmol)	0.400
DMSO 100%	1.500
DEPC treated water (sterile filtered, Sigma)	11.750
DNA	2.000
Total	20.000

[1]primer numbers in front of the slash refer to 3.1.3 cage swap, numbers behind the slash refer to 3.1.3 fecal transplantation and 3.1.5.

TABLE 9 PCR PROGRAM OF THE FIRST STEP OF THE 2-STEP PCR.

Step	Temperature [°C][1]	Time [s][1]	Cycles
Initialization	98	30/40	
Denaturation	98	5/20	
Annealing	52.5/55	10/40	15
Elongation	72	10/40	
Final elongation	72	120	

[1]numbers in front of the slash refer to 3.1.3 cage swap, numbers behind the slash refer to 3.1.3 fecal transplantation and 3.1.5.

TABLE 10 PCR REACTION MIXTURE OF THE SECOND STEP OF THE 2-STEP PCR.

	Volume per reaction [µl]
5x Phusion® HF Buffer	10.000
515/341 forward primer (20 µM)[1]	0.313
806/785 reverse rcbc 200 – 400 primer (2.5 µM)[1]	0.125
Phusion® HF DNA Polymerase Hotstart	0.200
d'NTPs (Bioline) (20 µmol)	1.000
DMSO 100%	1.500
DEPC treated water (sterile filtered, Sigma)	32.487
PCR product of the first reaction step	2.000
Total	50.000

[1]primer numbers in front of the slash refer to 3.1.3 cage swap, numbers behind the slash refer to 3.1.3 fecal transplantation and 3.1.5.

TABLE 11 PCR PROGRAM OF THE SECOND STEP OF THE 2-STEP PCR.

Step	Temperature [°C][1]	Time [s][1]	Cycles
Initialization	98	30/40	
Denaturation	98	5/20	
Annealing	50/55	10/40	10
Elongation	72	10/40	
Final elongation	72	120	

[1]numbers in front of the slash refer to 3.1.3 cage swap, numbers behind the slash refer to 3.1.3 fecal transplantation and 3.1.5.

Purification of PCR products was carried out according to the NucleoSpin® gel and PCR Clean-up kit (Macherey-Nagel; 3.1.3 cage swap) or the Agencourt AMPure XP system (Beckmann Coulter) (3.1.3 fecal transplantation, 3.1.5), respectively. Purified DNA was visualized by agarose gelelectrophoresis (2 % gel, 45 min, 100 V) and concentration was determined by the Qubit® dsDNA HS Assay Kit (Life Technologies). Samples were adjusted to 2 nM using the following formula:

$$\text{DNA concentration [nM]} = \frac{\text{DNA concentration [ng/µl]} * 1{,}000{,}000}{549 * 660} \qquad \text{[Equation 8]}$$

High-throughput 16S rRNA amplicon sequencing

16S rRNA sequencing and analysis were carried out by Thomas Clavel, PhD, at the ZIEL sequencing facility.

Samples were sequenced in paired-end modus (3.1.3 cage swap: PE200; 3.1.3 fecal transplantation, 3.1.5: PE275) using the MiSeq system (Illuminia) as described previously (Lagkouvardos et al., 2015). The raw data read files were demultipexed and each sample was processed using USEARCH (Edgar, 2010) according to the UPARSE approach (Edgar, 2013). All reads were truncated to the position with the first base revealing a quality score minor 3. For each sample, sequences were de-replicated and analyzed for chimeras with UCHIME (Edgar et al., 2011). Sequences from all samples were merged, sorted by abundance and operational taxonomic units (OTU) were filtered at a threshold of 97 % similarity. Taxonomic classification of OTUs was conducted by the RDP classifier (Wang et al., 2007) (80 % confidence). A phylogenetic tree using fasttree (Price et al., 2010) was constructed keeping all OTUs with a relative abundance above 0.5 % (3.1.3 cage swap, fecal transplantation) or 0.25 % (3.1.5) total sequences in at least one sample. Phylogenetic distances were calculated by the generalized Unifrac (Chen et al., 2012). The Shannon index was calculated as a correspondence to the effective number of species to estimate diversity within samples (α-diversity) (Jost, 2007).

3.7 Metabolomics

Metabolome analysis was performed in cooperation with Alesia Walker, PhD, from the group of Prof. Philippe Schmitt-Kopplin, Research Unit Analytical BioGeoChemistry, German Research Center for Environmental Health, Munich.

3.7.1 Metabolite extraction of cecal and hepatic samples

Samples were stored on dry ice until extraction. All instruments were flame-scarfed with methanol. Cecal contents (10 mg) or liver (50 mg) were placed into sterile ceramic bead tubes (NucleoSpin® Bead Tubes, Macherey-Nagel) containing a stainless metal bead (5 mm, Qiagen) and 1 ml of cold methanol (-20 °C, LC-MS CHROMASOLV®, FLUKA, Sigma Aldrich). Cecal samples were homogenized in a Tissue Lyser II (Qiagen) for 5 min at 30 Hz and mortared liver samples were incubated for 15 min. All samples were centrifuged twice (10 min, 21,000 *g*, 4 °C). Supernatants were transferred into sterile tubes (Eppendorf) and used for non-targeted metabolomics and cecal bile acid quantification.

3.7.2 Electron spray Fourier transform-ion cyclotron resonance mass spectrometry

Non-targeted metabolomics using electron spray Fourier transform-ion cyclotron resonance mass spectrometry (ESI-FT-ICR/MS) was performed for cecal and hepatic samples. Methanol extracts were analyzed in the negative ionization mode. FT-ICR mass spectra were generated using a 12 Tesla solariX™ mass spectrometer (Bruker) equipped with an Apollo II ESI source. External calibration of the system was performed with clusters of arginine by using 5 $mg*l^{-1}$ arginine solution in methanol resulting in calibration errors below 0.1 ppm for 4 selected m/z signals of arginine clusters (m/z 173.10440, 347.21607, 521.32775 and 695.43943). Direct infusion was performed for cecal samples in the manual mode while liver extracts were measured using the Gilson autosampler system (Gilson). Detailed information on instrument parameters is summarized in Table 12.

TABLE 12 ESI-FT-ICR/MS CONDITIONS

Analysis parameters	Cecal samples	Hepatic samples
Flow rate [µl*min^{-1}]	2	2
Mass range [Da]	122.9 – 1,000	122.9 – 1,000
Time of flight [msec]	0.8	0.65
Ion accumulation time [sec]	0.5	0.1
Acquired scans	450	450
Capillary voltage [V]	3,600	3,600
Drying gas flow rate [l*min^{-1}]	4	4
Drying gas temperature [°C]	180	180
Nebulizer gas flow rate [bar]	2	2
Spray shield [V]	-500	-500
Time domain [megaword]	2	2

3.7.3 Ultra performance liquid chromatography time of flight mass spectrometry

Bile acids in cecal content were quantified in the negative ionization mode using Ultra performance liquid chromatography (UPLC; Acquity™, Waters) coupled with time of flight mass spectrometry (TOF/MS; SYNAPT–G1–QTOF-HD mass spectrometer; Waters, Micromass).

Standard stock solutions of bile acids and 3 deuterated bile acids were prepared (1 mg*ml^{-1}; 1000 ppm). A mixture of all non-deuterated bile acids each concentrated to 50 ppm was diluted into 4 different concentration ranges (4, 3, 2, 1 and 0.1 ppm; Table S 3). These dilutions were used to determine a calibration curve for each bile acid. Before analysis, cecal samples were diluted 1:50 with pure methanol. Bile acid solutions and diluted cecal samples were measured in triplicates after being spiked with a deuterated bile acid mixture of d^4-deoxycholic acid (DCA), d^4-cholic acid (CA) and d^5-taurocholic acid (TCA) (final concentration of 0.5 ppm; Table S 3).

Diluted cecal extracts were separated using a reversed-phase column (C8: 1.7 µm, 2.1 x 150 mm, Acquity™ UPLC BEH™, Waters) with a flow rate of 350 µl*min^{-1}, an injection volume of 5 µl and a column temperature of 60 °C. Elution of bile acids was ensured by a solvent system including ammonium acetate (5 mM, Sigma Aldrich) combined with acetic acid (0.1 %, pH 4.2, Biosolve) in

water (milliQH_2O, Milli-Q Integral Water Purification System) and acetonitrile (LC-MS CHROMASOLV®, FLUKA, Sigma Aldrich). A gradient profile was applied by starting at 10 % acetonitrile for 1 min, increasing to 22 % within 2 min, then to 27 % within 4 min, followed by a linear gradient to 95 % within 13 min. The 95 % acetonitrile was held for 2.5 min, returning to 10 % acetonitrile within 2.5 min. ESI parameters were as followed: capillary, 0.5 kV; source temperature, 120 °C; desolvation temperature, 350 °C; cone gas flow, 20 $l*h^{-1}$; desolvation gas flow, 800 $l*h^{-1}$. The mass range was set to acquire the m/z range 50 – 1000. Bile acids used as external and internal standards can be found in Table S 3.

3.8 Statistics

Data were analysed using the SigmaPlot 12.5 and the Multi Experiment Viewer (MeV) software. 1-Way and 2-Way ANOVA followed by Tukey post-hoc testing examined statistical significance ($p < 0.05$) between mouse strains and diets. Repeated-measures ANOVA was applied for time course measurements including frequent recordings of body mass and composition as well as RER. Data for HP as well as fecal energy and fat content were adjusted by ANCOVA using S+ (TIBCO Spotfire). Figures were generated using GraphPad PRISM 6.

For microbiota analysis, data were processed in the R programming environment. The effect of feeding on OTU and taxonomic counts was tested using 1-way ANOVA followed by t-test for pairwise comparisons. Prior to testing, individual counts minor 0.5 % were zeroed, and only dominant taxonomic groups or molecular species (i.e. median sequence abundance above 1 % in at least 1 group) were considered. For β-diversity analysis, generalized Unifrac distances were calculated using the package GUniFrac (Chen et al., 2012).

For metabolome analysis, mass spectra were processed by internal calibration using the Compass DataAnalysis 4.0© (Bruker) and exported with a signal-to-noise ratio of 4 and a relative intensity ratio of 0.001 %. Alignment within an error of 1 ppm was performed using the Matrix Generator software

(in-house software of the Research Unit Analytical BioGeoChemistry, German Research Center for Environmental Health, Munich). The cut-off for further analysis of mass signals was set at 10 % abundance of mass signals, covering all samples. Sum formulas were generated by the NetCalc software (Tziotis et al., 2011). Annotation of mass signals was provided by the web-based MassTRIX server accounting for the ionization mode and the accuracy of the system (1 ppm) which includes a small but potential risk of false annotation. Metabolite clusters and heat maps were illustrated by the Hierarchical Clustering Explorer underlying Pearson's correlations and annotated metabolites were mapped into metabolic pathways using KEGG Mapper (http://www.genome.jp/kegg/tool/map_pathway2.html, 4th November 2014). Welch's t-test was conducted for pairwise comparisons hypothesizing unequal variances.

For bile acid quantification, data were processed using the Genedata Refiner MS software (Genedata). Bile acid concentrations were determined according to the calibration curve approach and the mean of triplicate measurements was calculated.

4 RESULTS

4.1 AKR/J mice are less obese when exposed to bedding of obesity resistant SWR/J mice

4.1.1 Cage swap reduces fat mass of AKR/J mice

Evidence for microbial impact on body weight development first emerged from germfree (GF) studies (Backhed et al., 2004; Fleissner et al., 2010; Turnbaugh et al., 2006), however, the influence of bacteria in conventional (CV) mice remains unexplored so far. Thus, cage swap of CV mice distinct in their capability to gain weight was performed to evaluate the extent of bacterial contribution on obesity development. In this respect, obesity-prone AKR/J and obesity-resistant SWR/J mice were transferred between cages twice weekly since weaning. At 12 weeks of age, mice were exposed to palm oil-based high-fat diet (pHFD) for 4 weeks. Phenotypically, an inter-strain adaptation was hypothesized.

At 8 weeks of age, CD-fed AKR/J mice were heavier than CD-fed SWR/J which was attributable to a distinct difference in lean mass (Figure 8, A-C). With the onset of pHFD feeding fat mass and hence, body mass steadily increased among AKR/J but not SWR/J mice (Figure 8, A, B). Considering the raw data, there was no difference in fat mass of AKR/J mice exposed to SWR/J environment (AKR/J Exp) compared to AKR/J control mice (AKR/J Ctrl) (9.7 ± 2.9 g vs. 11.1 ± 3.6 g) (Figure 9, A). However, correlation between fat mass and body mass indicated a lower fat mass in AKR/J Exp than AKR/J Ctrl mice (Figure 9, B). Cage swap of mice as a moderate strategy to induce microbiota transfer therefore yielded a 19 % reduction in fat mass compared to pHFD control mice (Figure S 1), which was significantly different when fat mass was adjusted for body mass (Figure 9, C).

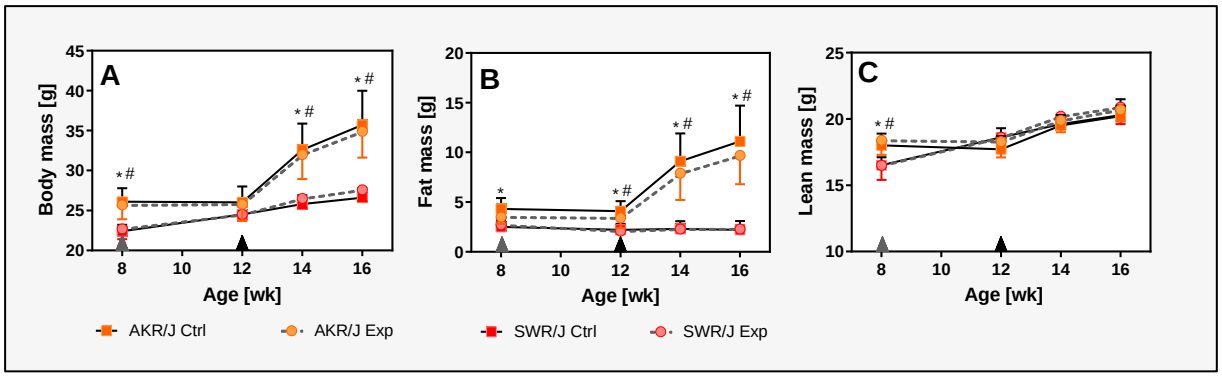

FIGURE 8 BODY MASS (A), FAT MASS (B), LEAN MASS (C) OF AKR/J AND SWR/J MICE DURING CAGE SWAP. Grey and black triangles indicate the onset of CD and pHFD feeding, respectively. AKR/J Ctrl: n = 12; AKR/J Exp: n = 12; SWR/J Ctrl: n = 12; SWR/J Exp: n = 12. Data are shown as means ± sd. Data with different symbols are significantly different. $p < 0.05$: * SWR/J Ctrl vs. AKR/J Ctrl; # SWR/J Exp vs. AKR/J Exp. CD – control diet. Ctrl – control. Exp – exposed. pHFD – palm oil-based high-fat diet.

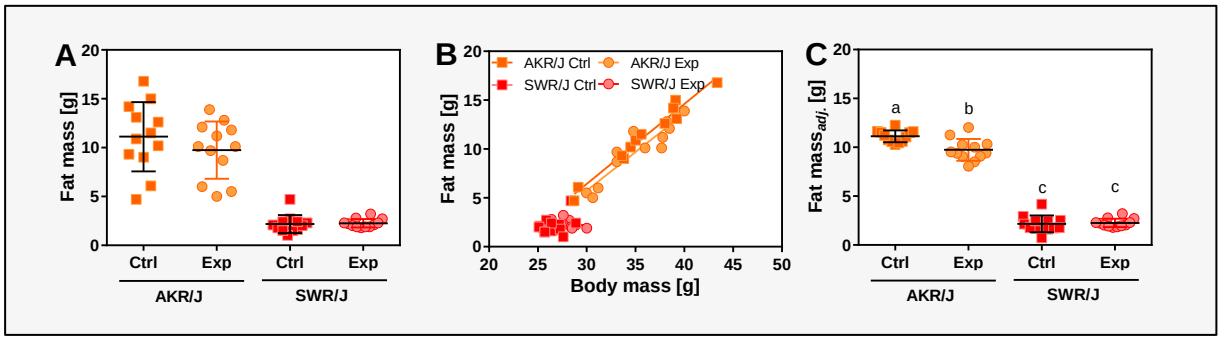

FIGURE 9 FAT MASS OF AKR/J AND SWR/J MICE FOLLOWING CAGE SWAP AND PHFD FEEDING. (A) Total fat mass of AKR/J and SWR/J Ctrl and Exp mice at 16 weeks of age (ns). (B) Linear regression between fat mass and body mass of AKR/J Ctrl ($r^2 = 0.97$; $p < 0.001$), AKR/J Exp ($r^2 = 0.85$; $p < 0.001$), SWR/J Ctrl ($r^2 = 0.16$; p = ns), and SWR/J Exp ($r^2 = 0.01$; p = ns) mice. (C) Fat mass adjusted for body mass according to linear regression formula of each subgroup (Table S 4). AKR/J Ctrl: n = 12; AKR/J Exp: n = 12; SWR/J Ctrl: n = 12; SWR/J Exp: n = 12. Different letters indicate statistical significance ($p < 0.05$). Ctrl – control. Exp – exposed. ns – not significant. pHFD – palm oil-based high-fat diet.

4.1.2 Changes in energy balance are not detectable among AKR/J mice

At the end of the experiment (age: 16 weeks) energy intake, excretion and resorption as well as diverse parameters of energy expenditure were scrutinized to clarify fat mass reduction in AKR/J Exp mice.

Parameters related to energy intake and resorption were similar among groups (Table 13). Taken into account that 1 g of fat corresponds to about 39 kJ of energy (Speakman, 2010), the energy imbalance necessary to generate a difference in body fat mass of 1.4 g within 4 weeks between AKR/J Ctrl and Exp mice is 1.95 kJ * d^{-1}. The energy density for pHFD used in the present study is about 22.7 kJ * g^{-1}. On a daily basis this refers to a difference of 0.09 g of pHFD consumed. The measurement accuracy required to detect such small variations between AKR/J Ctrl and AKR/J Exp mice during the two-day indirect calorimetry is thus questionable. In addition to this, energy expenditure adjusted for body composition did neither explain reduced fat mass of AKR/J Exp nor DIO resistance of SWR/J mice. The only factors which point to a lean phenotype of SWR/J mice were an increased physical activity level (PAL) as well as an enhanced respiratory exchange ratio (RER) toward carbohydrate oxidation at daytime (Table 13).

Hence, end-point recordings of energy balance parameters were not altered in a fashion explaining lean phenotypes.

TABLE 13 ENERGY BALANCE PARAMETERS OF SINGLE-HOUSED AKR/J AND SWR/J MICE FOLLOWING CAGE SWAP AND PHFD FEEDING. Data are shown as means (sd). AKR/J Ctrl: n = 12; AKR/J Exp: n = 12; SWR/J Ctrl: n = 12; SWR/J Exp: n = 12.

	AKR/J		SWR/J		ANOVA		
	Ctrl	Exp	Ctrl	Exp	Strain	Group	Strain x Group
Energy intake [kJ*d^{-1}]	72.4 (11.8)	74.5 (9.5)	75.9 (8.4)	75.3 (9.4)	ns	ns	ns
Gross fecal energy content [kJ*g^{-1}]	14.4 (0.5)	14.4 (0.3)	14.9 (0.8)	14.6 (0.5)	ns	ns	ns
Feces production [g*d^{-1}]	0.38 (0.05)	0.41 (0.06)	0.41 (0.04)	0.38 (0.13)	ns	ns	ns
Energy excretion [kJ*d^{-1}]	5.5 (0.8)	5.9 (0.9)	6.1 (0.9)	6.1 (0.8)	ns	ns	ns
Energy excretion$_{adj.}$ [kJ*d^{-1}]	5.6 (0.8)	5.9 (0.6)	6.1 (0.9)	6.1 (0.7)	ns	ns	ns
Energy resorption [kJ*d^{-1}]	66.4 (11.8)	68.7 (8.7)	69.7 (8.3)	69.2 (9.0)	ns	ns	ns
Efficiency of energy resorption [%]	91.6 (1.6)	92.2 (0.5)	91.9 (1.3)	91.9 (1.0)	ns	ns	ns
HP$_{30°C,pa}$ [mW]	260.5 (26.8)	248.5 (22.9)	197.2 (23.2)	204.9 (22.1)	p < 0.001	ns	ns
HP$_{adj.,30°C,pa}$ [mW]	237.3 (34.4)	229.8 (25.5)	220.2 (18.8)	223.9 (19.0)	ns	ns	ns
HP$_{at\ rest,\ 22°C,\ ad\text{-}lib}$ [mW]	768.9 (60.3)	770.4 (65.3)	641.7 (44.2)	618.8 (54.7)	p < 0.001	ns	ns
HP$_{adj.,at\ rest,\ 22°C,\ ad\text{-}lib}$ [mW]	627.9 (70.8)	625.8 (79.3)	601.0 (38.7)	582.5 (41.1)	p < 0.01	ns	ns
HP$_{22°C,ad\text{-}lib}$ [mW]	778.4 (96.6)	756.0 (103.1)	654.0 (90.2)	644.4 (105.5)	p < 0.001	ns	ns

	AKR/J		SWR/J		ANOVA		
	Ctrl	Exp	Ctrl	Exp	Strain	Group	Strain x Group
$HP_{adj.,22°C,ad\text{-}lib}$ [mW]	735.2 (76.3)	731.0 (85.0)	703.6 (52.8)	689.3 (60.3)	ns	ns	ns
$RER_{day\ time}$	0.80 (0.05)	0.81 (0.04)	0.84 (0.06)	0.85 (0.05)	p < 0.01	ns	ns
$RER_{night\ time}$	0.85 (0.05)	0.87 (0.04)	0.87 (0.05)	0.87 (0.05)	ns	ns	ns
PAL	1.14 (0.02)	1.15 (0.02)	1.20 (0.04)	1.22 (0.05)	p < 0.001	ns	ns

adj. – adjusted. *ad-lib* – *ad-libitum*. Ctrl – control. Exp – exposed. HP – heat production. ns – not significant. *pa* – post-absorptive. PAL – physical activity level ($HP_{22°C}/HP_{at\ rest,\ 22°C}$). pHFD – palm oil-based high-fat diet. RER – respiratory exchange ratio. Energy excretion was adjusted for energy intake and HP was adjusted for body composition. Regression formulas for adjustments can be found in

Table S 4. Energy resorption was not adjusted as there was no dependency on LM and FM (adjusted $r^2 = 0.009$, p = ns).

4.1.3 Cecal cell number and intestinal length are strain-specific and not altered by cage swap

Different fat mass in AKR/J Exp compared to AKR/J Ctrl mice was not fully explained by end-point energy balance measurements highlighting other factors such as the gut to be part of obesity management. Since nutrients are frequently absorbed in the upper and metabolized by bacteria in the lower gut, alterations in intestinal characteristics including the length of gut segments as well as the number of bacterial cells could contribute to obesity development and were, thus, investigated.

Interestingly, the small intestine was 1.6 cm longer and the colon was 0.9 cm shorter in SWR/J compared to AKR/J mice suggesting that there might be differences in the absorption of metabolites (Table 14). Moreover, the cecum was 25.6 mg heavier in mice exposed to cage swap indicating treatment effects potentially related to gut bacteria (Table 14). The number of bacterial cells per gram cecal mass was, however, not influenced by the experimental stimulation, but it was increased in SWR/J compared to AKR/J mice (Δ 4.2 * 10^{10} cells * g cecal content^{-1}) (Table 14).

In summary, intestinal characteristics investigated in the present study were strain-specific. In addition, cage swap led to increased cell counts in lean phenotypes as well as enhanced cecal mass in Exp mice indicating bacterial contribution to body mass development.

TABLE 14 INTESTINAL PARAMETERS OF AKR/J AND SWR/J MICE FOLLOWING CAGE SWAP AND PHFD FEEDING. Data are shown as means (sd). AKR/J Ctrl: n = 12; AKR/J Exp: n = 12; SWR/J Ctrl: n = 12; SWR/J Exp: n = 12.

	AKR/J		SWR/J		ANOVA		
	Ctrl	Exp	Ctrl	Exp	Strain	Group	Strain x Group
Small intestine [cm]	32.4 (1.4)	32.1 (1.7)	34.0 (1.4)	33.6 (1.2)	**p < 0.001**	**ns**	**ns**
Colon [cm]	7.1 (0.6)	7.2 (0.7)	6.3 (0.7)	6.2 (0.6)	**p < 0.001**	**ns**	**ns**
Cecal mass [mg]	156.8 (44.9)	190.9 (31.0)	168.6 (35.2)	185.8 (34.2)	**ns**	**p < 0.05**	**ns**
Cell counts * g cecal content^{-1} [*10^{10}]	10.8 (3.2)	9.0 (3.5)	13.3 (4.5)	14.9 (6.2)	**p < 0.01**	**ns**	**ns**

Ctrl – control. Exp – exposed. ns – not significant.

4.1.4 Fecal bacterial community structure changes occur in AKR/J mice due to cage swap

Despite minor changes in energy balance, there were major differences in intestinal characteristics between mouse strains. However, reduced fat mass in AKR/J Exp mice could neither be convincingly demonstrated by measurements of energy balance nor gut specificities. Microbiota transfer due to cage swap was initially assumed to affect body mass of mice, and might thus explain the lower fat mass of AKR/J Exp mice. In this respect, 16S rRNA of fecal bacteria was sequenced to assess whether bacterial community structure of AKR/J and SWR/J is different and whether cage swap successfully triggered bacterial transfer.

With respect to phylotype richness there were no differences among groups, although SWR/J mice seemed to be characterized by an overall lower diversity (Figure 10, A). α-diversity was, however, significantly altered according to the Shannon index, which takes into account the number and proportional abundance of phylotypes (Figure 10, B). Principal Coordinate Analysis (PCoA) on phylogenetic distances representing β-diversity revealed substantial inter-individual differences

between mice of the same group (Figure 10, C). In this respect, AKR/J Ctrl mice seemed to be phylogentically more distant to the majority of all other mice, especially to SWR/J Ctrl mice indicating differences in β-diversity between these 2 mouse genotypes (Figure 10, D-a). Of highest interest, PCoA further revealed an overlap between SWR/J and AKR/J Exp samples demonstrating that exposure to foreign environment induced microbiota transfer in AKR/J Exp mice (Figure 10, C). Moreover, cage swap led to significant shifts in the AKR/J Exp community structure toward SWR/J microbiota profiles (Figure 10, D-b). Hence, AKR/J Exp mice were prone to SWR/J environment as represented by differences in β-diversity confirming effective treatment at least in AKR/J mice.

Sequences were assigned to account for differences on the level of taxonomy. 1-Way ANOVA indicated differences within the phylum *Firmicutes*, especially the families *Lactobacillaceae*, *Erysipelotrichaceae* and unclassified *Clostridiales* (Figure 11, A-D). To account for interaction effects using 2-Way ANOVA (not shown) revealed increased sequence abundance for unclassified Clostridiales in AKR/J compared to SWR/J mice ($p < 0.05$) (Figure 11, D). Interestingly, levels of *Erysipelotrichaceae* were higher in SWR/J Ctrl compared to AKR/J Ctrl mice ($p < 0.01$), and sequence abundances of *Erysipelotrichaceae* in AKR/J Exp tended to be higher than in AKR/J Ctrl control mice ($p < 0.06$) (Figure 11, B), indicating assimilation of *Erysipelotrichaceae* in AKR/J Exp mice to levels found in SWR/J mice.

Taken together, results originating from high-throughput sequencing supported effective microbiota transfer by cage swap in AKR/J Exp mice. On the other hand, in SWR/J Exp mice there were no major changes in microbiota profile. Hence, cage swap as strategy to trigger microbial transfer was beneficial in obesity prone AKR/J mice. Lowered fat mass of these mice might thus be a consequence of an altered microbe-host crosstalk.

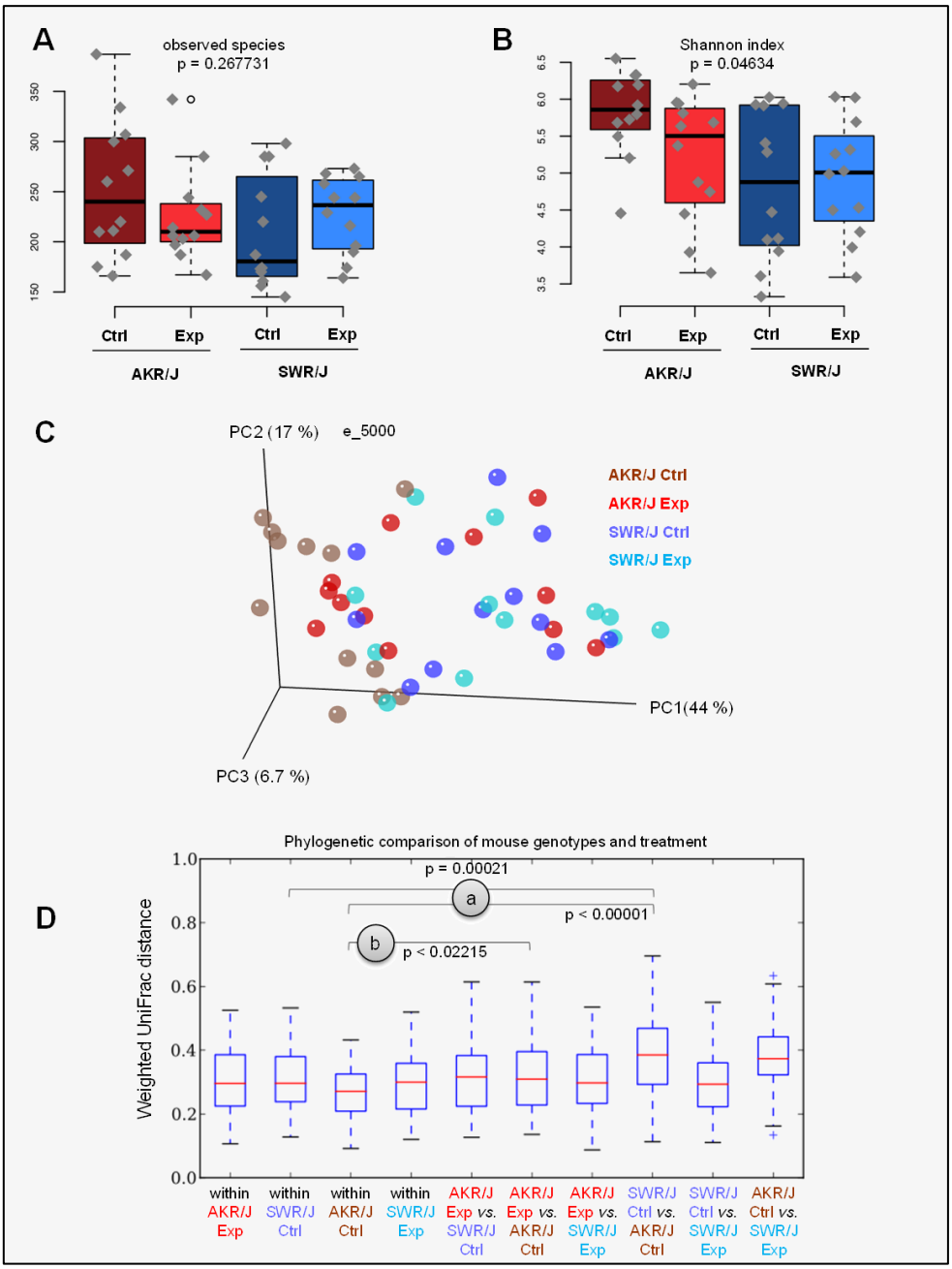

FIGURE 10 *A*- AND *B*-DIVERSITY OF FECAL 16S RRNA OF AKR/J AND SWR/J MICE DUE TO CAGE SWAP AND PHFD FEEDING. (A) Phylotype richness of AKR/J and SWR/J mice representing the number of observed species per sample. Sampling of 5,000 sequences was sufficient to cover diversity, whereas the number of molecular species observed per sample ranged between 170 and 250. The total number of OTUs in the dataset was 1,494. (B) Shannon index of α-diversity taking into account the number and proportional abundance of phylotypes. (C) Principal Coordinate Analysis (PCoA) on phylogenetic distances (weighted UniFrac) at even sampling of 5,000 sequences. Dots are color-coded according to mouse genotype-treatment combinations. (D) Phylogenetic comparison of mouse genotype and treatment. AKR/J Ctrl: n = 12; AKR/J Exp: n = 12; SWR/J Ctrl: n = 12; SWR/J Exp: n = 12. Ctrl – control. Exp – exposed. pHFD – palm oil-based high-fat diet.

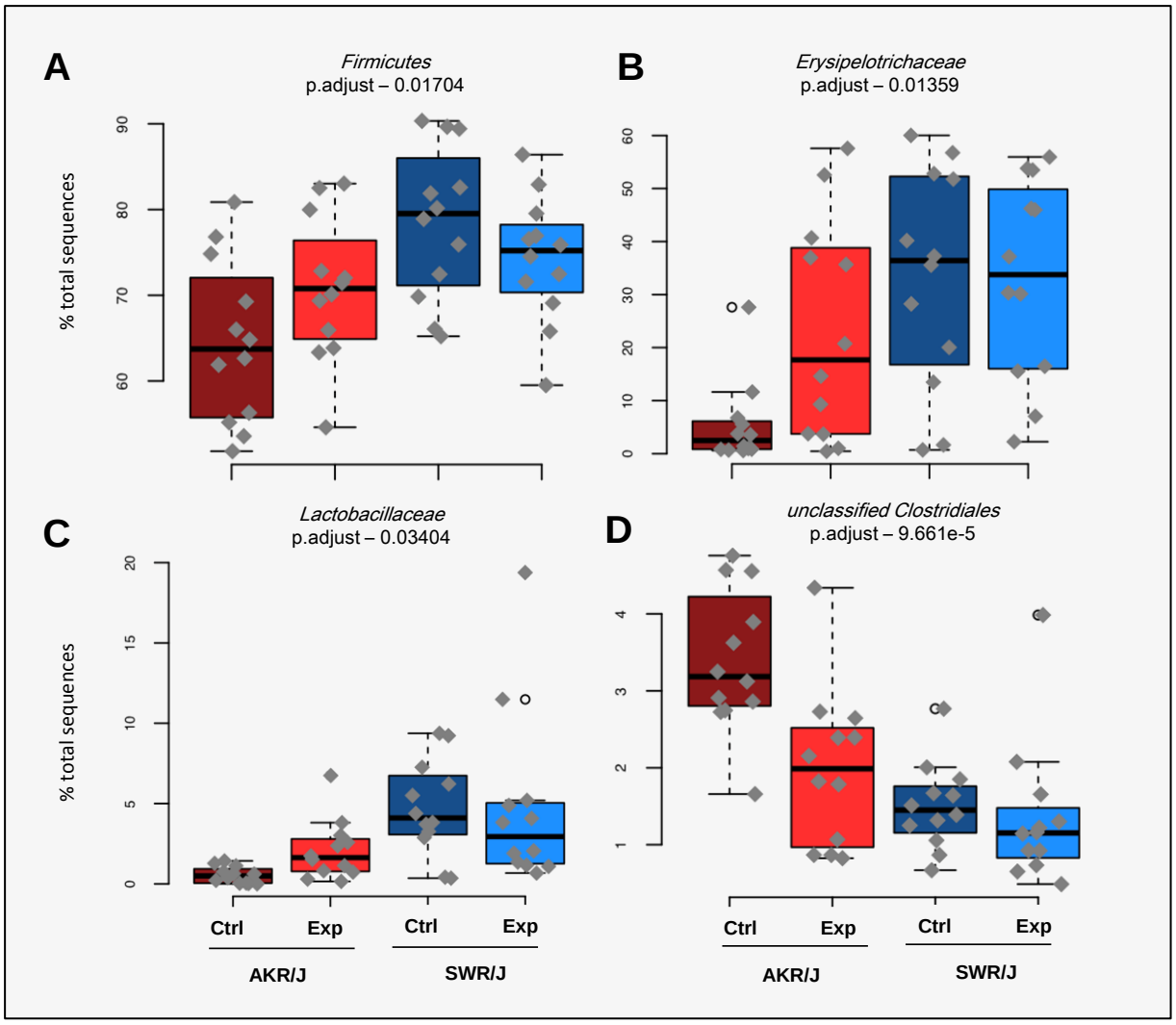

FIGURE 11 TAXONOMIC ASSIGNMENT OF FECAL BACTERIAL SPECIES OF AKR/J AND SWR/J MICE FOLLOWING CAGE SWAP. Sequence abundance of the *Firmicutes* (A) and related families *Lactobacillaceae* (B), *Erysipelotrichaceae* (C), and unclassified *Clostridiales* (D). AKR/J Ctrl: n = 12; AKR/J Exp: n = 12; SWR/J Ctrl: n = 12; SWR/J Exp: n = 12. Ctrl – control. Exp – exposed.

4.2 Fecal transplants of lean SWR/J mice reduce weight gain in AKR/J mice

4.2.1 Fecal microbiota transplantation reduces body and fat mass in AKR/J allogenic recipients

Based on the modest fat mass decline in AKR/J Exp mice (section 4.1), fecal microbiota transplantation was assumed to trigger stronger phenotype effects. In this respect, obesity prone AKR/J and obesity resistant SWR/J mice received fresh fecal homogenates from the other mouse strain (allogenic recipients) immediately before the onset of the 4-week-feeding trial using a palm oil-based high-fat diet (pHFD). Fecal transplantations were performed by oral gavage and rectal inoculation once weekly. Per mouse strain, three control (Ctrl) groups were examined to account for treatment effects using PBS inoculations (PBS Ctrl), fecal homogenates from the same mouse strain (autologous recipients) as well as donor mice assigned as untreated Ctrl.

During pHFD feeding AKR/J allogenic recipients had a lower body as well as fat mass, but a similar lean mass than respective controls (Figure 12, A-C). On the other hand, SWR/J mice did not respond to the treatment as indicated by similar body composition among groups (Figure 12, D-F). 2-Way repeated-measures ANOVA revealed that untreated AKR/J Ctrl mice gained significantly more body mass (Δ 11.5 g) and fat mass (Δ 8.7 g) during 4 weeks of pHFD feeding compared to all other AKR/J groups (body mass/fat mass: PBS Ctrl: Δ 9.4/7.7 g; autologous recipients: Δ 11.1/8.1 g; allogenic recipients: Δ 6.5/4.7 g), indicating that transplantation *per se* affects AKR/J mouse phenotype.

Hence, fecal transplants from obesity resistant SWR/J mice protected obesity prone AKR/J mice from massive weight gain, whilst the lean phenotype of SWR/J mice was not affected by foreign microbial transplants.

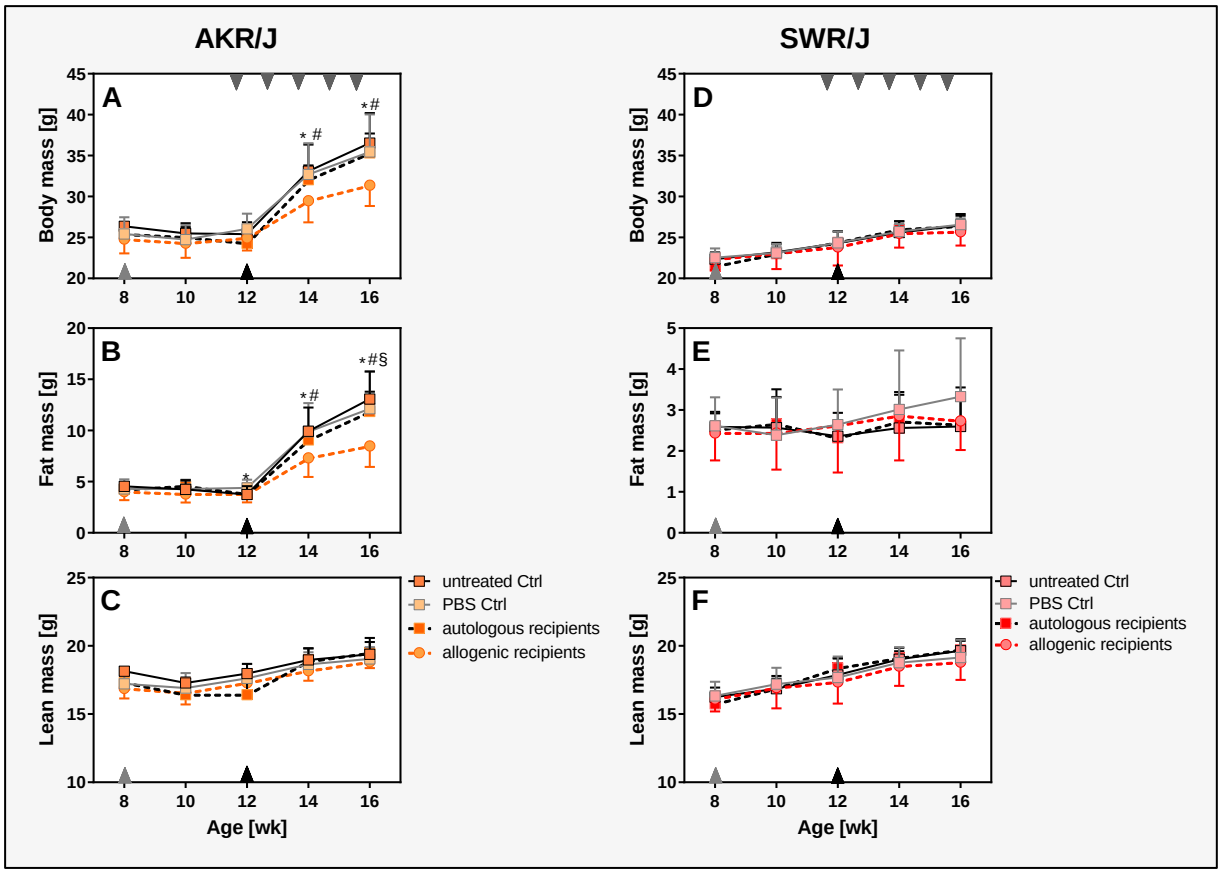

FIGURE 12 BODY MASS (A, D), FAT MASS (B, E) AND LEAN MASS (C, F) OF AKR/J AND SWR/J MICE DURING MICROBIOTA TRANSPLANTATIONS. Grey and black triangles indicate the onset of CD and pHFD feeding, respectively. Grey inverse triangles in (A) and (D) on top of the figure indicate the time points of fecal microbiota transplantation. AKR/J untreated Ctrl n = 10; AKR/J PBS Ctrl: n = 11; AKR/J autologous recipients: n = 5; AKR/J allogenic recipients: n = 10; SWR/J untreated Ctrl n = 10; SWR/J PBS Ctrl: n = 8; SWR/J autologous recipients: n = 5; SWR/J allogenic recipients: n = 8. Data are shown as means ± sd. $p < 0.05$: * untreated Ctrl vs. allogenic recipients; # PBS Ctrl vs. allogenic recipients; § autologous recipients vs. allogenic recipients. CD – control diet. Ctrl – control. pHFD – palm oil-based high-fat diet.

4.2.2 Disturbances in energy balance are not detectable in AKR/J allogenic recipients

AKR/J allogenic recipients gained less body as well as fat mass than respective controls. In this respect, disturbances in energy balance were assumed to explain the lean phenotype of these mice.

Neither energy resorption nor excretion changed in AKR/J allogenic recipients compared to respective controls following data adjustments (Table 15,

Table S 4). However, energy excretion corrected for energy intake was strain-dependent indicating that increased energy loss in SWR/J mice might contribute to DIO resistance. Diverse parameters of energy expenditure such as basal metabolic rate, resting energy expenditure and daily energy expenditure, which are represented as heat production, were calculated and adjusted for differences in body composition (Table 15). Following adjustments, resting energy expenditure ($HP_{adj., at\ rest, 22°C, ad-lib}$) and daily energy expenditure ($HP_{adj., 22°C, ad-lib}$) were similar among groups. Basal metabolism ($HP_{adj., 30°C, pa}$) appeared to be slightly increased in allogenic recipients compared to PBS Ctrl mice (Δ 20.3 mW) (Table 15), indicating that basal metabolism might influence body mass development at least in AKR/J mice. Respiratory exchange ratio (RER) and physical activity level (PAL) were higher in SWR/J than AKR/J mice highlighting increased carbohydrate oxidation and providing an explanation for the lean phenotype of SWR/J mice. Moreover, nocturnal RER levels of autologous and allogenic recipients were increased compared to untreated Ctrl (Table 15), which might suggest an impact of transplanted bacteria on substrate oxidation in states when mice are active.

Overall, despite minor changes in basal metabolic rate, sensitivity of end-point measurements might be too small to unravel disturbances in energy balance that explain the lean phenotype of AKR/J allogenic recipients.

TABLE 15 ENERGY BALANCE PARAMETERS OF SINGLE-HOUSED, PHFD-FED AKR/J AND SWR/J MICE FOLLOWING MICROBIOTA TRANSPLANTATIONS. Data are shown as means (sd). AKR/J untreated Ctrl: n = 6; AKR/J PBS Ctrl: n = 10; AKR/J autologous recipients: n = 5; AKR/J allogenic recipients: n = 9; SWR/J untreated Ctrl: n = 7; SWR/J PBS Ctrl: n = 6; SWR/J autologous recipients: n = 5; SWR/J allogenic recipients: n = 4. Different letters indicate significant interactions ($p < 0.05$).

	AKR/J				SWR/J				ANOVA			Post-hoc testing
	untreated Ctrl	PBS Ctrl	autologous recipients	allogenic recipients	untreated Ctrl	PBS Ctrl	autologous recipients	allogenic recipients	Strain	Group	Strain x Group	Group effects
Energy intake [kJ*d^{-1}]	63.2 (12.6)	43.3 (13.9)	48.8 (7.6)	45.2 (14.3)	71.2 (19.4)	59.2 (7.2)	60.5 (13.5)	61.4 (6.6)	**p < 0.01**	**p < 0.05**	**ns**	untreated Ctrl/PBS Ctrl
Gross fecal energy content [kJ*g^{-1}]	14.6 (0.3)	14.0 (0.4)	14.2 (0.1)	14.8 (1.2)	14.6 (0.4)	14.4 (0.3)	14.9 (0.7)	14.6 (0.4)	**p < 0.05**	**p < 0.05**	**ns**	
Feces production [g*d^{-1}]	0.35 (0.04)	0.32 (0.04)	0.38 (0.05)	0.35 (0.03)	0.44 (0.04)	0.39 (0.03)	0.40 (0.04)	0.40 (0.01)	**p < 0.001**	**p < 0.01**	**ns**	untreated Ctrl/PBS Ctrl
Energy excretion [kJ*d^{-1}]	5.2 (0.5)	4.5 (0.6)	5.4 (0.6)	5.1 (0.7)	6.5 (0.8)	5.5 (0.5)	6.0 (0.8)	5.3 (2.0)	**p < 0.001**	**p < 0.01**	**ns**	untreated Ctrl/PBS Ctrl; PBS Ctrl/autologous recipients
Energy excretion$_{adj.}$ [kJ*d^{-1}]	5.1 (0.5)	4.9 (0.6)	5.5 (0.6)	5.3 (0.7)	5.8 (0.5)	5.4 (0.6)	5.7 (0.7)	5.5 (0.3)	**p < 0.05**	**ns**	**ns**	
Energy resorption [kJ*d^{-1}]	55.8 (14.8)	38.8 (13.7)	43.4 (7.5)	40.1 (13.9)	65.1 (20.6)	53.6 (7.3)	54.5 (13.2)	55.6 (6.7)	**p < 0.01**	**p < 0.05**	**ns**	untreated Ctrl/PBS Ctrl
Energy resorption$_{adj.}$ [kJ*d^{-1}]	61.6 (16.1)	44.8 (13.8)	46.5 (9.8)	42.8 (13.6)	57.6 (18.5)	49.5 (12.4)	47.4 (13.7)	49.7 (6.3)	**ns**	**ns**	**ns**	

	AKR/J				SWR/J				ANOVA			Post-hoc testing
	untreated Ctrl	PBS Ctrl	autologous recipients	allogenic recipients	untreated Ctrl	PBS Ctrl	autologous recipients	allogenic recipients	Strain	Group	Strain x Group	Group effects
Efficiency of energy resorption [%]	91.1 (1.6)	89.0 (2.9)	88.8 (1.9)	87.2 (6.1)	90.4 (2.3)	90.4 (1.6)	89.9 (1.8)	90.5 (1.1)	ns	ns	ns	
$HP_{30°C,pa}$ [mW]	278.5 (13.3)	263.5 (16.0)	267.5 (22.7)	258.0 (15.7)	223.0 (17.1)	210.1 (11.7)	218.1 (9.8)	233.8 (30.7)	p < 0.001	ns	ns	
$HP_{adj.,30°C,pa}$ [mW]	244.0 (15.7)	241.8 (11.8)	247.4 (17.8)	254.9 (10.4)	243.1 (16.3)	229.0 (10.7)	238.3 (7.2)	256.5 (29.3)	ns	p < 0.01	ns	PBS Ctrl/allogenic recipients
$HP_{at\ rest,\ 22°C,\ ad\text{-}lib}$ [mW]	645.0 (40.5)	646.5 (25.8)	659.5 (38.7)	627.4 (26.3)	567.8 (69.0)	548.4 (26.8)	557.4 (32.7)	556.9 (44.6)	p < 0.001	ns	ns	
$HP_{adj.,at\ rest,\ 22°C,\ ad\text{-}lib}$ [mW]	579.0 (38.3)	608.2 (28.1)	621.9 (30.0)	624.8 (13.9)	601.1 (64.9)	583.3 (24.5)	590.5 (37.0)	600.7 (35.3)	ns	ns	ns	
$HP_{22°C,ad\text{-}lib}$ [mW]	753.7 (16.1)	723.8 (43.3)	725.2 (32.5)	704.6 (34.8)	683.2 (50.1)	653.8 (29.3)	707.4 (47.7)	667.4 (46.4)	p < 0.001	ns	ns	
$HP_{adj.,22°C,ad\text{-}lib}$ [mW]	753.7 (17.7)	723.8 (43.4)	725.2 (36.4)	704.6 (36.7)	683.2 (54.1)	653.8 (31.7)	707.4 (53.3)	667.4 (49.6)	ns	ns	ns	
$RER_{day\ time}$	0.76 (0.01)	0.76 (0.01)	0.76 (0.01)	0.76 (0.01)	0.81 (0.02)	0.80 (0.01)	0.79 (0.01)	0.79 (0.01)	p < 0.001	ns	ns	

	AKR/J				SWR/J				ANOVA			Post-hoc testing
	untreated Ctrl	PBS Ctrl	autologous recipients	allogenic recipients	untreated Ctrl	PBS Ctrl	autologous recipients	allogenic recipients	Strain	Group	Strain x Group	Group effects
$RER_{night\ time}$	0.82 (0.01)	0.83 (0.02)	0.84 (0.01)	0.84 (0.01)	0.84 (0.01)	0.85 (0.01)	0.85 (0.01)	0.84 (0.01)	**p < 0.001**	**p < 0.01**	**ns**	untreated Ctrl/autologous recipients; untreated Ctrl/allogenic recipients
PAL	1.17 (0.09)^{ab}	1.12 (0.03)^{a}	1.10 (0.03)^{a}	1.12 (0.03)^{a}	1.21 (0.08)^{b}	1.19 (0.05)^{b}	1.27 (0.08)^{b}	1.20 (0.05)^{b}	**p < 0.001**	**ns**	**p < 0.05**	

adj. – adjusted. *ad-lib* – *ad-libitum*. Ctrl – control. HP – heat production. ns – not significant. *pa* – post-absorptive. PAL – physical activity level ($HP_{22°C}/HP_{at\ rest,\ 22°C}$). pHFD – palm oil-based high-fat diet. RER – respiratory exchange ratio. Energy excretion was adjusted for energy intake. Energy resorption and HP were adjusted for body composition. Regression formulas for adjustments can be found in Table S 4.

.

.

4.2.3 Total fat mass of AKR/J allogenic recipients is characterized by smaller fat depots

Fecal transplants from obesity resistant SWR/J mice protected AKR/J mice from massive weight gain, which was attributed to reduced fat but not lean mass. Since energy balance recordings did not detect major differences explaining the lean phenotype, tissue dissections were performed to account for differences in metabolically active organs.

AKR/J mice revealed heavier liver (Δ 0.35 g), epididymal white adipose tissue (eWAT) (Δ 1,257 mg) and inguinal white adipose tissue (iWAT) depots (Δ 408 mg). Additionally, they had increased cecum weights (Δ 14.7 mg), a shorter small intestine (Δ 2.2 cm), and a longer colon (Δ 1.2 cm) compared to SWR/J mice indicating strain-specific differences in endogenous metabolism as well as in gut physiology (Table 16). Moreover, liver (Δ 0.17 g), eWAT (Δ 240 mg) as well as iWAT (Δ 169 mg) weights were lower for allogenic compared to autologous recipients or PBS Ctrl, respectively (Table 16), which corresponds to the reduced total fat mass in AKR/J allogenic recipient mice as measured by magnetic resonance imaging.

Taken together, organ dissections hint to strain-specific endogenous metabolism including the gut, which might contribute to obesity resistance in SWR/J but not AKR/J mice. Moreover, reduced total fat mass of AKR/J allogenic recipient mice as measured by NMR could be confirmed by smaller fat mass depots indicating alterations in lipid metabolism induced by SWR/J fecal transplants.

TABLE 16 ORGAN MASSES OF PHFD-FED AKR/J AND SWR/J MICE FOLLOWING MICROBIOTA TRANSPLANTATIONS. Data are shown as means (sd). AKR/J PBS Ctrl: n = 11; AKR/J autologous recipients: n = 5; AKR/J allogenic recipients: n = 10; SWR/J PBS Ctrl: n = 7; SWR/J autologous recipients: n = 5; SWR/J allogenic recipients: n = 8.

	AKR/J			SWR/J			ANOVA			Post-hoc testing
	PBS Ctrl	autologous recipients	allogenic recipients	PBS Ctrl	autologous recipients	allogenic recipients	Strain	Group	Strain x Group	Group effects
Liver [g]	1.71 (0.20)	1.80 (0.07)	1.56 (0.14)	1.36 (0.12)	1.43 (0.16)	1.33 (0.14)	**p < 0.001**	**p < 0.05**	**ns**	autologous recipients/allogenic recipients
eWAT [mg]	1,684.5 (443.5)	1,816.9 (258.5)	1,298.2 (357.4)	369.2 (169.5)	253.2 (73.9)	276.2 (123.2)	**p < 0.001**	**p < 0.05**	**ns**	PBS Ctrl/allogenic recipients
iWAT [mg]	734.4 (247.4)	811.6 (170.0)	524.3 (147.9)	357.2 (163.1)	234.6 (42.8)	238.8 (71.3)	**p < 0.001**	**p < 0.01**	**ns**	PBS Ctrl/allogenic recipients
Small intestine [cm]	31.5 (2.3)	32.3 (1.9)	29.9 (3.1)	33.4 (1.0)	33.2 (0.7)	33.7 (2.2)	**p < 0.01**	**ns**	**ns**	
Colon [cm]	7.4 (0.6)	6.8 (0.4)	6.9 (0.7)	5.9 (0.4)	5.5 (0.2)	6.0 (0.4)	**p < 0.001**	**ns**	**ns**	
Cecum [mg]	157.7 (26.4)	145.0 (23.0)	138.3 (31.5)	143.2 (38.7)	114.6 (19.6)	128.3 (19.3)	**p < 0.05**	**ns**	**ns**	

eWAT – epididymal white adipose tissue. iWAT – inguinal white adipose tissue. ns – not significant. pHFD – palm oil-based high-fat diet.

4.2.4 Lean phenotype of AKR/J allogenic recipients is not linked to specific bacterial transfer

16S rRNA amplicons from feces of AKR/J and SWR/J mice were sequenced to validate whether the treatment strategy of microbial transplantation was effective.

There were no major changes in the number of dominant molecular species due to mouse genotype or bacterial transplantation (Figure 13, A). Regarding *β*-diversity, samples clustered according to the mouse genotype but seemed to be independent of treatment (Figure 13, B). AKR/J mice that received the SWR/J transplants were, however, less distant to SWR/J mice, although, there were strong inter-individual differences (Figure 13, B). Moreover, taxonomic assignment revealed significant inter-strain differences in the families *Bacteroidaceae*, a representative of the phylum *Bacteroidetes*, as well as *Lactobacillaceae* and *Clostridiales*, both belonging to the phylum *Firmicutes* (Figure 14, A-C). In that matter, *Bacteroidaceae* in contrast to *Lactobacillaceae* and *Clostridiales* dominated in feces of AKR/J compared to SWR/J mice (Figure 14, A-C). Since there seemed to be no consistent effects observable in feces, cecal contents were also analyzed. *β*-diversity analysis thereby indicated the same clusters as for fecal samples (Figure 15), highlighting a genotype but no treatment effect. Both, allogenic recipients of AKR/J and SWR/J mice, however, tended to be less distant to each other concerning inter-genotype grouping effects (Figure 15).

In summary, the lean phenotype of AKR/J mice could neither be related to distinct differences in energy balance nor linked to transfer of specific bacteria from SWR/J donor mice suggesting that other compounds of stool homogenates are involved in mediating phenotype effects.

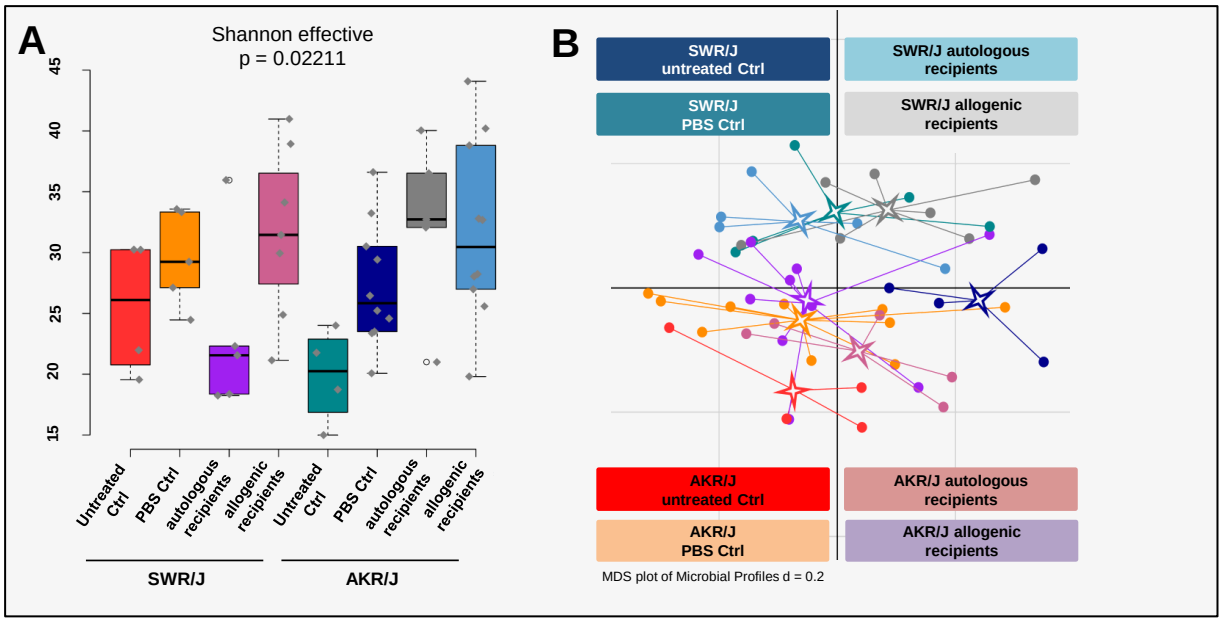

FIGURE 13 *A*- AND *B*-DIVERSITY OF FECAL 16S RRNA OF PHFD-FED AKR/J AND SWR/J MICE FOLLOWING MICROBIOTA TRANSPLANTATION. (A) Shannon effective counts of species. Sampling of 5,960 sequences was sufficient to cover diversity, whereas the number of molecular species observed per sample ranged between 53 and 87. The total number of OTUs in the dataset was 104. (B) Principal Coordinate Analysis (PCoA) on phylogenetic distances (weighted UniFrac) at even sampling of 5,960 sequences. Dots are color-coded according to mouse genotype-treatment combinations. AKR/J untreated Ctrl: n = 4; AKR/J PBS Ctrl: n = 10; AKR/J autologous recipients: n = 5; AKR/J allogenic recipients: n = 10; SWR/J untreated Ctrl: n = 4; SWR/J PBS Ctrl: n = 5; SWR/J autologous recipients: n = 5; SWR/J allogenic recipients: n = 7. Ctrl – control. pHFD – palm oil-based high-fat diet.

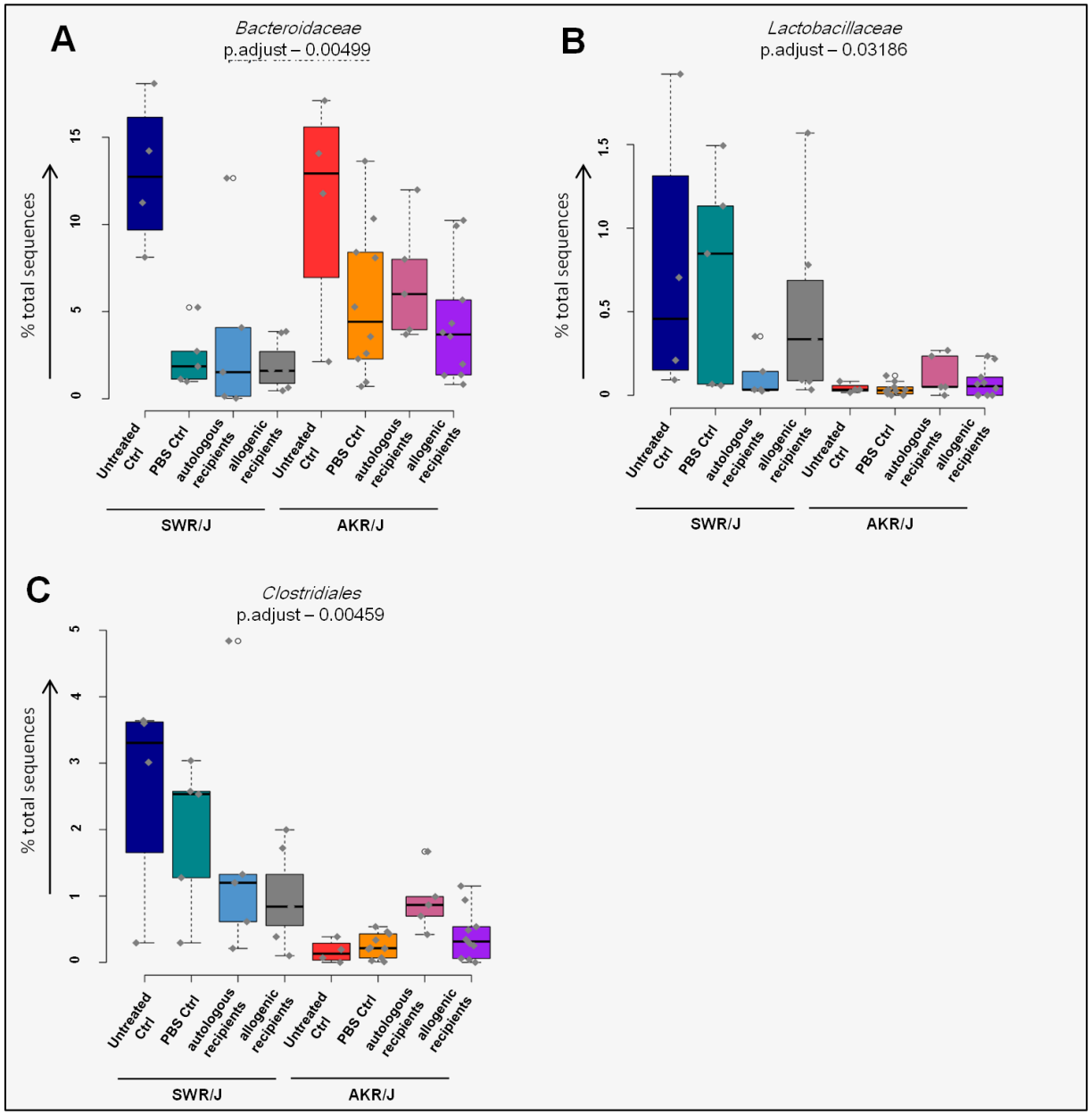

FIGURE 14 TAXONOMIC ASSIGNMENT OF FECAL BACTERIAL SPECIES OF PHFD-FED AKR/J AND SWR/J MICE FOLLOWING MICROBIOTA TRANSPLANTATIONS. (A) Sequence abundance of the family *Bacteroidaceae* belonging to the phylum *Bacteroidetes*. (B) Sequence abundance of the family *Lactobacillaceae* and (C) *Clostridiales*, both belonging to the phylum *Firmicutes*. AKR/J untreated Ctrl: n = 4; AKR/J PBS Ctrl: n = 10; AKR/J autologous recipients: n = 5; AKR/J allogenic recipients: n = 10; SWR/J untreated Ctrl: n = 4; SWR/J PBS Ctrl: n = 5; SWR/J autologous recipients: n = 5; SWR/J allogenic recipients: n = 7. Ctrl – control. pHFD – palm oil-based high-fat diet.

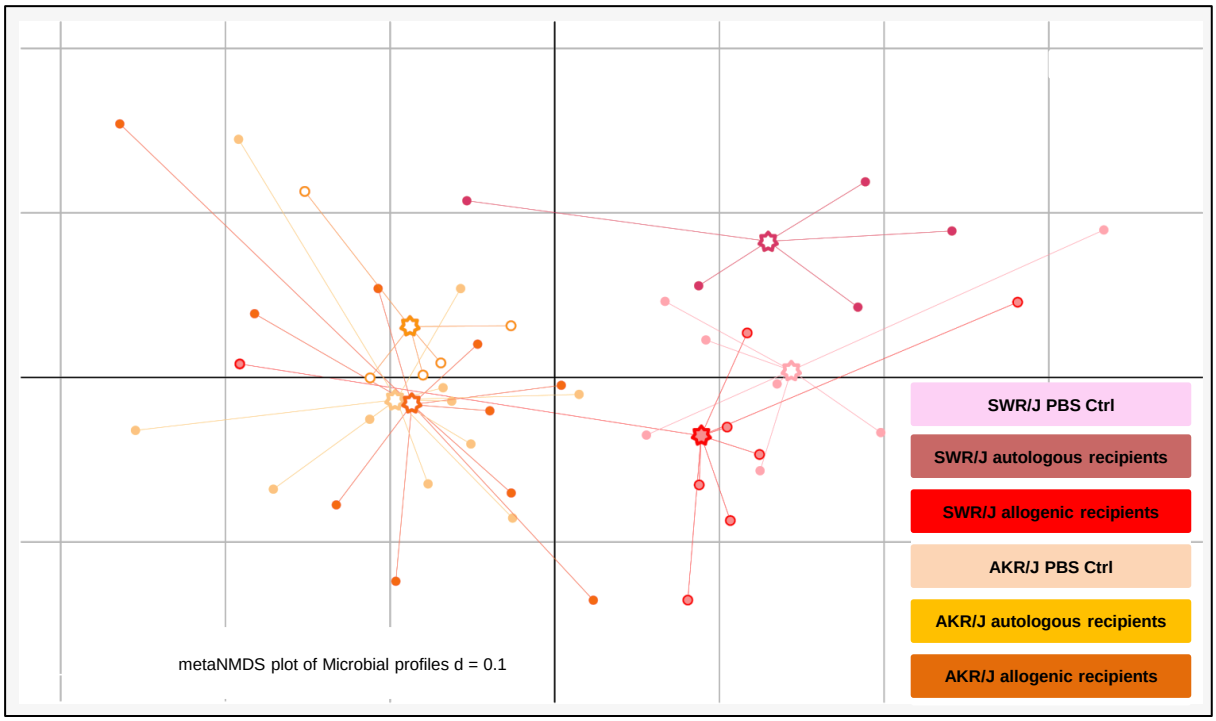

FIGURE 15 *β*-DIVERSITY OF CECAL 16S RRNA OF PHFD-FED AKR/J AND SWR/J MICE FOLLOWING MICROBIOTA TRANSPLANTATIONS. Principal Coordinate Analysis (PCoA) on phylogenetic distances (weighted UniFrac) at even sampling of 13,000 sequences. Dots are color-coded according to mouse genotype-treatment combinations. AKR/J PBS Ctrl: n = 11; AKR/J autologous recipients: n = 5; AKR/J allogenic recipients: n = 10; SWR/J PBS Ctrl: n = 7; SWR/J autologous recipients: n = 5; SWR/J allogenic recipients: n = 8. Ctrl – control. pHFD – palm oil-based high-fat diet.

4.3 Cohousing of obese and lean Mc4r^{W16X} mice does not affect phenotype

Cohousing of genetically obese knockin (ki) with lean wildtype (wt) mice was chosen to evaluate diet-independent and environmental effects on phenotypic outcomes. In this respect, Mc4r^{W16X}/C57BL/6J ki and wt mice were housed in groups with a 1:3 (ki 1+3) or 3:1 (wt 1+3) ratio of ki:wt to ensure the dominance of one respective genotype. Thus, coprophagy was assumed to mediate microbiota transfer and body mass assimilation toward the dominating genotype. Mice were cohoused from weaning until 13 weeks of age and were fed a standard chow diet throughout the experiment. Control (Ctrl) mice belonging to each respective genotype were housed in groups of 4 mice per cage.

After 2 weeks of cohousing ki mice already gained more body as well as fat mass than wildtype mice, whereas lean mass was not different among groups (Figure 16, A-F). However, phenotypes were not

affected due to cohousing. In this respect, energy balance was not influenced by the treatment strategy, and genotype effects also vanished after adjustment for body composition (Table 17, Table S 4). Solely, energy intake and concomitantly energy excretion were enhanced in ki mice compared to wt mice leading to a net increase in energy resorption which explains the obese phenotype.

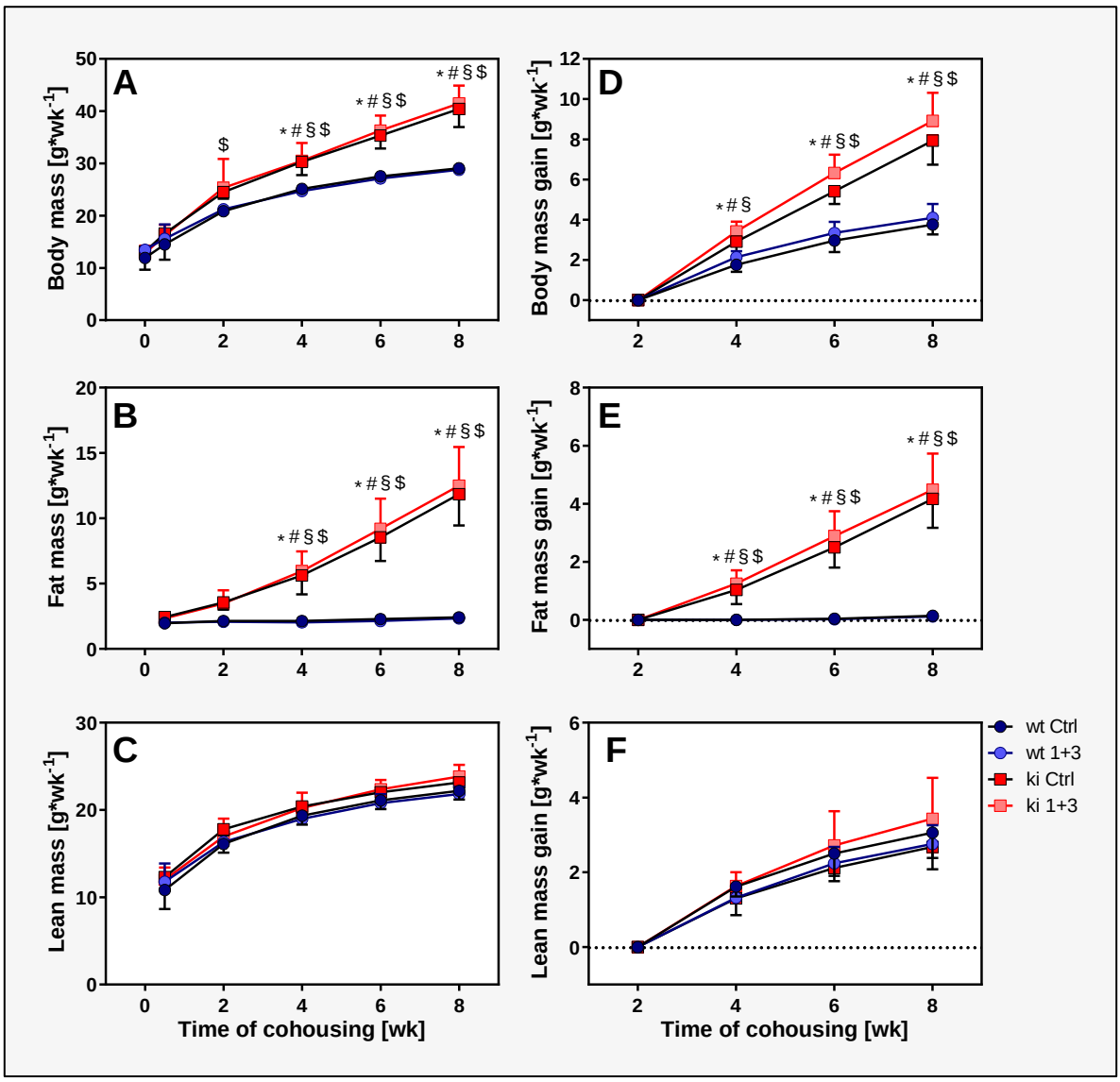

FIGURE 16 BODY MASS (A), FAT MASS (B) AND LEAN MASS (C) AS WELL AS GAIN OF BODY MASS (D), FAT MASS (E) AND LEAN MASS (F) OF CHOW-FED MC4R^{W16X} KI AND WT MICE DURING COHOUSING. wt Ctrl: n = 6; wt 1+3: n = 5; ki Ctrl: n = 6; ki 1+3 : n = 6. Data are shown as means ± sd. $p < 0.05$: * wt Ctrl vs. ki 1+3; # ki Ctrl vs. wt 1+3; § wt 1+3 vs. ki 1+3; $ wt Ctrl vs. ki Ctrl. Ctrl – control. ki – knockin. wt – wildtype.

TABLE 17 ENERGY BALANCE PARAMETERS OF SINGLE-HOUSED, CHOW-FED MC4R^{W16X} WILDTYPE (WT) AND KNOCKIN (KI) MICE FOLLOWING COHOUSING (1+3). Data are shown as means (sd). wt Ctrl: n = 4; wt 1+3: n = 4; ki wt: n = 6; ki 1+3: n = 6.

	wt		ki		ANOVA		
	Ctrl	1+3	Ctrl	1+3	Genotype	Group	Genotype x Group
Energy intake [kJ*d^{-1}]	66.2 (12.0)	54.5 (10.3)	72.3 (9.5)	75.5 (9.0)	**p < 0.01**	ns	ns
Gross fecal energy content [kJ*g^{-1}]	15.6 (0.1)	15.7 (0.2)	15.5 (0.3)	15.4 (0.2)	ns	ns	ns
Feces production [g*d^{-1}]	0.81 (0.03)	0.73 (0.06)	0.92 (0.17)	0.97 (0.12)	**p < 0.01**	ns	ns
Energy excretion [kJ*d^{-1}]	12.6 (0.5)	11.5 (1.0)	14.3 (2.6)	14.9 (1.8)	**p < 0.01**	ns	ns
Energy resorption [kJ*d^{-1}]	53.7 (11.7)	43.0 (10.0)	58.8 (9.1)	61.3 (8.7)	**p < 0.05**	ns	ns
Efficiency of energy resorption [%]	80.6 (3.4)	78.4 (4.3)	81.1 (2.3)	81.0 (2.3)	ns	ns	ns
$HP_{30°C,pa}$ [mW]	217.1 (37.6)	208.7 (18.2)	270.5 (28.9)	250.5 (22.2)	**p < 0.01**	ns	ns
$HP_{adj.,30°C,pa}$ [mW]	237.8 (24.6)	235.4 (16.8)	263.0 (23.7)	234.2 (29.0)	ns	ns	ns
$HP_{at\ rest,\ 22°C,\ ad\text{-}lib}$ [mW]	469.7 (48.5)	436.6 (30.0)	545.1 (59.7)	528.8 (48.4)	**p < 0.01**	ns	ns
$HP_{adj.,at\ rest,\ 22°C,\ ad\text{-}lib}$ [mW]	504.9 (32.3)	477.1 (18.2)	527.5 (58.0)	496.0 (61.1)	ns	ns	ns
$HP_{22°C,ad\text{-}lib}$ [mW]	581.6 (46.0)	531.7 (42.8)	661.9 (52.3)	690.1 (47.1)	**p < 0.001**	ns	ns
$HP_{adj.,22°C,ad\text{-}lib,}$ [mW]	642.9 (24.3)	602.3 (31.4)	631.1 (42.3)	632.9 (27.9)	ns	ns	ns
$RER_{day\ time}$	0.87 (0.05)	0.87 (0.06)	0.88 (0.07)	0.87 (0.07)	ns	ns	ns
$RER_{night\ time}$	0.96 (0.03)	0.96 (0.05)	0.95 (0.08)	0.97 (0.08)	ns	ns	ns
PAL	1.24 (0.04)	1.22 (0.03)	1.22 (0.07)	1.31 (0.14)	ns	ns	ns

adj. – adjusted. *ad-lib* – *ad-libitum*. Ctrl – control. HP – heat production. ki – knockin. ns – not significant. *pa* – post-absorptive. PAL – physical activity level ($HP_{22°C}$/$HP_{at\ rest,\ 22°C}$). RER – respiratory exchange ratio. wt – wildtype. HP was adjusted for body composition. Regression formulas can be found in

Table S 4. Energy resorption and energy excretion were not adjusted as there was no dependency on LM and FM (adjusted r^2 = 0.13, p = ns) or energy intake (adjusted r^2 = 0.05, p = ns), respectively.

Heavier organs such as heart, kidney, liver, iBAT and eWAT were attributable to the obese phenotype of ki mice (Table 18). Neither the length of the small intestine nor the colon nor the cecal mass nor the bacterial counts in the cecum were affected due to cohousing or genotype (Table 18).

TABLE 18 ORGAN MASSES OF CHOW-FED COHOUSED (1+3) AND CONTROL (CTRL) MC4R^{W16X} WILDTYPE (WT) AND KNOCKIN (KI) MICE. Data are shown as means (sd). wt Ctrl: n = 6; wt 1+3: n = 6; ki wt: n = 6; ki 1+3: n = 6.

	wt		ki		ANOVA		
	Ctrl	1+3	Ctrl	1+3	Genotype	Group	Genotype x Group
Body length [cm]	9.9 (0.4)	10.1 (0.1)	10.3 (0.3)	10.4 (0.4)	**p < 0.05**	**ns**	**ns**
Small intestine [cm]	32.7 (2.6)	34.3 (2.0)	35.3 (2.7)	35.3 (2.9)	**ns**	**ns**	**ns**
Colon [cm]	7.0 (0.6)	6.8 (0.9)	7.4 (0.6)	7.4 (1.0)	**ns**	**ns**	**ns**
Cecum [mg]	453.0 (27.3)	493.8 (113.0)	499.7 (108.3)	540.3 (115.9)	**ns**	**ns**	**ns**
Liver [g]	1.46 (0.22)	1.48 (0.12)	2.03 (0.25)	2.19 (0.38)	**p < 0.001**	**ns**	**ns**
eWAT [mg]	275.5 (8.0)	288.3 (71.5)	1,594.2 (511.1)	1,657.0 (533.3)	**p < 0.001**	**ns**	**ns**
Heart [mg]	147.8 (15.5)	139.9 (9.0)	168.6 (18.6)	175.8 (13.3)	**p < 0.001**	**ns**	**ns**
Kidney [mg]	387.9 (9.5)	360.9 (29.4)	416.6 (37.8)	425.8 (42.8)	**p < 0.01**	**ns**	**ns**
iBAT [mg]	64.7 (13.4)	60.2 (17.7)	186.7 (43.8)	180.5 (45.3)	**p < 0.001**	**ns**	**ns**
Cell counts * g cecal content^{-1} [*10^{10}]	19.5 (3.2)	18.4 (7.3)	21.9 (5.7)	19.4 (4.8)	**ns**	**ns**	**ns**

Ctrl – control. eWAT – epididymal white adipose tissue. iBAT – interscapular brown adipose tissue. ki – knockin. ns – not significant. wt – wildtype.

Overall, the basic hypothesis on phenotypic assimilation of cohoused genotypes could be discarded. Moreover, genotypic differences in energy balance parameters disappeared after accounting for confounders. However, defects in satiety signaling of Mc4r^{W16X} ki mice persisted as indicated by increased energy intake. Microbiota effects that could have happened due to cohousing might thus be hidden by the strong genetic background of these mice.

4.4 Obesity resistance of germfree mice is dependent on the dietary fat source

4.4.1 Lard-fed germfree mice are resistant to diet-induced obesity

Diet-induced obesity (DIO) resistance of germfree (GF) mice that happens in the presence of a Western-style diet draws attention to the need to extensively investigate the underlying mechanisms and reasons responsible for this phenotype (Backhed et al., 2007; Fleissner et al., 2010; Rabot et al., 2010). Albeit dietary variations in sugar and fat provoked body mass gain in these mice (Fleissner et al., 2010), the responsible compounds leading to inconsistencies in body mass development are unexplored so far. To evaluate the prevalent question on whether dietary composition triggers DIO resistance of GF mice, 12-week-old male GF and conventional (CV) C57BL/6N mice were fed either a high-fat diet derived from lard (lHFD) or palm oil (pHFD) for 4 weeks, respectively.

During the first 3 weeks of HFD feeding, CV mice showed a massive body mass gain irrespective of the dietary fat quality (Figure 17, A). In GF mice, however, obesity was observed only in mice exposed to pHFD, but not lHFD. Hence, lHFD-fed GF mice resembled the lean phenotype of both CV and GF mice on control diet (CD) (Figure 17, A). Consequently, at the end of the 4-week-feeding trial lHFD-fed GF mice had a lower body mass compared to other HFD-fed groups, which was attributable to a low fat mass, while lean mass was similar among groups (Figure 17, B-D). Interestingly, CD-fed GF mice were heavier than CV counterparts, albeit this was not in line with differences in fat mass and might therefore be explained by cecal enlargement (GF CD: 3,163 ± 344 mg; CV CD: 225 ± 42 mg). Overall, the lean phenotype of GF mice is linked to lHFD but not pHFD feeding.

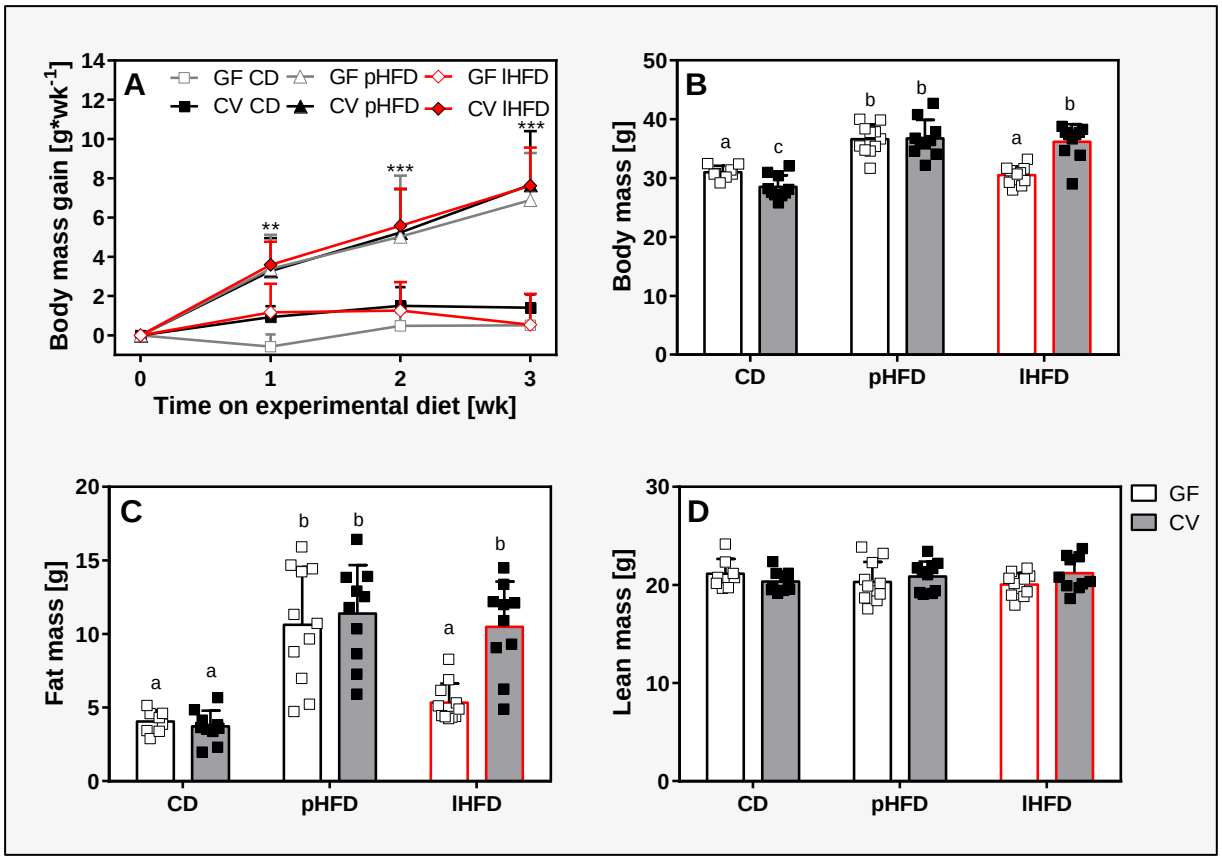

FIGURE 17 BODY MASS GAIN AND BODY COMPOSITION OF CD-, PHFD- AND LHFD-FED GF AND CV MICE. (A) Body mass gain during the first 3 weeks of experimental diet. **p<0.01 and ***p<0.001 for GF lHFD, GF CD, and CV CD relative to GF pHFD, CV pHFD, and CV lHFD. (B) Body mass, (C) fat mass and (D) lean mass at the end of the 4-week-feeding trial. Data with different superscript letters indicate significance ($p < 0.05$). CV CD: n = 10; CV pHFD: n = 10; CV lHFD: n = 10; GF CD: n = 8; GF pHFD: n = 11; GF lHFD: n = 11. Data are shown as means + sd including dots representing single values. CD – control diet. CV – conventional. GF – germfree. lHFD/pHFD – lard-/palm oil-based high-fat diet.

4.4.2 Basal metabolism and respiratory exchange ratio are increased in lard-fed germfree mice

Altered energy balance including energy expenditure and excretion was hypothesized for the lean phenotype of lHFD-fed GF mice. Energy expenditure was highly influenced by body composition (Table S 4). ANCOVA was thus applied to detect differences independent of lean mass and fat mass. Following adjustments, daily energy expenditure ($HP_{adj.,\ 22\ °C,\ ad\text{-}lib}$) was affected by diet (Figure 18, A). On pHFD, adjusted daily energy expenditure was higher than on CD. Although there were no significant interaction effects, daily energy expenditure was slightly increased in lHFD-fed GF

compared to CV counterparts (GF: 663.3 mW; SPF: 643.6 mW). Guided by this result, basal metabolic rate was evaluated as one major component of daily energy expenditure and as a potential factor contributing to this difference. Interestingly, adjusted basal metabolic rate ($HP_{adj.,\ 30\ °C,\ pa}$) of lHFD-fed GF mice was 13.1 % higher than that of CV counterparts (GF: 246.7 mW; CV: 218.2 mW), and it was also increased compared to CD- and pHFD-fed mice (Figure 18, B).

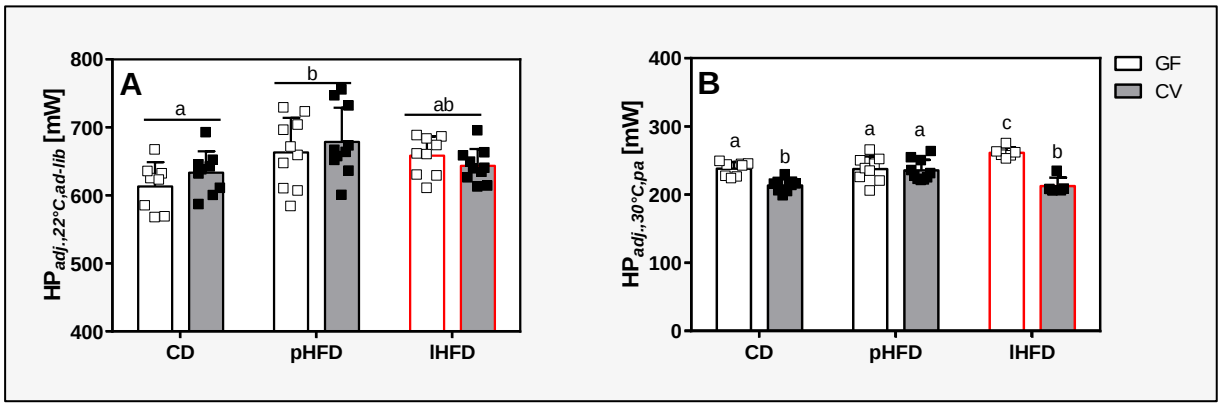

FIGURE 18 HEAT PRODUCTION (HP) OF CD-, PHFD- AND LHFD-FED GF AND CV MICE. (A) HP of *ad-libitum* fed C57BL/6N mice measured at ambient temperature (22 °C) reflecting daily energy expenditure. (B) HP of C57BL/6N mice in the post-absorptive state measured at thermoneutrality (30 °C) representing basal metabolism. Data with different superscript letters indicate significance ($p < 0.05$). CV CD: n = 9; CV pHFD: n = 10; CV lHFD: n = 10 / 5 (B); GF CD: n = 8; GF pHFD: n = 9; GF lHFD: n = 10 / 6 (B). HP was adjusted for body composition according to regression formulas found in

Table S 4. Data are shown as means + sd including dots representing single values. *adj.* – adjusted. *ad-lib* – *ad-libitum*. CD – control diet. CV – conventional. GF – germfree. HP – heat production. lHFD/pHFD – lard-/palm oil-based high-fat diet. *pa* – post-absorptive.

Next, respiratory exchange ratio (RER) was determined to assess potential differences in substrate oxidation and utilization pointing toward DIO resistance of lHFD-fed GF mice (Figure 19, A-D). CD- fed mice revealed a distinct day-night rhythm with increased RER levels at nighttime favoring carbohydrate oxidation and decreased levels at daytime favoring fat oxidation when mice are usually dormant (Figure 19, A-B). This characteristic was becoming less intensive when mice were exposed to a HFD due to steadily fat oxidation. Within GF mice, however, lHFD compared to pHFD induced increased RER levels in the early night phase, an effect absent in CV mice (Figure 19, A-B). Direct comparison between GF and CV mice belonging to the same feeding group thereby indicated that

RER levels, especially at the beginning of the night were lowered in pHFD-fed GF mice (Figure 19, D), but were not different among lHFD-fed mice (Figure 19, C).

Taken together, the lean phenotype of lHFD-fed GF mice is associated with an increased basal metabolic rate and different substrate oxidation capacities compared to obese, pHFD-fed counterparts. The latter may be due to impaired dietary fat resorption.

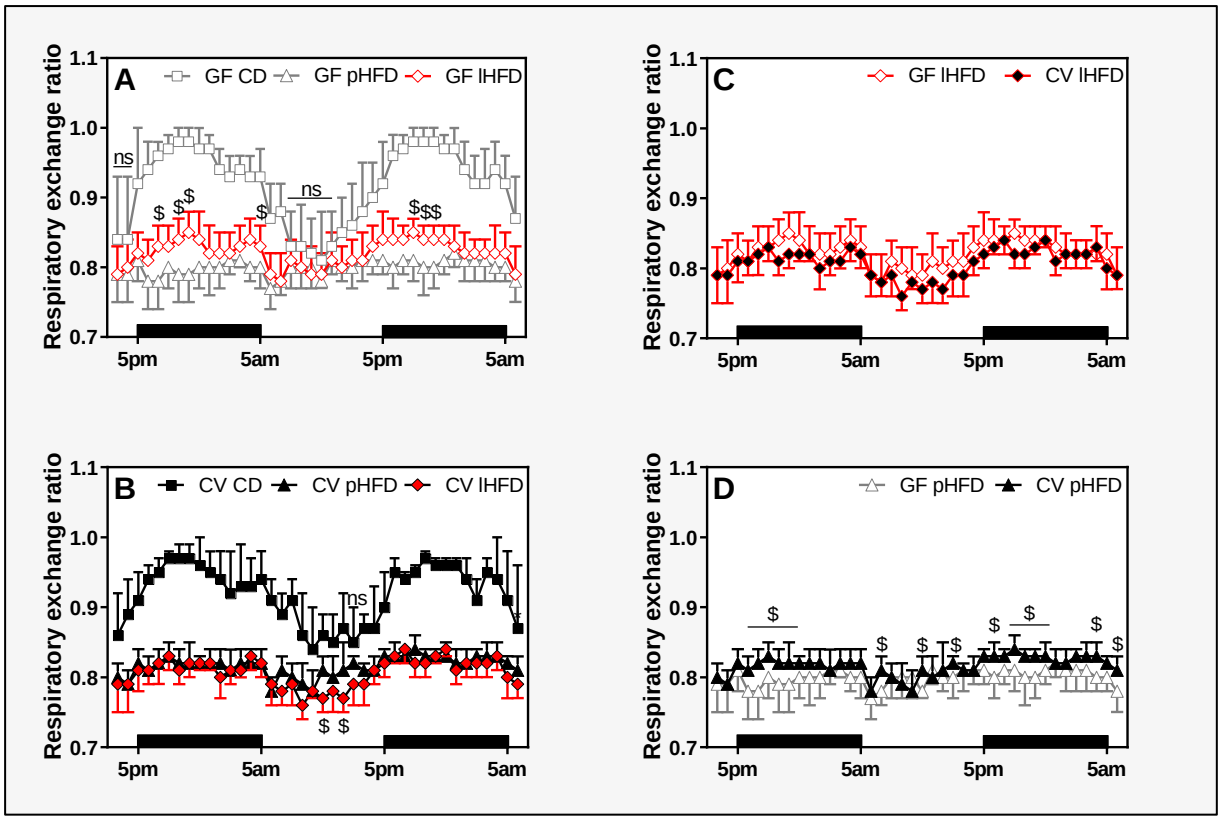

FIGURE 19 RESPIRATORY EXCHANGE RATIO (RER) OF CD-, PHFD- AND LHFD-FED GF AND CV MICE. (A) RER of GF mice. $ GF pHFD vs. GF lHFD: $p < 0.05$ (B) RER of CV mice. $ CV pHFD vs. CV lHFD: $p < 0.05$. CD-fed mice were distinct to HFD-fed mice at all time points unless otherwise labeled with ns. (C) Comparison of RER between lHFD-fed GF and CV mice (p = ns). (D) Comparison of RER between pHFD-fed GF and CV mice. $ GF pHFD vs. CV pHFD: $p < 0.05$. Black bars above the x-axis indicate nocturnal phases. CV CD: n = 9; CV pHFD: n = 10; CV lHFD: n = 10; GF CD: n = 8; GF pHFD: n = 9; GF lHFD: n = 10. Data are shown as means ± sd. CD – control diet. CV – conventional. GF – germfree. lHFD/pHFD – lard-/palm oil-based high-fat diet. ns – not significant.

4.4.3 Fecal loss of energy and fat is enhanced in lean germfree mice

Excretion of fecal energy as well as fat was studied by FT-IR measurement of group-housed mice during the first and the last week of the feeding trial to further pursue the hypothesis of altered energy balance in lHFD-fed GF mice. Data were adjusted for feces production and energy or fat intake, respectively (

Table S 4). In GF mice, a higher amount of fecal energy got lost in CD- and lHFD- compared to pHFD-fed mice and CV counterparts (Figure 20, A). Among CV mice, however, there was no difference within HFD-fed groups, however, energy excretion was higher compared to CD after adjustment (Figure 20, B). Appropriately, fat excretion was decreased in pHFD but not CD- and lHFD-fed GF mice, whereas fecal fat contents were similar between CV mice (Figure 20, B). The amount of fat measured in the feces of HFD-fed CV mice was, however, significantly higher compared to GF counterparts (Figure 20, B), which might be due to loss of fatty acids derived from bacterial membranes. Taken together, increased fat excretion in lHFD-fed GF mice indicates lower intestinal fat resorption, well in line with the increased respiratory exchange ratio toward decreased fat oxidation in these mice.

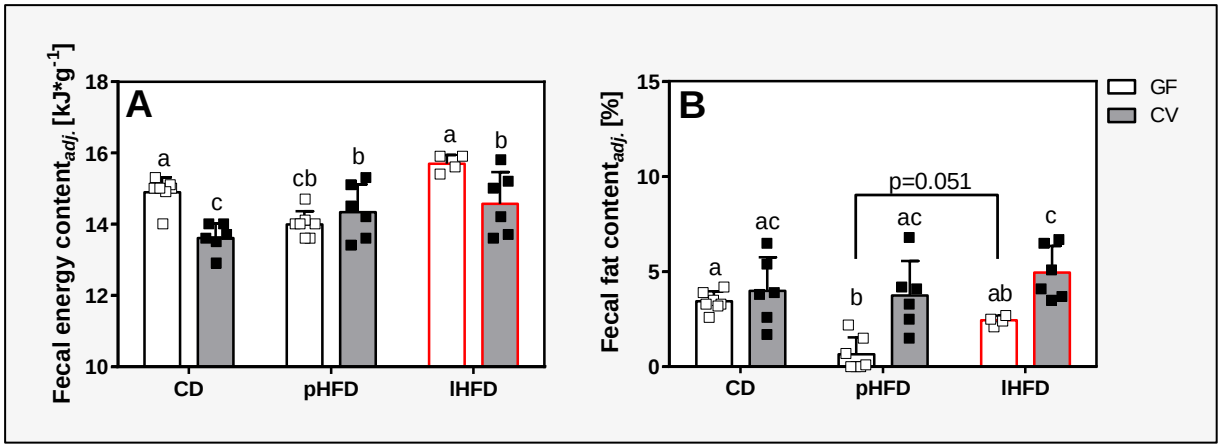

FIGURE 20 FECAL ENERGY (A) AND FAT (B) CONTENT OF GROUP-HOUSED GF AND CV MICE. Data including the first and the last week of the feeding trial. Different superscript letters indicate significance ($p < 0.05$). CV CD: n = 6; CV pHFD: n = 6; CV lHFD: n = 6; GF CD: n = 7; GF pHFD: n = 7; GF lHFD: n = 4. Data are shown as means + sd including dots representing cage means for the first and the last week of the feeding trial. Fecal energy and fat contents were adjusted for daily feces production and daily energy (A) or fat (B) intake, respectively, according to regression formulas found in

Table S 4. *adj.* – adjusted. CD – control diet. CV – conventional. GF – germfree. lHFD/pHFD – lard-/palm oil-based high-fat diet.

Concomitant to increased fecal energy loss, a decreased energy resorption was assumed to favor DIO resistance in lHFD-fed GF mice. Thus, energy resorption, a potential predictor of body mass development, was calculated and correlated to body mass gain. Within GF mice, energy uptake was lowest due to CD and highest for pHFD feeding, but there was no difference compared to lHFD (Figure 21, A). Providing CV mice both kinds of HFD markedly increased energy resorption, especially within the lHFD group (Figure 21, A). Interestingly, albeit microbiota status did not affect energy resorption in the presence of CD and pHFD, the amount of assimilated energy was lower in lHFD-fed GF than CV mice (Figure 21, A). As initially assumed, energy resorption positively correlated with body mass gain resulting in similar energy resorption rates after adjustment for this confounder. However, in lHFD-fed CV mice energy resorption still remained increased (Figure 21, B, C). Thus, energy resorption tended to be lower in lean compared to obese mice and thus, partly explains differences in body mass gain. In summary, the lean phenotype of lHFD-fed GF mice is accompanied with increased fecal energy and fat excretion as well as by a trend of decreased energy resorption.

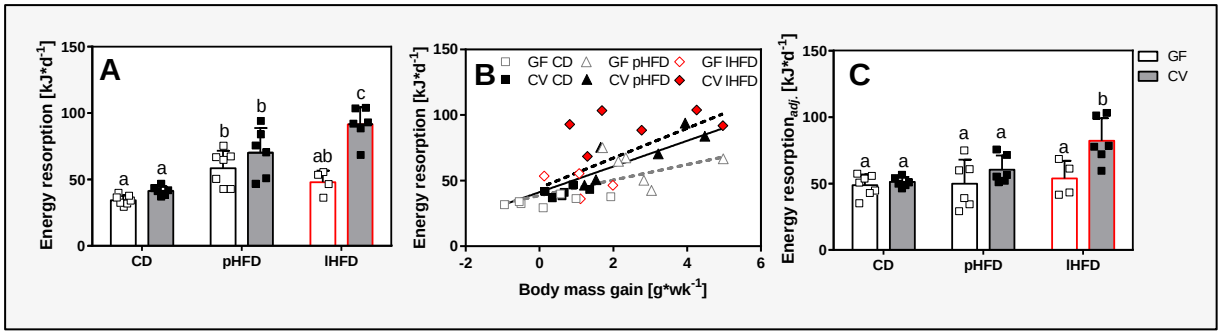

FIGURE 21 RAW (A) AND ADJUSTED (C) ENERGY RESORPTION OF GROUP-HOUSED GF AND CV MICE. Data include the first and the last week of the feeding trial. Different superscript letters indicate significance ($p < 0.05$). CV CD: n = 6; CV pHFD: n = 6; CV lHFD: n = 6; GF CD: n = 7; GF pHFD: n = 7; GF lHFD: n = 4. Data are shown as means + sd including dots representing cage means for the first and the last week of the feeding trial. (B) Dotted black line: linear regression among CV mice; dotted grey line: linear regression among GF mice; continuous black line: linear regression of GF and CV mice. Linear regression used for adjustment (C) includes both GF and CV mice and the corresponding regression formula can be found in

Table S 4. *adj.* – adjusted. CD – control diet. CV – conventional. GF – germfree. lHFD/pHFD – lard-/palm oil-based high-fat diet.

4.4.4 Lard feeding enhances jejunal transepithelial resistance in germfree mice

A disturbed gut barrier has been linked to obesity development in CV mice and is assumed to include decreased transepithelial resistance (TER) (Cani et al., 2007; Cani et al., 2008; Everard et al., 2011; Muccioli et al., 2010). However, recent data were unable to link gut barrier dysfunction and obesity (Kless et al., 2015). Thus, jejunal TER was investigated to clarify the bacterial impact on gut barrier integrity related to obesity. Moreover, the present study aimed to assess whether increased energy excretion and, hence, DIO resistance in lHFD-fed GF mice is accompanied with altered gut function.

CV compared to GF mice exhibited a massively decreased jejunal TER (Figure 22, A), indicating bacterial contribution toward lowered gut barrier integrity. Interestingly, jejunal TER was highest in lHFD-fed GF mice compared to CD- and pHFD-fed GF mice as well as CV counterparts (Figure 22, A), reflecting a potential link between increased jejunal TER, increased energy excretion and DIO resistance in these mice. On the other hand, there was no difference in jejunal TER within lean and obese CV mice (Figure 22, A), questioning obesity-related gut barrier breakdown. However, linear regression analysis revealed a negative correlation between jejunal TER and body mass gain in CD- and lHFD- fed mice (Figure 22, B, D), as well as among GF and CV mice (Figure 22, E-F). A higher jejunal TER was thus accompanied with a lower body mass gain, which finally indicates a connection between body mass development and gut barrier integrity, albeit this was not true for pHFD-fed mice ($r^2 = 0.02$, p = ns) (Figure 22, C).

Overall, the lean phenotype of lHFD-fed GF mice is accompanied with increased jejunal TER which hints to altered gut physiology contributing to decreased energy resorption as well as increased energy and fat excretion.

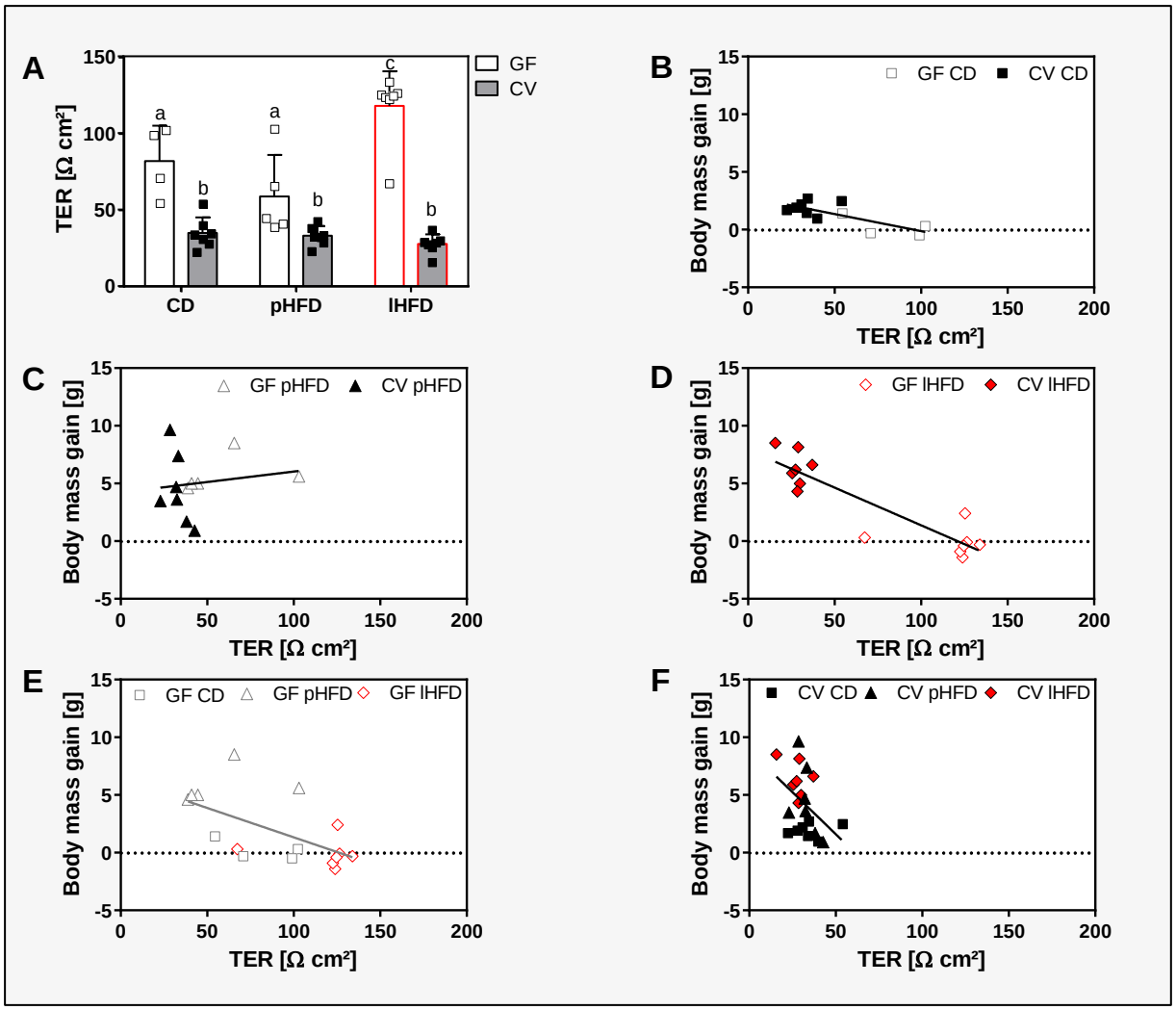

FIGURE 22 JEJUNAL TRANSEPITHELIAL RESISTANCE (TER) OF CD-, PHFD- AND LHFD-FED GF AND CV MICE Different superscript letters indicate significance ($p < 0.05$). (A) Data are shown as means + sd including dots representing single values. (B) Linear regression between jejunal transepithelial resistance and body mass gain of CD-fed GF and CV C57BL/6N mice ($r^2 = 0.59$, $p < 0.01$). (C) Linear regression between jejunal TER and body mass gain of pHFD-fed GF and CV mice ($r^2 = 0.02$, p = ns). (D) Linear regression between jejunal TER and body mass gain of lHFD-fed GF and CV ($r^2 = 0.81$, $p < 0.001$). (E) Linear regression between jejunal TER and body mass gain of GF mice ($r^2 = 0.35$, $p < 0.05$). (F) Linear regression between jejunal TER and body mass gain of CV mice ($r^2 = 0.19$, $p < 0.05$). CV CD: n = 7; CV pHFD: n = 7; CV lHFD: n = 7; GF CD: n = 4; GF pHFD: n = 5; GF lHFD: n = 7. CD – control diet. CV – conventional. GF – germfree. lHFD/pHFD – lard-/palm oil-based high-fat diet.

4.4.5 Cecal and hepatic metabolic fingerprints are associated with microbiota status and diet

Metabolome analysis of cecal contents and liver tissue were performed by ESI-FT-ICR/MS to identify potential pathways implicated in DIO resistance of lHFD-fed GF mice. Mass spectra were processed and signals were finally annotated by the MassTRIX server including a small but potential risk of false annotation. Metabolic pathways involved in DIO resistance of lHFD-fed GF mice were analyzed using KEGG Mapper.

Mass signals of cecal contents as shown by cluster analysis were clearly different to microbiota status and diet underlining the influence of bacteria and diet within the cecum (Figure 23). In liver samples, assembly of mass signals in response to the feeding status (fed/fasted) made discrimination according to microbiota status and diet less obvious (Figure 24). Integration of cecal mass signals into KEGG metabolic pathways were thus performed independent of the feeding state, whilst in liver, samples were analyzed in the fed state since there were no outliers as confirmed by Principal Component Analysis (PCA) (not shown). The following results refer to significant differences found in HFD-fed GF but not CV mice.

In both, cecal content and hepatic tissue, metabolites that belong to the biosynthesis of unsaturated fatty acids dominated in pHFD- compared to lHFD-fed GF mice (Figure 25, Figure 26, Table S 5, Table S 6). On the other hand, lHFD feeding provoked a higher number of cecal and hepatic metabolites related to arachidonic acid metabolism as well as steroid hormone biosynthesis in GF mice (Figure 25, Figure 26, Table S 5, Table S 6). Cecal mass signals were therefore attributable to progestagens, glucocorticoids, androgens as well as estrogens (Table S 5). However, cecal urocortisol or cortolone, both degradation products of cortisol, were found to be higher due to pHFD feeding (Table S 5). In the liver, lHFD triggered degradation of androgens as well as glucocorticoids (Table S 6). Increased cecal steroid levels further highlighted potential cholesterol effects mediated by lHFD in GF mice (Figure 25, Table S 5).

Taken together, cecal and hepatic fingerprints were associated with microbiota status and diet. The lean phenotype of lHFD-fed GF mice coincided with cecal metabolites belonging to steroid hormone biosynthesis indicating a potential cholesterol-derived pathway in mediating DIO resistance.

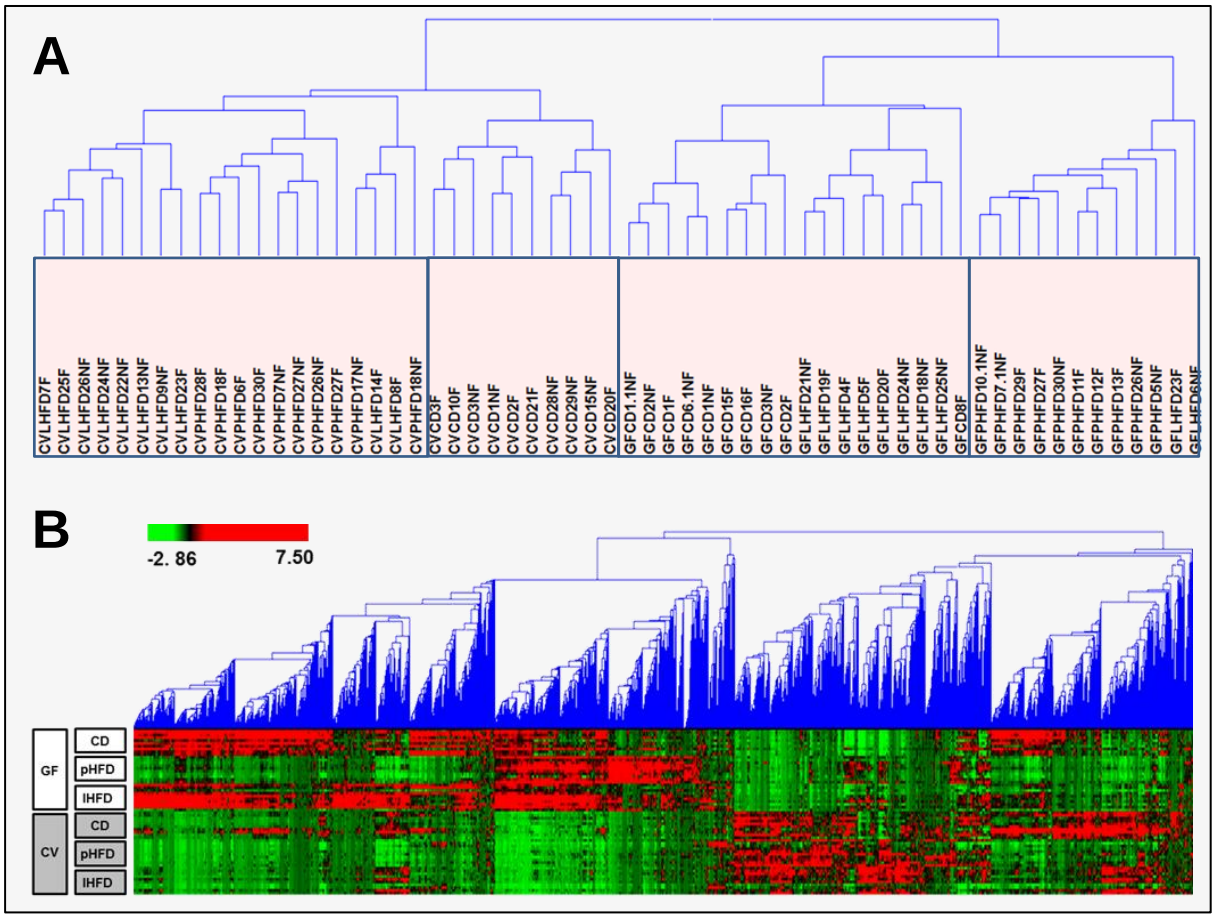

FIGURE 23 HIERARCHICAL CLUSTERING FOLLOWING METABOLOME ANALYSIS OF CECAL CONTENTS OF CD-, PHFD AND LHFD-FED GF AND CV MICE. (A) Hierarchical clustering of masses and (B) samples. 9948 masses were used for clustering analysis. Similarity measures were based on Pearson Correlation Coefficient. Clusters in (A) represented in boxes correspond to a minimum similarity value of 0.572. CV CD: n = 10; CV pHFD: n = 10; CV lHFD: n =10; GF CD: n = 10; GF pHFD: n = 10; GF pHFD: n = 10. Fasted: n = 5/group; not fasted: n = 5/group. Analysis was performed in the negative mode of ESI-FT-ICR/MS. CD – control diet. CV – conventional. F – fasted. GF – germfree. lHFD/pHFD – lard-/palm oil-based high-fat diet. NF – not fasted.

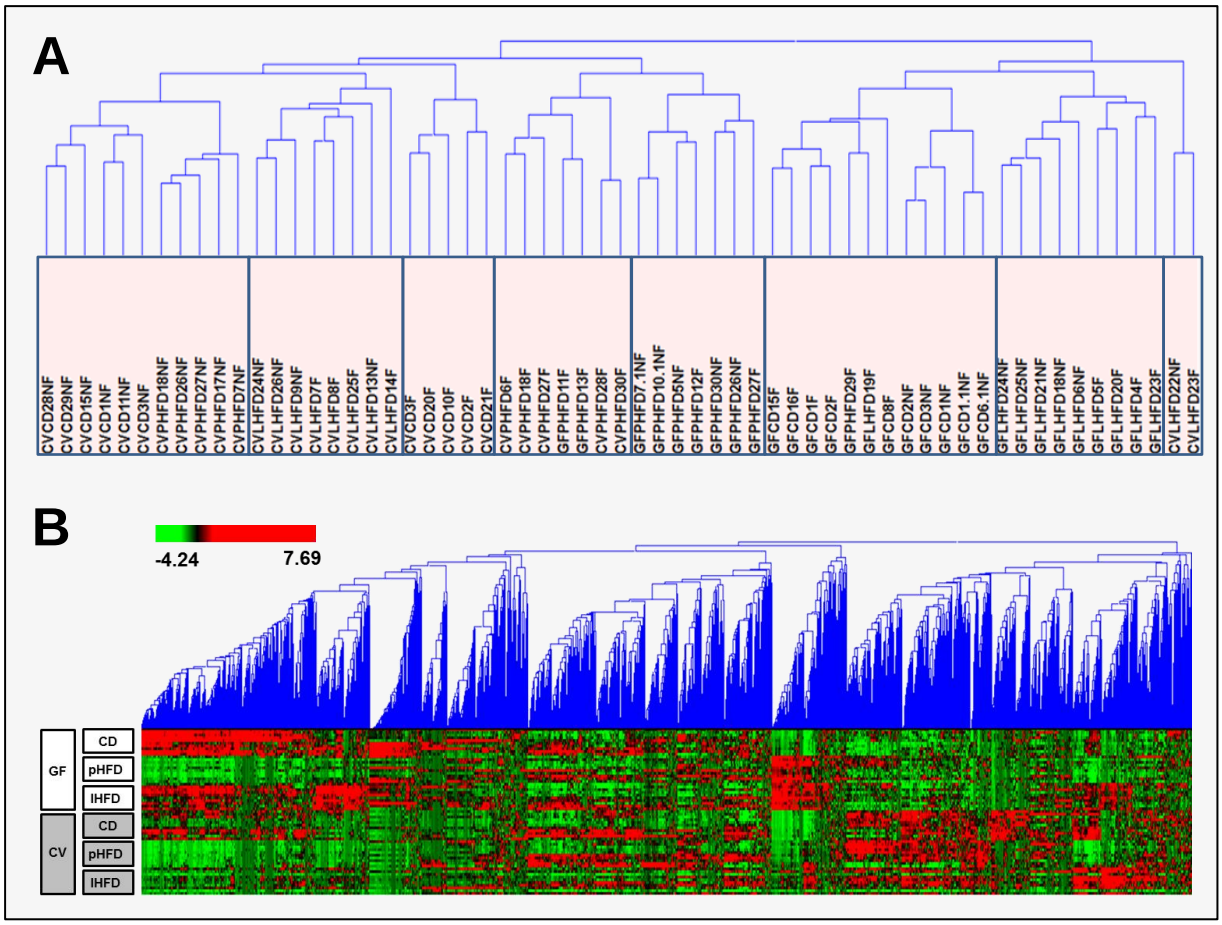

FIGURE 24 HIERARCHICAL CLUSTERING FOLLOWING METABOLOME ANALYSIS OF LIVER TISSUE OF CD-, PHFD AND LHFD-FED GF AND CV MICE. (A) Hierarchical clustering of masses and (B) samples. 5075 masses were used for clustering analysis. Similarity measures were based on Pearson Correlation Coefficient. Clusters in (A) represented in boxes correspond to a minimum similarity value of 0.544. CV CD: n = 11; CV pHFD: n = 10; CV lHFD: n =10; GF CD: n = 10; GF pHFD: n = 10; GF pHFD: n = 10. Fasted: n = 5/group; not fasted*: n = 5/group (*CV CD: n = 6). Analysis was performed in the negative mode of ESI-FT-ICR/MS. CD – control diet. CV – conventional. F – fasted. GF – germfree. lHFD/pHFD – lard-/palm oil-based high-fat diet. NF – not fasted.

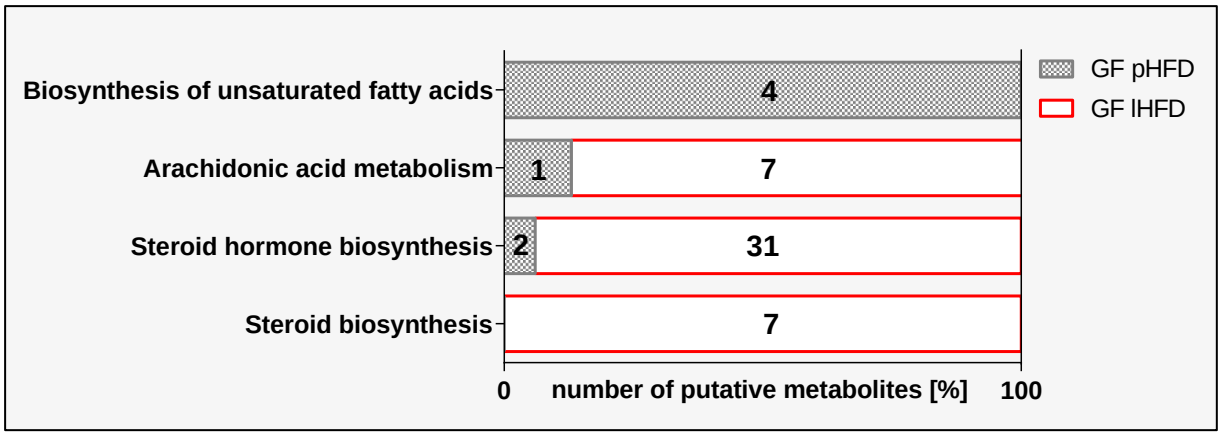

FIGURE 25 OUTPUT OF KEGG METABOLIC PATHWAY ANALYSIS OF CECAL METABOLITES. Numbers indicate metabolites significantly increased in lHFD- (white bars) or pHFD- (grey bars) fed GF mice, but not in CV counterparts. GF pHFD: n = 10; GF lHFD: n = 10. CV – conventional. GF – germfree. lHFD/pHFD – lard-/palm oil-based high-fat diet.

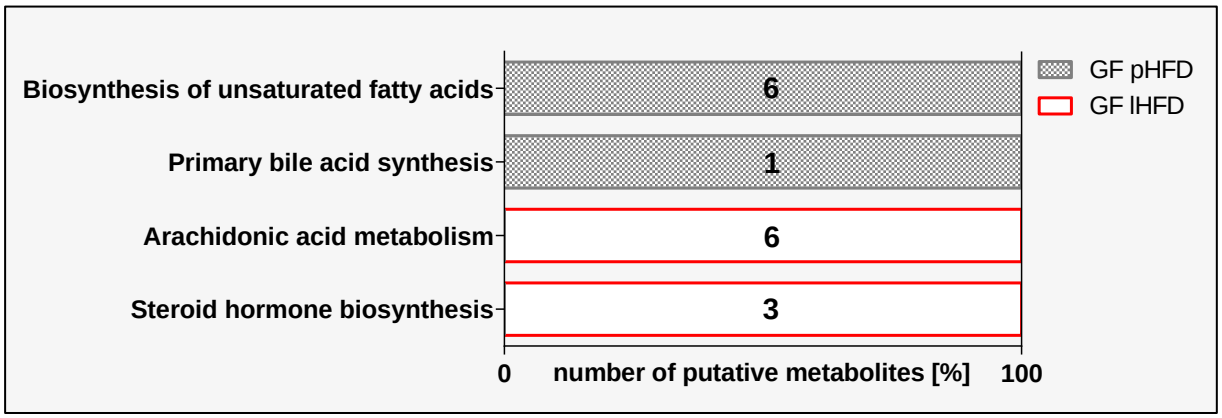

FIGURE 26 OUTPUT OF KEGG METABOLIC PATHWAY ANALYSIS OF HEPATIC METABOLITES. Numbers indicate metabolites significantly increased in lHFD- (white bars) or pHFD- (grey bars) fed GF mice, but not in CV counterparts. GF pHFD: n = 5; GF lHFD: n = 5. CV – conventional. GF – germfree. lHFD/pHFD – lard-/palm oil-based high-fat diet.

4.4.6 Cecal bile acid levels are decreased in lean germfree mice

To deepen metabolome analysis, quantification of bile acids was performed by UPLC-TOF/MS. Besides their role in lipid absorption and cholesterol catabolism, bile acids act as signaling molecules that activate the nuclear hormone receptor Farnesoid X Receptor (FXR), a transcription factor that negatively controls both, the biosynthesis and enterohepatic recycling of bile acids (Watanabe et al., 2011). Moreover, bile acids are known to mediate DIO resistance by increasing energy expenditure (Watanabe et al., 2011; Watanabe et al., 2006). Thus, bile acids were hypothesized to play a central role in mediating DIO resistance in lHFD-fed GF mice. Cecal bile acid levels were increased in CV

compared to GF mice which was represented by a higher diversity including primary as well as bacterial-derived, secondary bile acids (Figure 27). The low complexity found in GF mice was reflected by few taurine conjugated primary bile acids since GF mice are devoid of bacterial deconjugation (Figure 27, A). Amongst them, TCA and (α+β) TMCA were highest in pHFD- compared to CD- and lHFD-fed GF mice, as well as CV counterparts (Figure 27, A, B). In CV mice, DCA was increased irrespective of the HFD type, whereas LCA levels were just higher due to pHFD feeding. Furthermore, there was a positive correlation between body mass and cecal bile acid levels (Figure 28), which hint toward an increased bile acid-mediated fat uptake leading to obesity. Increased fecal fat excretion observed in DIO resistant, lHFD-fed GF mice might thus be a consequence of lowered cecal bile acid levels which consequently lead to altered endogenous substrate metabolism.

Guided by this hypothesis, a potential link between cecal bile acid levels and respiratory exchange ratio (RER) was examined. Interestingly, there was a negative correlation between total cecal bile acid levels and RER (Figure 29). This inverse relationship was most striking when mice resided in basal metabolism (Figure 29), rather than daily habitual needs (Figure S 3). In this respect, pHFD-fed GF mice revealed highest cecal bile acid concentrations which were concomitant with lowest RER levels (Figure 29, A), reflecting increased bile acid-mediated fat uptake, and consequently, higher fat oxidation rates. Moreover, neither bile acid levels nor RER differed between CD- and lHFD-fed mice (Figure 29, A). In CV mice, however, lHFD feeding increased total bile acid pool compared to CD and there was no difference to pHFD (Figure 29, B). Overall, total cecal bile acid concentration was strikingly higher in CV compared to GF mice but both revealed a negative correlation between the RER and cecal bile acids (Figure 29, C-D), indicating a link between substrate oxidation and cecal bile acid levels.

Taken together, the data does not support the hypothesis of linking DIO resistance in lHFD-fed GF mice to increased cecal bile acid levels. However, the negative correlation between cecal bile acid levels and RER suggests reduced bile acid-mediated fat uptake and oxidation resulting in increased fecal fat excretion and DIO resistance in lHFD-fed GF mice.

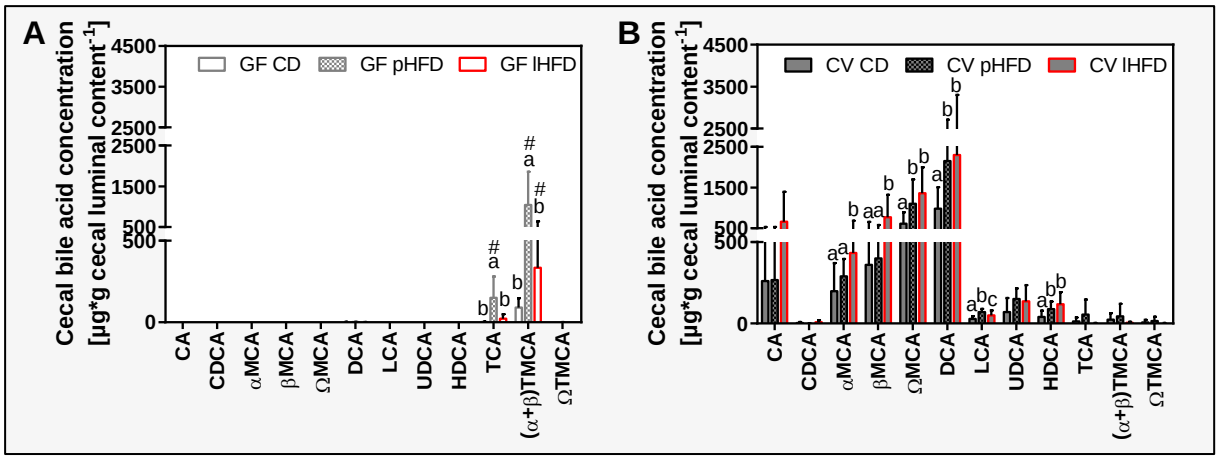

FIGURE 27 CECAL BILE ACID CONCENTRATIONS OF CD-, PHFD- AND LHFD-FED GF AND CV MICE. Different superscript letters indicate significant differences within a certain bile acid and among GF (A) or CV (B) mice, respectively ($p < 0.05$). # GF vs. CV: $p < 0.05$. CV CD: n = 10; CV pHFD: n = 10; CV lHFD: n = 10; GF CD: n = 10; GF pHFD: n = 10; GF lHFD: n = 10. Data are shown as means + sd. CA – cholic acid. CD – control diet. CDCA – chenodeoxcholic acid. CV – conventional. DCA – deoxycholic acid. GF – germfree. LCA – lithocholic acid. lHFD/pHFD – lard-/palm oil-based high-fat diet. MCA – muricholic acid. UDCA – ursodeoxycholic acid. HDCA – hyodeoxycholic acid. T – taurine-conjugated species.

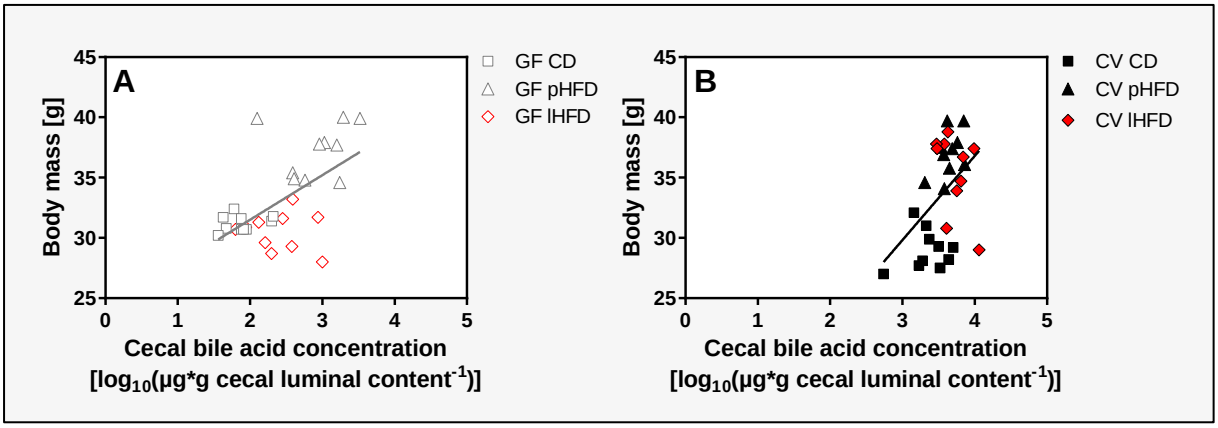

FIGURE 28 CORRELATION BETWEEN BODY MASS AND TOTAL CECAL BILE ACID CONCENTRATIONS OF CD-, PHFD- AND LHFD-FED GF AND CV MICE. Linear regression between body mass and total cecal bile acid concentration of GF mice (A) ($r^2 = 0.35$, $p < 0.001$) and CV mice (B) ($r^2 = 0.20$, $p < 0.05$). CV CD: n = 10; CV pHFD: n = 10; CV lHFD: n = 10; GF CD: n = 10; GF pHFD: n = 10; GF lHFD: n = 10. CD – control diet. CV – conventional. GF – germfree. lHFD/pHFD – lard-/palm oil-based high-fat diet.

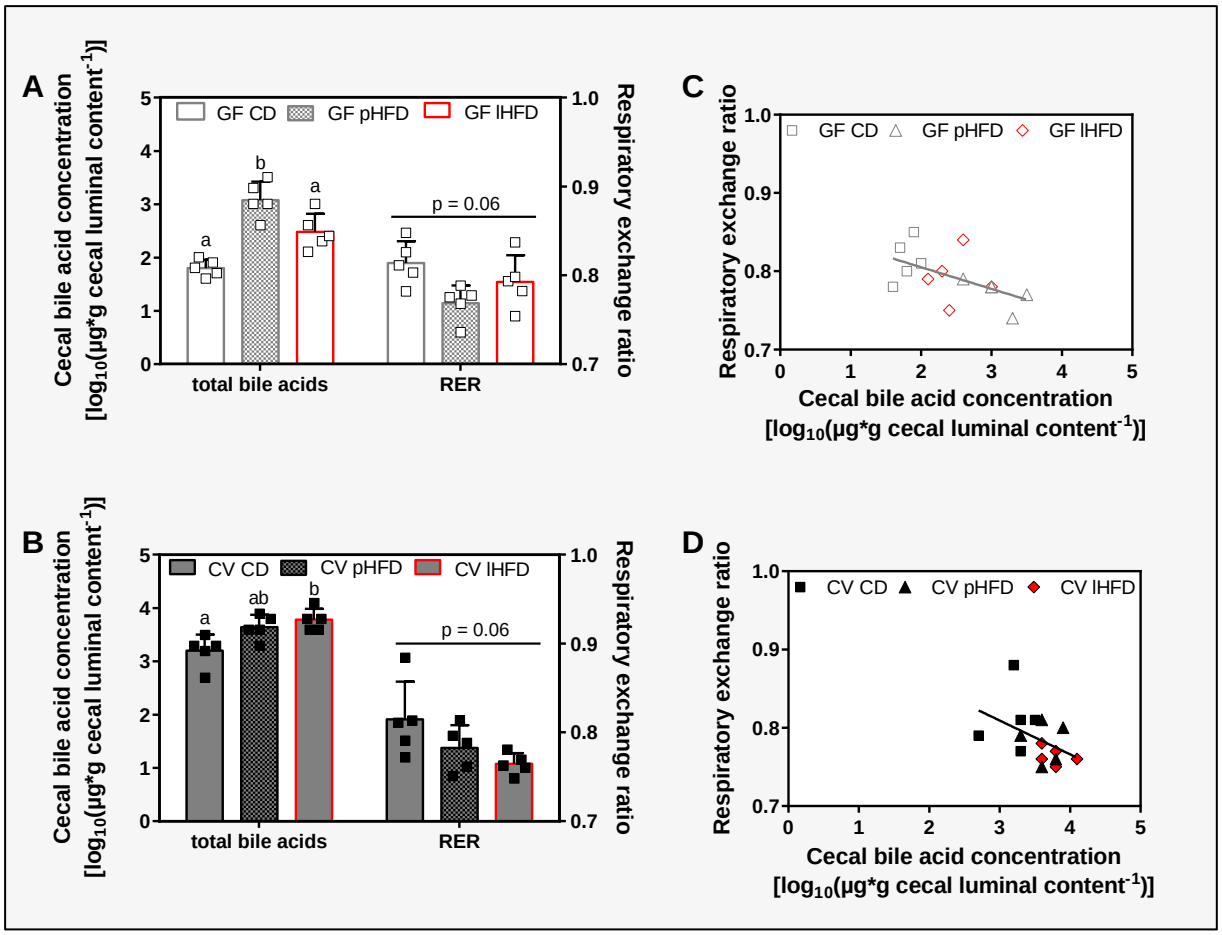

FIGURE 29 TOTAL CECAL BILE ACID CONCENTRATION AND RESPIRATORY EXCHANGE RATIO (RER) MEASURED DURING BASAL METABOLISM OF CD-, PHFD- AND LHFD-FED GF (A) AND CV (B) MICE. (A-B) Data are shown as means + sd including dots representing single values. Different superscript letters indicate significance ($p < 0.05$). (C-D) Linear regression analysis between RER and cecal bile acid concentration of fasted GF ($r^2 = 0.26$, $p < 0.05$) (C) and CV mice ($r^2 = 0.22$, p = ns) (D). CV CD: n = 5; CV pHFD: n = 5; CV lHFD: n = 5; GF CD: n = 5; GF pHFD: n = 5; GF lHFD: n = 5. CD – control diet. CV – conventional. GF – germfree. lHFD/pHFD – lard-/palm oil-based high-fat diet.

4.4.7 Hepatic Cyp7a1 and Nr1h4 gene expression is lowered in lard-fed germfree mice

Since increased steroid hormone and decreased cecal bile acid levels were found in lHFD-fed GF mice, hepatic gene expression using qRT-PCR was investigated to better understand the molecular mechanisms underlying DIO resistance in lHFD-fed GF mice. The liver was analyzed as it represents the tissue controlling synthesis and degradation of cholesterol, synthesis of bile acids as well as sterol uptake and expression of transcription factors involved in sterol homeostasis.

Higher gene expression levels were found for Hmgcs, Hmgcr, Dhcr7 and Ldlr in GF compared to CV mice pointing toward an increased endogenous biosynthesis and sensitivity for hepatic cholesterol uptake (Figure 30), although hepatic cholesterol levels were not distinct among groups (Figure S 2).

Guided by these results, extensive hepatic cholesterol conversion was assumed to play a role in DIO resistance of lHFD-fed GF mice. Interestingly, Cyp7a1, the key enzyme for cholesterol-derived primary bile acid synthesis, was higher in pHFD-fed GF mice than CD- or lHFD-fed and CV counterparts (Figure 30), confirming hepatic cholesterol degradation. On the other hand, there was no indication for neither increased acidic bile acid synthesis fueled by the Cyp27a1 nor enhanced cholesterol translocation mediated via Abcg5 and Abcg8 among mice. Gene expression of Akr1d1 which reduces bile acid intermediates as well as progesterone, androstenedione, 17-α-hydroxyprogesterone and testosterone was higher in GF than CV mice highlighting gut microbiota-host signaling. Additionally, transcript levels of Hsd11b1 which is involved central obesity by conversion of 11-dehydocorticosterone into corticosterone failed to show any differences among groups. Overall, Cyp7a1 represented the only gene that was decreased in lean GF mice contributing to cholesterol degradation.

Interestingly, Nr1h4 expression that encodes FXRα and counteracts Cyp7a1 expression was enhanced in pHFD-fed GF mice compared to lHFD but not CD. On the other hand, Nr1h2 and Nr1h3 that encode LXRβ and LXRα proteins, respectively, and are known to stimulate Cyp7a1 expression were similar among groups. In this respect, Nr1h4 regulation happened in the same direction as Cyp7a1 expression suggesting potential bile acid-mediated positive feedback mechanism.

In summary, decreased hepatic Cyp7a1 gene expression in lean GF mice may explain decreased cecal bile acid levels due to a reduced capacity of hepatic cholesterol-to-bile acid conversion, which thereby appears as the regulating mechanism in mediating DIO resistance in lHFD-fed GF mice.

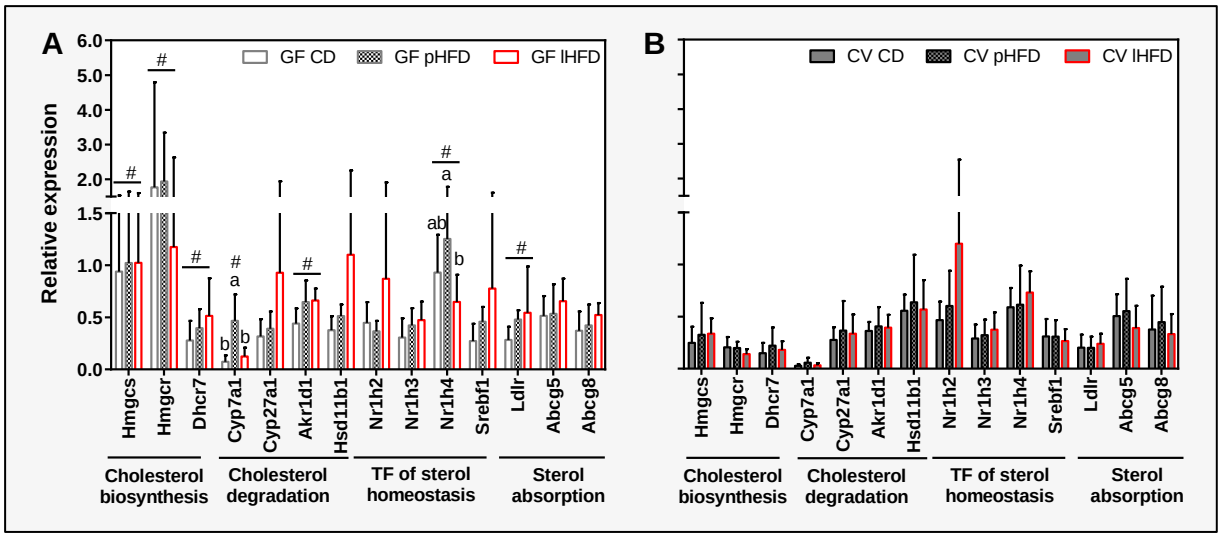

FIGURE 30 HEPATIC GENE EXPRESSION OF CD-, PHFD- AND LHFD-FED GF AND CV MICE. Different superscript letters indicate significance ($p < 0.05$). CV CD: n = 6; CV pHFD: n = 5; CV lHFD: n = 5; GF CD: n = 6; GF pHFD: n = 6; GF lHFD: n = 5. Data are shown as means + sd. Different superscript letters indicate significant differences within a certain gene among GF mice ($p < 0.05$). # GF vs. CV: $p < 0.05$. Abcg5 – ATP-binding cassette sub-family G member 5. Abcg8 – ATP-binding cassette sub-family G member 8. Akr1d1 – aldo-keto-reductase family member 1. CD – control diet. CV – conventional. Cyp7a1 – cholesterol 7 alpha-hydroxylase. Cyp27a1 – cholesterol 27 alpha-hydroxylase. Dhcr7 – 7-dehydrocholesterol reductase. Hmgcr – 3-hydroxy-3-methylglutaryl Coenzyme A reductase. GF – germfree. Hmgcs – 3-hydroxy-3-methylglutaryl Coenzyme A synthase 1. Hsd11b1 – hydroxysteroid (11-β) dehydrogenase 1. Ldlr – low density lipoprotein receptor. lHFD/pHFD – lard-/palm oil-based high-fat diet. Nr1h2 – nuclear receptor subfamily 1, group H, member 2 (liver X receptor β). Nr1h3 – nuclear receptor subfamily 1, group H, member 3 (liver X receptor α). Nr1h4 – nuclear receptor subfamily 1, group H, member 4 (farnesoid X receptor α). Srebf1 – sterol regulatory element binding transcription factor 1. TF – transcription factor.

4.4.8 Cecal gut microbiota is altered by diet

The fact that lHFD-fed CV mice were obese when compared to GF counterparts implied that bacterial colonization is at least partly responsible for loss of the lean phenotype. The presence of specific gut bacteria was therefore investigated in cecal samples by high-throughput sequencing of 16S rRNA amplicons.

α-diversity analysis indicated no difference in the richness of molecular species, yet HFD-fed mice were characterized by higher Shannon effective counts which refers to most dominant bacteria (Figure 31, A). *β*-diversity revealed significant diet-dependent clusters. Lean, CD-fed mice were distant

compared to HFD groups (Figure 31, B). Albeit there was a partial overlap between obese groups, the center of both bacterial profiles was phylogenetically distant to each other (Figure 31, B). The relative sequence abundance of *Clostridiales* spp. was increased, whereas that of *Bacteroidales* decreased under both HFD feeding conditions (Figure 31, C), but there were no significant changes at any taxonomic levels between the two HFDs (data not shown). Molecular species related to *Acetatifactor muris* (OTU25, 96.6 % sequence similarity; OTU4, 92.0 %) and to the cholesterol-to-coprostanol converting *Eubacterium coprostagnoligenes* (OTU31, 95.4 %) were higher in the cecum of lHFD-fed mice (Figure 31, D). On the other hand, *Flavonifractor plautii* (OTU316, 94.2 %) and *Hydrogenoanaerobacterium saccharovorans* (OTU9, 92.9 %) were more abundant under pHFD feeding (Figure 31, D).

In summary, a few lHFD-specific bacteria were identified by high-throughput sequencing, which may have contributed to the loss of the lean phenotype as seen in lHFD-fed GF mice.

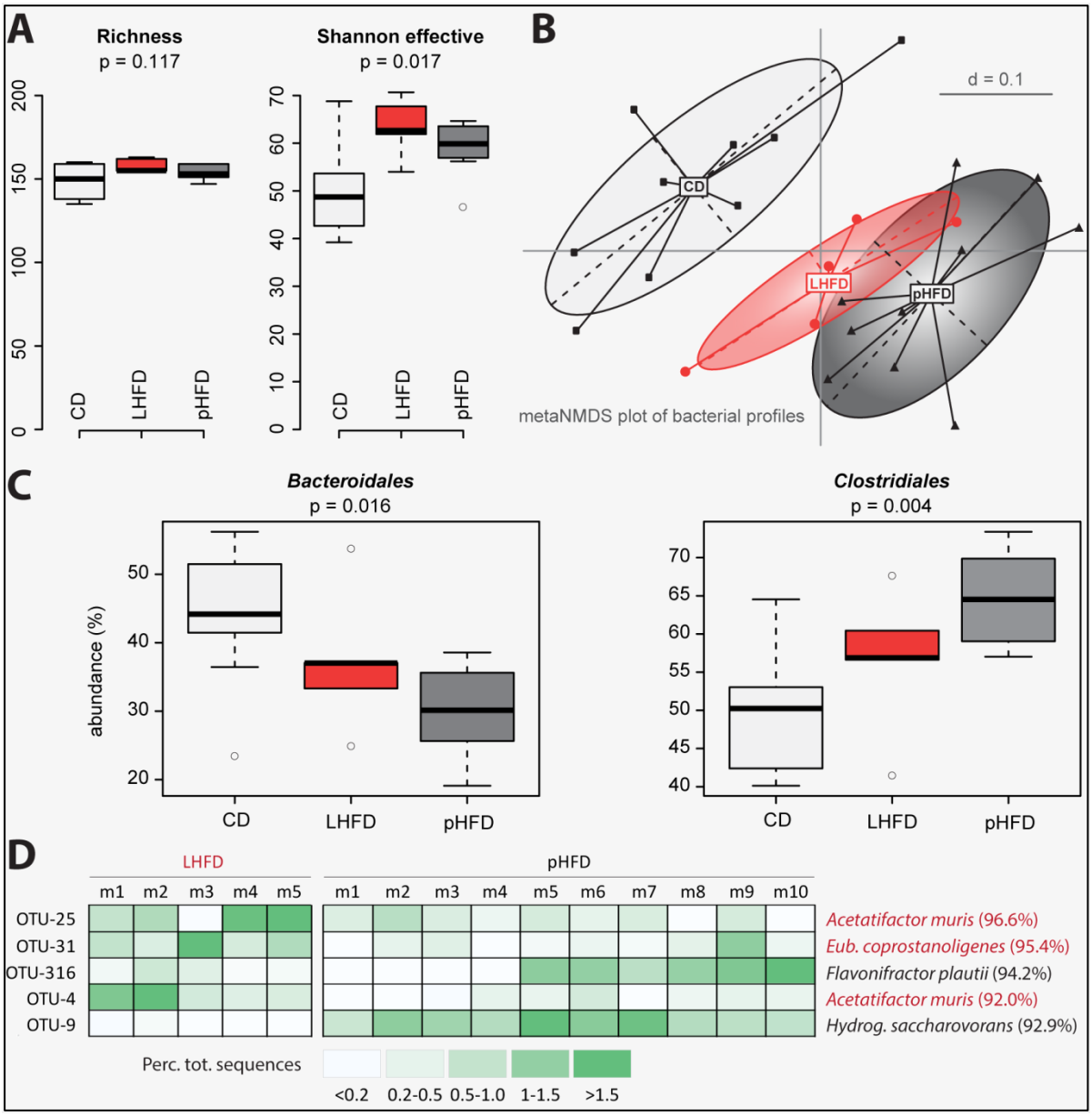

FIGURE 31 CECAL SEQUENCING OF BACTERIAL 16S RRNA OF CD-, PHFD- AND LHFD-FED CV MICE. (A) *α*-diversity analysis. (B) *β*-diversity indicated by multidimensional scaling based on general UniFrac distances. CD: black squares; pHFD: black triangles; lHFD: red dots. (C) Relative sequence abundance of *Bacteroidales* and *Clostridiales*, significantly different between lean and obese mice. (D) Heat map of the top 5 operational taxonomic units (OTU) significantly different between CV lHFD and pHFD. The identity of OTUs was obtained using EzTaxon based on sequences of approximately 380 bp. Red font: increased abundance in lHFD-fed CV mice; black font: increased abundance in pHFD-fed CV mice. Each square corresponds to a single sample. Distinct shades of green correspond to the relative abundance of total sequences. Numbers in brackets correspond to sequence similarity. CV CD: n = 9; CV pHFD: n= 10; CV lHFD: n = 5. Mice were fasted and maintained at thermoneutrality for 6 hours until cecal sampling. CD – control diet. CV – conventional. GF – germfree. lHFD/pHFD – lard-/palm oil-based high-fat diet.

5 DISCUSSION

The present study was conducted to elucidate the gut microbiota-host-diet interaction in obesity. The impact of bacteria on body mass development was therefore addressed by environmental exposure and fecal transplantations of diet-induced obesity (DIO) prone (AKR/J) and resistant (SWR/J) as well as cohousing of genetically obese (Mc4r^{W16X}/C57BL/6J) mice. It could be shown that microbial transfer by cohousing of genetically obese mice was insufficient to trigger changes in body or fat mass indicating that the genetic background dominated bacterial effects. In DIO mouse models, however, environmental conditioning using cage swap between obesity prone AKR/J and obesity resistant SWR/J mice slowed fat mass development in AKR/J mice, and even stronger effects were induced by frequent fecal transplantations. Furthermore, it was found that the type of host accounts for effects in the DIO model: AKR/J mice were responsive while SWR/J mice resisted changes in fat mass when provoked with bacteria of the other mouse strain. These findings hint toward a more sensitive microbial community structure in obese mice being susceptible to foreign stimuli whereas that of lean mice appears stable. Interestingly, exposure of AKR/J mice to the SWR/J environment via cage swap led to significant shifts toward SWR/J microbiota profiles highlighting a potential role of gut microbiota on fat mass development. However, bacterial sequencing following microbiota transplantation failed to detect the causative microbiota transfer for both mouse strains thereby it is assumed that non-microbial factors played a role in mediating the effects on body composition.

Given that body mass gain of GF mice relies on dietary composition, the present study further focused on the gut microbiota-host-diet interaction by feeding germfree (GF) and conventional (CV) C57BL/6N mice HFDs with different fat sources. While CV mice gained body mass irrespective of the dietary fat, GF mice put on weight when exposed to palm oil but not to lard. Molecular pathways and metabolites pointed at lard-derived cholesterol as the key player in mediating DIO resistance in GF

mice. Cecal bacterial profiles of CV mice clustered according to diet, and could therefore not be attributed to body mass *per se*.

5.1 Host phenotype is influenced by genetic background rather than by gut microbiota

The success of microbiota transfer in curing diseases such as *Clostridium difficile* infections has convincingly been shown earlier (Bakken, 2009; Bakken et al., 2011; Gough et al., 2011). However, less is known about the role of gut microbiota in obesity development. So far, mouse studies dealing with the bacterial influence on body mass were predominately performed in recolonized GF mice (Backhed et al., 2004; Turnbaugh et al., 2006). This resembles an artificial approach to elicit bacteria related metabolic pathways. The actual extent of the gut microbiota to trigger obesity thus remains unsolved. Already colonized mice represent a more realistic tool to investigate the impact of gut microbiota on body mass development. Hence, strain-specific obesity onset as a transmissible trait due to variations in gut microbiota composition was examined in conventional (CV), DIO resistant (SWR/J) and prone (AKR/J) mice as well as in a genetic mouse model of obesity (Mc4r^{W16X}/C57BL/6J).

5.1.1 The stronger the intervention, the higher the phenotypic outcome

GF mice have been discussed as an unsuitable model to represent the complex flora of a patient's intestine (Damman et al., 2012). Moreover, recolonization of these mice implied diverse microbial treatment strategies which render comparisons challenging (Backhed et al., 2004; Crawford et al., 2009; Ridaura et al., 2013; Turnbaugh et al., 2006). Thus, the present study investigated the type of treatment in three CV mouse models (DIO resistant SWR/J, DIO prone AKR/J, and genetically obese Mc4r^{W16X}/C57BL/6J) to clarify the bacterial impact on obesity development.

It could be shown that fat mass reduction strongly depended on the strength of the stimulus. In AKR/J mice, fat mass was reduced by 19 % using cage swap or even 35 % using fecal transplants from SWR/J mice (Figure S 1). SWR/J mice, however, resisted DIO irrespective of the treatment and cohousing Mc4r^{W16X}/C57BL/6J knockin (ki) with wildtype (wt) mice further did not induce any changes in body composition for either genotype (Figure 16). Hence, body weight change was the most pronounced, the higher the stimulus, although this happened to be strain-dependent.

Cage swap and cohousing are environmental conditioning strategies that induce microbial transfer by coprophagy. In contrast to cohousing studies related to gut inflammation (Bel et al., 2014; Hansen et al., 2012; Macia et al., 2015; Stecher et al., 2010), publications conducted on obesity management are scarce and the data for bacterial impact on weight loss of genetically obese ob/ob mice investigated by antibiotics is inconsistent (Dubuc and Willis, 1978; Henao-Mejia et al., 2012; Membrez et al., 2008; Ridaura et al., 2013). Albeit Mc4r^{W16X}/C57BL/6J mice were housed at a ki:wt ratio of 3:1 and *vice versa*, the present study failed to elicit phenotypic differences, consequently neglecting bacterial sequencing of 16S rRNA amplicons. This result underlines the strong genetic impact that might have overwhelmed bacterial contribution on body mass development. Environmental stimuli induced by cohousing are apparently too weak for lowering body mass in genetically obese Mc4r^{W16X}/C57BL/6J ki mice.

Interestingly, strain-dependent behavior has been proposed to affect coprophagy (Dimitriu et al., 2013), which could explain distinct efficacy of cohabiting mouse strains to assimilate allochthonous microbiota. In this respect, cage swap and fecal transplantation were effective in lowering fat mass of AKR/J mice and even more, fat mass reduction via cage swap was attributable to bacterial changes toward SWR/J microbiota profiles. On the other hand, higher effects in AKR/J mice due to fecal transplantation failed to detect specific causative SWR/J microbes but are likely triggered by particles found in complex SWR/J feces such as fibres, mucus, proteins, fat, bile acids. Fecal transplantations from lean donors have been shown to improve insulin sensitivity indicating a relationship between

bacterial translocation and host metabolism (Vrieze et al., 2012). Hence, in the present study transfer of gut microbiota, or at least fecal contents such as metabolites might have reprogrammed host signaling toward a fat lowering manner.

Altogether, cage swap and fecal transplantation reduced fat mass of obesity prone AKR/J mice which could partly be attributed to microbial changes. However, lacking effects in SWR/J mice and as examined by cohousing of genetically obese with lean mice indicates that not the gut microbiota *per se* but also the experimental design including mouse strains and treatment strategy highly affects phenotypic outcomes.

5.1.2 AKR/J mice but not SWR/J mice are ready to microbial transfer

In a screen of 100 inbred mouse strains, the microbiota profile of AKR/J and SWR/J mice was first examined by Parks and colleagues to evaluate the impact of HFD on gut bacterial composition (Parks et al., 2013). However, strain-dependent variations in microbial community structure of those mice accompanied with different phenotypes were not ruled out as reasons for the underlying resistance of SWR/J but not AKR/J to develop obesity.

In the present study, fat mass in AKR/J mice was lower upon fecal microbiota transplantation compared to cage swap, but phenotype of SWR/J mice remained unchanged. Interestingly, α-diversity of fecal bacteria was strain-specific for the cage swap experiment (Figure 10), but there were no major changes in the number of dominant molecular species according to mouse genotype or bacterial therapy following fecal transplantation (Figure 13). On the other hand, β-diversity revealed high inter-individual variations (Figure 10, Figure 13, Figure 15). For both experiments, the family *Lactobacillaceae* was persistently higher in SWR/J rather than AKR/J mice, which has been linked to obesity prevention or obesity onset depending on the species level (Park et al., 2013; Poutahidis et al., 2013; Yoo et al., 2013; Zeng et al., 2013). However, there is inconsistency between experiments in the number of bacterial sequences belonging to the family *Clostridiales*. Time-shifted cohorts

accompanied with environmental changes within the animal holding area as well as distinct breeding pairs might be responsible for experimental variations in gut microbiota profiles. Moreover, it is also conceivable that modifications in bacterial community structure induced by cage swap not only relies on coprophagy, but also on bacteria from the fur of foreign mouse strains that transfer over to bedding, while microbiota transplantation is limited to stool contents from the foreign mouse strain. Additionally, strain-specific pheromones prevalent in mouse cages might influence mouse behavior and thus body mass development. Bacterial exposure due to cage swap could thus be more complex compared to pure fecal transplantations and might further explain inconsistencies between experiments.

A less diverse bacterial profile in the guts of obese mice implicates unfilled microbial niches whereby 'lean' microbes settle and trigger a lowered body mass (Turnbaugh et al., 2009). Hence, a more sensitive, obese microbial community structure seems to favor colonization of foreign microbes which trigger metabolic alterations. Settlement of specific causative bacteria due to cage swap, i.e. belonging to the familly *Lactobacillaceae*, might therefore encourage fat mass lowering effects in AKR/J mice. Responsive bacteria induced by fecal microbiota transplantations that might alter fat mass of AKR/J mice remain, however, undetected. Beyond methodical limitations to identify successful bacterial transfer implicated in lowering body weight, there are further possibilities by which fecal transplantation might have affected AKR/J phenotype. First, bacterial-derived metabolites such as short-chain fatty acids (SCFA) as well as bile acids have been frequently discussed in obesity development and prevention and represent a valuable approach to investigate (Tremaroli and Backhed, 2012). Moreover, it is conceivable that altered enzymatic systems within the gut might affect endogenous transmission and metabolism. In addition to that, diversity of microbial genes was shown to distinguish lean and obese phenotypes more accurately than host genes (DeWeerdt, 2014). Given that lower bacterial gene richness corresponds with higher body fat contents (DeWeerdt, 2014), hints toward treatment-induced differences in bacterial gene diversity between AKR/J phenotypes. A metagenomics analysis could, thus, be a valuable tool to more closely characterize the bacterial impact on fat mass outcome between those mice.

Taken together, strain-specific differences in gut microbiota of obesity prone AKR/J and obesity resistant SWR/J mice might contribute to different phenotypes. Weight-lowering mechanisms in AKR/J mice, however, remain a matter of debate since cage swap but not fecal transplantation led toward SWR/J microbiota profiles.

5.1.3 Treatment strategy does not change strain-specific gut morphology and metabolism

Variations in substrate uptake related to differences in gut morphology are another possibility for obesity development. In this respect, the length of gut segments and parameters of energy balance were examined to evaluate treatment-induced, gut-associated assimilations between mouse strains as well as between genotypes of Mc4r^{W16X}/C57BL/6J mice.

Since cohousing of genetically obese with lean mice did not impact body composition it is comprehensible that there weren't any differences in neither energy balance parameters, nor gut length or bacterial counts. Additionally, Mc4r^{W16X}/C57BL/6J ki mice were heavier than wt mice due to overeating, a finding in accordance with previous results (Bolze et al., 2011).

Treatment-dependent gut adaptations were assumed to contribute to the lean phenotype in AKR/J mice. The small intestine was longer and the colon was shorter in SWR/J compared to AKR/J mice in both, cage swap as well as after fecal transplantation indicating altered gut physiology (Table 14, Table 16). The longer colon in AKR/J mice is likely to support increased resorption capacity of bacterial-derived metabolites such as SCFA. And an increased small intestinal length in SWR/J mice could favor increased carbohydrate uptake. Overall, increased RER levels in SWR/J mice underline the hypothesis of increased carbohydrate oxidation protecting against obesity (Table 13, Table 15). There is, however, no indication toward any influences of the treatment strategy explaining the reduced fat mass in AKR/J mice.

As further heat production and energy resorption were similar after adjustment for body composition, there might be endogenous mechanisms responsible for fat mass lowering effects in AKR/J mice. In this respect, future investigations should include additional focus on gut physiology, liver and fat metabolism-related genes, proteins as well as metabolites. Moreover, energy balance measurements were solely performed at the end of the experiment without marked effects. However, small but sustained differences could lead to distinct obesity outcomes which may not be accurately detectable at one respective time point. It could therefore be worth investigating energy balance parameters more frequently or at least, at an earlier time point. In addition to this, indirect calorimetry-based energy expenditure relies on oxygen consumption and carbon dioxide production, whereby anaerobic metabolism provided by bacteria is neglected. The bacterial contribution to host heat production, thus, demonstrates a valuable approach to examine as it is unexplored so far.

5.1.4 Summary related to the treatment strategies in conventional mice

Based on previous publications, recolonization of GF mice indicated a distinct bacterial impact on body mass development (Backhed et al., 2004; Turnbaugh et al., 2006). Bacterial transfer into mice harboring a complex microbiota is, however, scarce and the real extent with which bacteria influence obesity remain unsolved. In this respect, obesity prone AKR/J and obesity resistant SWR/J mice as well as a genetic mouse model of obesity (Mc4rW16X/C57BL/6J ki and wt) were chosen to evaluate treatment strategies on phenotypic outcome and gut bacterial adaptations.

This study shows that the strength of the stimulus determines the obese phenotype of AKR/J mice, whereas SWR/J stayed resistant to microbial transfer and to develop obesity. Compared to pHFD-fed AKR/J controls, cage swap induced a fat mass reduction by 19 % and fecal transplantation by even 35 %. Moreover, cage swap was accompanied with changes in AKR/J bacterial composition toward SWR/J profiles indicating bacterial settlement related to lean phenotypes. Albeit fecal transplantation revealed distinct fat mass reduction in AKR/J mice treated with SWR/J fecal transplants, causative

bacteria remained undetected. Thus, other components of feces as well as environmental factors are further candidates for weight lowering effects.

Beyond the strength of the treatment strategy, there was also a strong genetic influence that certainly overwhelmed bacterial effects by cohousing on phenotypes of Mc4r^{W16X}/C57BL/6J ki and wt mice. Higher stimuli are therefore assumed to be needed to unravel bacterial effects on body composition as decisive bacteria might not be transferred due to environmental exposure. Strikingly, it is known that in addition to gut communication obesity also involves metabolic alterations within the liver and fat tissue. Hence, cohousing studies of CV mice likely include the interplay between gut inhabitants and metabolically active organs.

Altogether, these findings elaborate the difficulty to detect microbial alterations in CV mouse models due to environmental exposure and fecal transplantations. Alterations in body composition are, hence, not simply ascribed to the gut microbiota *per se*, but seem to strongly rely on the interaction of host genetics, diet and treatment.

5.2 Dietary fat and the gut microbiota alter diet-induced obesity in mice

During the last decade, close attention has been paid to the impact of gut microbiota on energy metabolism (Karlsson et al., 2013; Tremaroli and Backhed, 2012). Inconclusive data on DIO resistance in GF mice, however, highlight the need for clarification with respect to the role of specific dietary compounds in regulating microbe-host interactions.

5.2.1 Lard-fed germfree mice are protected against obesity by affecting energy balance

Detailed analysis of published research pointed at the possible role of dietary fat source, as feeding of beef tallow and lard was accompanied by DIO resistance (Backhed et al., 2007; Rabot et al., 2010), while plant fats such as coconut oil were not (Fleissner et al., 2010). However, causal dietary ingredients remain undetected. Thus, one asset was to elucidate the influence of the dietary fat source on body mass development by feeding GF and CV mice either a high-fat diet based on palm oil (pHFD) or lard (lHFD). Contrary to pHFD, lHFD protected GF mice from obesity indicating a direct crosstalk between fat-derived ingredients and host metabolism, which was modified by the gut microbiota. In this respect, the present study demonstrates for the first time that the type of dietary fat, in particular cholesterol sources, impacts progression of DIO resistance in GF, but not CV mice.

Positive energy balance is key to obesity development. Hence, one primary aim was to perform extensive mouse phenotyping as this has been rather superficially addressed in published studies to unravel mechanisms underlying gut microbiota-host-diet interactions (Backhed et al., 2004; Bruckner-Kardoss and Wostmann, 1978; Levenson et al., 1969). Using ANCOVA to account for different metabolic capacities of body composition rather than body mass *per se* demonstrated an increased basal metabolic rate in lHFD-fed GF mice. So far, basal metabolism has never been investigated in GF mice in the context of obesity development, although it constitutes the major part of daily energy

expenses (Leibel et al., 1995; Ravussin and Bogardus, 1989). Interestingly, it has been shown that housing density increases temperature within mouse cages and that social thermoregulation is accompanied with less brown adipose tissue thermogenesis (Himms-Hagen and Villemure, 1992; Smith et al., 2005). It is thus likely that group-housed mice as in the present study might be exposed to higher within-cage temperatures resembling thermoneutrality (29 – 33 °C) rather than ambient temperature (22 °C). Hence, basal metabolic rate as measured by indirect calorimetry of single-housed mice might better reflect normal housing conditions than daily energy expenditure. Consequently, increased basal metabolic rate of lHFD-fed GF mice is one important factor in the development of DIO resistance.

The respiratory exchange ratio (RER) was investigated to account for variations in endogenous substrate oxidation which might be accompanied with DIO resistance in lHFD-fed GF mice. A sustained and augmented RER was found at the beginning of the nocturnal phases in lHFD- compared to pHFD-fed GF mice confirming the hypothesis of different substrate metabolism. Moreover, this assumption was supported by the negative correlation between the RER and cecal bile acid concentrations, which agrees with literature data (da-Silva et al., 2011; Ockenga et al., 2012; Watanabe et al., 2006). Bile acids are known to facilitate intestinal fat absorption (Evans et al., 2013), possibly triggering fat uptake and induction of endogenous fat oxidation as represented by lowered RER levels in pHFD-fed GF mice. Corresponding to this, those mice revealed reduced fat and energy excretion as compared to lHFD-fed counterparts underlining the increased capacity of fat utilization and obesity onset. *Vice versa*, the increased RER toward carbohydrate oxidation, together with decreased bile acid levels and concomitantly increased fat excretion in lHFD-fed GF mice supports the model of DIO resistance. In addition, to get the fat solubilized and incorporated into mixed micelles for absorption, lHFD-fed animals may have to invest more energy as heat to allow the fat emulsion to be formed and that may also become rate limiting for proper absorption. The lack of any bacteria might further restrict formation of lHFD-specific metabolites used as energy substrates in the lower small intestine and colon of GF mice.

Measurements of energy resorption that could explain DIO resistance in GF mice are still scant and published research rather relies on one of both factors (intake or excretion of energy) to evaluate the bacterial contribution on energy harvest. However, energy resorption represents net energy uptake that can be utilized by the host for metabolic processes and fat storage. Hence, energy resorption of group-housed mice was calculated to elucidate differences explaining the lean phenotype of GF mice. Energy resorption was similar between lean phenotypes and lower compared to obese mice indicating a positive correlation with body mass gain. Thus, jejunal transepithelial resistance (TER) was investigated to assess whether decreased energy resorption was accompanied with altered gut function. Interestingly, jejunal TER was massively increased in GF compared to CV mice, which might be due to differences in gut morphology, i.e. mucin coatings, as indicated by others (Smith et al., 2007). Additionally, regression analysis indicated that jejunal TER negatively correlated to body mass gain indicating a clear impact of jejunal TER on DIO resistance of lHFD-fed GF mice. The relation of body mass gain with a decreased energy resorption and an increased jejunal TER highlights a possible link between energy resorption and jejunal TER in obesity progression. However, further studies are needed to unravel a direct connection between jejunal TER and energy resorption.

5.2.2 Enterohepatic circulation of cholesterol and bile acids impact on mouse phenotypes

Being part of the enterohepatic circulation, bile acids and cholesterol are extensively modified by gut microbiota and liver. In this context, bile acids facilitate intestinal fat and cholesterol uptake, but have also been associated with increased energy expenditure and DIO resistance in mice (Watanabe et al., 2011; Watanabe et al., 2006). Thus, cecal as well as liver metabolome were extensively studied to elucidate potential pathways mediating DIO resistance in GF mice.

9-fold higher dietary cholesterol levels in lHFD compared to pHFD indicate a possible impact on endogenous cholesterol metabolism. However, cholesterol levels of both tissues were similar among CV mice highlighting a balance between endogenous synthesis and dietary intake (Figure S 2).

Interestingly, cecal cholesterol levels were higher in pHFD- compared to lHFD-fed GF mice, although pHFD did not contain any cholesterol and there weren't any differences in hepatic cholesterol *de novo* biosynthesis as represented by similar hepatic Hmgcr expression and liver-derived cholesterol levels (Figure S 2). Thus, it is likely that other tissues, i.e. the gut, build up cholesterol (Dietschy and Siperstein, 1965). Moreover, an inhibited re-uptake of endogenously derived cholesterol is also conceivable, which in the presence of plant sterols has been shown earlier (Patel, 2008). Additionally, cholesterol precedes the synthesis of bile acids, steroid hormones and vitamin D. Thus, dietary ingredients such as cholesterol in lHFD or plant sterols in pHFD might favor different cholesterol pathways. In this respect, lHFD feeding in GF mice was accompanied with increased cecal steroid hormone biosynthesis. On the other hand, pHFD led to higher cecal bile acid concentrations. In summary, dietary challenge influences the direction of cholesterol conversion which was highlighted by increased cecal steroid hormone biosynthesis in lHFD- and higher bile acid levels in pHFD-fed GF mice.

Among cecal steroid hormones, 17β-estradiol levels were higher in lean than obese GF and CV mice, thus, representing a candidate metabolite implicated in DIO resistance (Table S 5). Several studies provide evidence for a role of 17β-estradiol in energy balance regulation by reducing body weight, and increasing insulin sensitivity and glucose tolerance (Chen et al., 2009; Cooke et al., 2001; Heine et al., 2000). In addition, estrogens stimulate energy expenditure (Gao et al., 2007; Heine et al., 2000; Xu et al., 2011), which is well in line with the increase in basal metabolic rate and 17β-estradiol levels observed in lean lHFD-fed GF mice. Interestingly, FXRα has been reported to link bile acid and steroid metabolism (Baptissart et al., 2013). In that matter, several findings suggest a negative correlation between bile acids and sex hormone synthesis (testosterone and estrogen) via FXRα signaling (Baptissart et al., 2013). Concurrent lower cecal bile acid and higher steroid hormone levels in lHFD-fed GF mice may thus be due to reduced hepatic Nr1h4 gene expression. Overall, it is likely that increased levels of 17β-estradiol as a cholesterol derivative can interfere with bile acid metabolism to

decrease fat absorption and promote DIO resistance via enhanced energy expenditure in lHFD-fed GF mice. Quantification of cecal 17β-estradiol is, however, needed to further support this hypothesis.

Cecal bile acid levels were quantified to elucidate a potential link to DIO resistance in lHFD-fed GF mice. However, taurine-conjugated cholic and muricholic acid, as major representatives of GF bile acid profiles, were higher in pHFD- compared to lHFD-fed GF mice. Together with this, total cecal bile acid levels were also increased in obese CV mice, negating the hypothesis of bile acid-mediated DIO resistance. In this respect, increased cecal bile acid levels more readily correspond to an enhanced need to transport fat in obese phenotypes. Thus, bile acid-mediated DIO resistance as described previously might be related to circulating rather than cecal bile acid levels (Watanabe et al., 2006). For this purpose, bile acid quantification in other tissues (liver, plasma) could be worth investigating to consider this hypothesis. In summary, DIO resistance in lHFD-fed GF mice related to increased bile acid levels could not be confirmed by the present study, but still, differences in cecal bile acid composition might contribute to lean and obese GF phenotypes.

Taken together, metabolome analysis indicated a potential role of cholesterol-derived cecal steroid hormone and bile acid synthesis in DIO progression of GF mice.

5.2.3 Cyp7a1 gene expression may be related to cecal bile acid levels in germfree mice

Hepatic expression of genes involved in cholesterol metabolism was investigated to unravel potential pathways associated with metabolome data that take place in DIO resistance of lHFD-fed GF mice. However, gene expression differed due to microbiota status rather than diet. Interestingly, Cyp7a1 and Nr1h4 were the only genes highly expressed in pHFD- but not lHFD-fed GF mice indicating an impact of both genes in obesity progression. However, this observation is unexpected since elevated bile acids in the gut are known to repress expression of Cyp7a1 in the liver by a FXRα/FGF15/19 mediated mechanism, and bile acid dependent activation of FXRα in hepatocytes represses Cyp7a1 gene

transcription (Kir et al., 2012; Martinez-Augustin and Sanchez de Medina, 2008). Moreover, expression of Nr1h4, which encodes FXRα, was increased in liver of pHFD-fed GF mice. Thus, in the GF state other factors modulate the feedback control of Cyp7a1 by FXRα.

5.2.4 The gut microbiota alters diet-host crosstalk

The striking difference in energy balance as found between lean and obese GF mice on either high-fat diet dissolved in the presence of gut microbiota, suggesting that microorganisms in the gut alter the diet-host crosstalk. High-throughput sequencing pointed at a few lHFD-specific bacteria, which may have contributed to the obese phenotype of lHFD-fed CV mice. These bacteria included 2 molecular species related to the species *Acetatifactor muris*, which was first isolated from the cecum of an obese mouse (Pfeiffer et al., 2012), as well as an OTU related at the genus level to *Eubacterium coprostanoligenes*, a species capable of producing coprostanol from cholesterol (Freier et al., 1994). Hence, the presence of intestinal microorganisms is essential in regulating diet-host interactions including few candidate bacteria related to obesity and cholesterol conversion which might contribute to obesity development in lHFD-fed CV mice.

5.2.5 Summary related to gut microbiota-host-diet crosstalk in obesity development

Present data clearly demonstrates that dietary fat origin is linked to important alterations of cholesterol-derived metabolites underlying the development of DIO in GF mice. Briefly, lHFD-fed GF mice were protected against obesity, which was accompanied with increased fecal fat excretion. Increased fecal fat excretion might be linked to decreased hepatic Cyp7a1 gene expression, and hence, lower cecal bile acid levels that mediate intestinal fat uptake. Consequently, being devoid of dietary fat, carbohydrates may preferentially be oxidized endogenously as indicated by increased RER

levels. Moreover, positive correlations between body mass gain and energy resorption as well as jejunal TER indicate potential changes in gut morphology that may have contributed to the lean phenotype of lHFD-fed GF mice. Certain metabolites that belong to steroid hormone biosynthesis, i.e. 17β-estradiol, were found in cecal contents of these mice and are thus probably involved in molecular signaling pathways leading to increased basal metabolic rate and DIO resistance. Interestingly, the presence of intestinal microorganisms was essential in regulating diet-host interactions as represented by loss of the lean phenotype in CV counterparts. Molecular assays pointed a few specific taxa of particular interest. However, further mechanistic studies are needed to test the causative role of these and closely related bacteria in DIO, and to assess the implication of certain metabolites such as 17β-estradiol as identified in the present study.

6 CONCLUSION

In the context of gut microbiota-host-diet interaction, the present study evaluated the microbial impact on body mass development by using diverse treatment strategies (cage swap, cohousing, fecal transplantation) on mice either resistant (SWR/J) or prone (AKR/J) to diet- or genetically-induced obesity (Mc4r^{W16X}/C57BL/6J). In a further approach, the crosstalk between dietary compounds, bacteria and host was investigated in germfree (GF) and conventional (CV) C57BL/6N mice in the presence of high-fat diet based on palm oil (pHFD) or lard (lHFD).

Exposure to SWR/J environment via cage swap decreased fat mass of AKR/J mice. Effects were even more pronounced in AKR/J allogenic recipient mice following microbial transplantation of SWR/J feces. Reduced fat mass of AKR/J mice due to cage swap was accompanied with microbial changes toward SWR/J fecal bacterial profiles. However, microbial transfer into AKR/J allogenic recipients induced by fecal transplantation could not be found indicating that other factors, i.e. fecal components (bile acids, short-chain fatty acids) may play a role for the lean phenotype of these mice. It is also conceivable that small but undetectable continuous alterations in energy balance as well as less abundant bacteria contribute to slowed obesity progression in AKR/J allogenic recipients. Moreover, the lean phenotype of SWR/J mice was not influenced by any kind of treatment, thus, suggesting a stable SWR/J microbial community structure. Like in diet-induced obesity (DIO) resistant SWR/J mice, also cohousing of genetically obese Mc4r^{W16X}/C57BL/6J knockin (ki) with lean wildtype (wt) mice failed to induce changes in body composition indicating a strong genotype-dependent effect on body mass development. Overall, these results highlight that transfer of microbes into CV mice is dependent on treatment strategy and genotype and that changes in body composition are small compared to published colonization reports of GF mice.

Inconsistencies about whether GF mice are DIO resistant have been related to diet. Thus, diet as another factor within the gut microbiota-host interplay was investigated in GF and CV mice exposed to

lard- or palm oil-based high-fat diet for 4 weeks. Current data suggest for the first time that cholesterol may act as a candidate component to induce DIO resistance in GF mice. Moreover, this study provides a model for lard-derived obesity protection: a decreased hepatic Cyp7a1 expression might entail lower concentrations of cecal bile acids which further correspond to a higher fecal fat excretion. This hypothesis is emphasized by increased RER levels, especially during the early night phase pointing toward reinforced carbohydrate oxidation. Moreover, there might be further mechanisms including cholesterol metabolites in cecum and liver, i.e. steroid hormone such as 17β-estradiol that may trigger increased basal metabolic rate and jejunal transepithelial resistance, which contribute to DIO resistance of lHFD-fed GF mice. Interestingly, obesity was prevalent in CV mice irrespective of the dietary fat source. Loss of the lean phenotype might be accompanied with few bacterial taxa related to cholesterol metabolism and obesity as found in lHFD-fed CV mice.

Taken together, the present work examined the gut microbiota-host-diet interaction in obesity aiming at effective treatment strategies in CV mouse models as well as dietary compounds mediating DIO resistance in GF mice. It could be shown that the strength of the treatment (fecal transplantation > cage swap) influenced fat mass development in DIO prone AKR/J but not DIO resistant SWR/J mice. This hypothesizes a highly sensitive obese microbial community structure of AKR/J mice being susceptible to foreign microbial settling as demonstrated by cage swap. However, insensitivity to treatment as found for SWR/J and genetically obese Mc4r^{W16X}/C57BL/6J ki and wt mice highlights genotype effects rather than microbial stimuli that influence phenotypic outcome. An interaction between gut microbiota and diet was assumed since CV but not GF C57BL/6N mice developed obesity irrespective of dietary fat source (pHFD, lHFD). Of highest interest, a mechanism to explain DIO resistance in lHFD-fed GF mice was hypothesized to involve cholesterol-derived metabolites to counteract obesity progression.

7 OUTLOOK

Experimental strategies to transfer microbiota into germfree (GF) rodent guts were mostly performed by oral gavage. The present study suggests that environmental conditioning via cage swap is equally viable compared with the more challenging microbial transplantation via the oral and rectal route into conventional (CV) mice. AKR/J was the only mouse strain sensitive to treatment, albeit microbiota settlement just occurred via cage swap and not fecal transplantation into AKR/J allogenic recipients. On the other hand, SWR/J mice not only resisted obesity but also transfer of AKR/J microbiota. Thus, new experiments including higher stimuli mediated by increased bacterial number are conceivable to achieve detectable microbiota settling within the gut following transplantations. Moreover, decreased fat mass of AKR/J allogenic recipients not attributable to SWR/J microbiota settlement indicates that other fecal compounds may contribute to the lean phenotype. Insofar, metabolome analysis of SWR/J fecal transplants and AKR/J tissues may be worth finding other components mediating lowered fat mass. Isolation of certain bacteria and metabolites as well as targeted transfer into both, GF and CV mice, could be a valuable tool to treat obesity.

Published research indicated that GF mice are not generally protected against obesity and that dietary compounds might be involved in mediating DIO resistance in GF mice. Guided by this hypothesis, GF and CV mice were fed a high-fat diet based on palm oil (pHFD) or lard (lHFD). It could be shown that lHFD- but not pHFD-fed GF mice are DIO resistant and that obesity in CV mice occurred irrespective of the fat source. Moreover, effects were assumed to be mediated by cholesterol-derived metabolites. Based on these results, a closer metabolome analysis including plasma and feces is indicated to confirm this hypothesis. Since dietary cholesterol is supposed to be the driving compound for DIO resistance, supplementation of cholesterol in the presence of pHFD is necessary. Reversibility of pHFD-induced obesity by subsequent lHFD feeding represents another proof-of-concept experiment. Moreover, circulating bile acids were suggested to play an important role in DIO resistance of lHFD-

fed GF mice. With respect to this, Cyp7a1 gene expression was decreased in lean GF mice. Hence, a GF Cyp7a1 knockout mouse model could help to clarify endogenous mechanisms protecting against obesity and further allows metabolic comparisons of GF and CV mice with respect to bile acid turnover.

Taken together, further mechanistic studies will be needed to test the causative role of bacteria in DIO, and to assess the implication of certain metabolites as identified in the present study. This study highlights the importance of dietary fat source for research using DIO models and provides novel insight into the physiological relevance of gut microbiota and cholesterol-derived metabolites interactions.

8 SUMMARY

The gut is occupied by a vast number of bacteria which were recently shown to be involved in body weight management. In mice, several mechanisms were suggested by which bacteria communicate and alter endogenous host metabolism. Since germfree (GF) mice represent the model of choice, the overall extent of gut bacteria in obesity development of conventional (CV) mice remains elusive. Body weight of GF mice was further shown to be dependent on the type of high-fat diet (HFD), albeit dietary compounds responsible for this discrepancy are still unknown.

Therefore, the present study first aimed to clarify the magnitude of bacterial contribution on obesity development by using mild (cage swap, cohousing) to strong (fecal transplantations) stimuli to achieve microbiota transfer in CV mice. In this respect, mouse strains prone (AKR/J) or resistant (SWR/J) to diet-induced obesity (DIO) as well as genetically obese mice (Mc4r^{W16X}/C57BL/6J) were chosen to unravel which of the factors including diet, genetics or gut microbiota influence body composition. In addition to that, the dietary fat source (lard and palm oil) was investigated to identify candidate components and related metabolic pathways involved in DIO resistance of GF mice.

Environmental conditioning due to cohousing of obese Mc4r^{W16X}/C57BL/6J knockin with lean wildtype mice failed to induce phenotypic changes of either genotype. Cage swap between DIO resistant SWR/J and DIO prone AKR/J mice also did not affect body composition of SWR/J mice. DIO prone AKR/J mice, however, revealed less fat mass expansion when exposed to SWR/J environment. Reduced fat mass in AKR/J mice due to cage swap with SWR/J mice was accompanied with changes in gut microbiota toward SWR/J profiles indicating a relation between microbial settlement and phenotypic outcome. Even more pronounced effects on body mass were obvious in AKR/J allogenic recipient mice following microbial transplantation of SWR/J feces. Nonetheless, fecal transplantation of SWR/J microbiota into AKR/J allogenic recipient mice failed to unravel a connection between

lowered fat mass and profound fecal or cecal microbial changes. In this respect, other fecal components are hypothesized to trigger strain-specific responsiveness.

In a further approach, the interplay between gut microbiota and dietary fat was investigated to clarify existing inconsistencies regarding DIO resistance in GF mice. Based on present data, DIO resistance in GF mice occurred in the presence of lard but not palm oil. Mechanistically, a decreased hepatic Cyp7a1 gene expression in lard-fed GF mice likely contributed to reduced cecal bile acid concentrations and increased fecal fat excretion. Moreover, reduced cecal bile acid levels together with increased fecal fat excretion suggest altered endogenous substrate oxidation which could be confirmed by higher respiratory exchange ratios during the early night phases. DIO resistance of lard-fed GF mice was further accompanied with increased jejunal transepithelial resistance and basal metabolic rate. Metabolites such as cholesterol-derived steroid hormones were upregulated in cecum and liver of these mice and thus, represent a putative pathway contributing to the lean phenotype. In this respect, lard-fed GF mice were DIO resistant due to altered energy balance involving endogenous mechanisms potentially related to bile acid- and steroid hormone-signaling. On the other hand, loss of the lean phenotype in lard-fed CV mice was accompanied with particular bacterial taxa so far related to cholesterol conversion and obesity development indicating that the presence of intestinal microorganisms is essential in regulating diet-host interactions.

Taken together, the present study provides novel insight into the physiological relevance of gut microbiota-host-diet interaction in obesity research. It further highlights the importance of carefully choosing mouse strain, treatment strategy and dietary fat source to study DIO models. Further mechanistic studies are, however, needed to test the causative role of bacteria in DIO, and to assess the implication of certain metabolites as identified in the present study.

9 ZUSAMMENFASSUNG

Der Darm ist mit einer Vielzahl an Bakterien besiedelt, die unlängst in Zusammenhang mit der Körpergewichtsregulation gebracht wurden. Bei Mäusen sind bereits einige Mechanismen bekannt, die für eine Kommunikation zwischen Bakterien und einem veränderten Wirtsmetabolismus sprechen. Da keimfreie (GF) Mäuse bislang jedoch das Modell der Wahl darstellten, gibt es noch keine genauen Belege über das tatsächliche Ausmaß von Darmbakterien hinsichtlich der Entstehung von Übergewicht bei konventionellen (CV) Mäusen. Hinzu kommt, dass das Körpergewicht bei GF Mäusen wahrscheinlich von der Art der Hochfettfütterung (HFD) abhängt, die dafür verantwortlichen Bestandteile sind jedoch noch unerforscht.

Die vorliegende Studie hatte daher zunächst zum Ziel mit einfachen (Käfigwechsel, *Cohousing*) bis hin zu ausgeprägten (fäkale Transplantation) Stimuli, den Einfluss von Bakterien an der Entstehung von Adipositas zu klären und damit eine Mikrobiotaübertragung bei CV Mäusen zu forcieren. Aufgrund dessen wurden Mausstämme verwendet, die empfänglich (AKR/J) wie auch resistent (SWR/J) gegenüber Diät-induzierter Adipositas (DIO) sind oder infolge eines Gendefekts (Mc4r^{W16X}/C57BL/6J) Übergewicht entwickeln. Dabei sollte geklärt werden, welche der Faktoren Diät, Gene oder Darmmikrobiota das Körpergewicht beeinflussen. Zusätzlich wurde die Fettquelle des Futters (Schweineschmalz und Palmfett) untersucht um spezifische Komponenten und damit verbundene metabolische Signalwege zu identifizieren, die für die Resistenz der DIO bei GF Mäusen eine Rolle spielen.

Eine Umwelt-bedingte Konditionierung durch *Cohousing* von übergewichtigen Mc4r^{W16X}/C57BL/6J *Knockin* mit schlanken Wildtyp-Mäusen zeigte keine Veränderung im Phänotyp beider Genotypen. Käfigwechsel zwischen DIO resistenten SWR/J und DIO empfänglichen AKR/J Mäusen beeinflusste zudem nicht die Körperzusammensetzung bei SWR/J Mäusen. Demgegenüber wiesen DIO sensitive AKR/J Mäuse eine geringere Fettmassezunahme auf, sobald sie mit dem SWR/J Umfeld exponiert

wurden. Eine reduzierte Fettmasse bei AKR/J Mäusen als Folge des Käfigwechsels mit SWR/J Mäusen war verbunden mit mikrobiellen Veränderungen in Richtung SWR/J Profile. Dies deutet auf einen Zusammenhang zwischen mikrobiellem Übergang und dem Phänotyp hin. Stärkere Effekte auf das Körpergewicht waren sogar bei AKR/J allogenen Empfänger-Mäusen infolge mikrobieller Transplantation mit SWR/J Fäzes vorhanden. Hingegen konnte die verringerte Fettmasse bei AKR/J allogenen Empfänger-Mäusen aufgrund fäkaler Transplantation mit SWR/J Mikrobiota nicht auf profunde Veränderungen der fäkalen, wie auch zäkalen Mikrobiota zurückgeführt werden. Aufgrund dessen werden andere Stuhlbestandteile für eine Stamm-spezifische Reaktion vermutet.

In einem weiteren Ansatz wurde das Zusammenspiel zwischen Darmmikrobiota und Nahrungsfett untersucht, um die bestehende Diskrepanz hinsichtlich einer DIO Resistenz bei GF Mäusen aufzuklären. Basierend auf den vorliegenden Daten entwickelten GF Mäuse in Gegenwart von Schweineschmalz, nicht jedoch Palmöl, eine DIO Resistenz. Mechanistisch zeigte sich dies in einer verminderten hepatischen Cyp7a1 Genexpression bei Schweineschmalz-gefütterten GF Mäusen, was vermutlich zu der reduzierten zäkalen Gallensäurekonzentration und erhöhten fäkalen Fettausscheidung beitrug. Darüber hinaus deutete eine verminderte Gallensäurekonzentrationen zusammen mit einer erhöhten fäkalen Fettausscheidung auf eine veränderte endogene Substratoxidation hin, was durch erhöhte respiratorische Austauschraten während der frühen Nachtphasen bestätigt werden konnte. DIO Resistenz bei Schweineschmalz-gefütterten GF Mäusen ging außerdem mit einem erhöhtem jejunalem transepithelialem Widerstand sowie Grundumsatz einher. Stoffwechselprodukte wie beispielsweise Cholesterol-abstammende Steroidhormone waren hochreguliert in Zäkum und Leber dieser Mäuse und stellen somit einen möglichen Signalweg dar, der den schlanken Phänotyp begünstigt. Somit waren Schweineschmalz-gefütterte GF Mäuse DIO resistent aufgrund einer veränderten Energiebilanz, welche endogene Mechanismen wie beispielweise potentielle Gallensäuren- und Steroidhormonwirkungen umfasst. Andererseits war der Verlust des schlanken Phänotyps bei CV Mäusen mit bestimmten bakteriellen Taxa verbunden, die bislang in Zusammenhang mit Cholesterolumwandlung und Adipositasentwicklung gebracht wurden.

Dieses Ergebnis verdeutlicht, dass die Anwesenheit von intestinalen Mikroorganismen essenziell für die Regulation von Diät-Wirt Interaktionen ist.

Zusammenfassend bietet die vorliegende Studie neue Einblicke für die Adipositasforschung hinsichtlich der physiologischen Relevanz der Darmmikrobiota-Wirt-Diät Interaktion. Des Weiteren hebt sie die Wichtigkeit bei der sorgfältigen Wahl des Mausstamms, der Behandlungsstrategie und der Nahrungsfettquelle bei DIO Modellen hervor. Weitere mechanistische Studien werden jedoch benötigt um die ursächliche Rolle von Bakterien bei DIO zu untersuchen und den Einfluss von bestimmten Stoffwechselprodukten, die in der vorliegenden Studie identifiziert wurden, zu beurteilen.

10 REFERENCES

Aranda, A., and Pascual, A. (2001). Nuclear hormone receptors and gene expression. Physiological reviews *81*, 1269-1304.

Armougom, F., Henry, M., Vialettes, B., Raccah, D., and Raoult, D. (2009). Monitoring bacterial community of human gut microbiota reveals an increase in Lactobacillus in obese patients and Methanogens in anorexic patients. PloS one *4*, e7125.

Arslan, N. (2014). Obesity, fatty liver disease and intestinal microbiota. World journal of gastroenterology : WJG *20*, 16452-16463.

Backhed, F. (2011). Programming of host metabolism by the gut microbiota. Annals of nutrition & metabolism *58 Suppl 2*, 44-52.

Backhed, F., Ding, H., Wang, T., Hooper, L.V., Koh, G.Y., Nagy, A., Semenkovich, C.F., and Gordon, J.I. (2004). The gut microbiota as an environmental factor that regulates fat storage. Proceedings of the National Academy of Sciences of the United States of America *101*, 15718-15723.

Backhed, F., Ley, R.E., Sonnenburg, J.L., Peterson, D.A., and Gordon, J.I. (2005). Host-bacterial mutualism in the human intestine. Science *307*, 1915-1920.

Backhed, F., Manchester, J.K., Semenkovich, C.F., and Gordon, J.I. (2007). Mechanisms underlying the resistance to diet-induced obesity in germ-free mice. Proceedings of the National Academy of Sciences of the United States of America *104*, 979-984.

Bakken, J.S. (2009). Fecal bacteriotherapy for recurrent Clostridium difficile infection. Anaerobe *15*, 285-289.

Bakken, J.S., Borody, T., Brandt, L.J., Brill, J.V., Demarco, D.C., Franzos, M.A., Kelly, C., Khoruts, A., Louie, T., Martinelli, L.P., et al. (2011). Treating Clostridium difficile infection with fecal microbiota transplantation. Clinical gastroenterology and hepatology : the official clinical practice journal of the American Gastroenterological Association *9*, 1044-1049.

Baptissart, M., Vega, A., Martinot, E., Baron, S., Lobaccaro, J.M., and Volle, D.H. (2013). Farnesoid X receptor alpha: a molecular link between bile acids and steroid signaling? Cellular and molecular life sciences : CMLS *70*, 4511-4526.

Bel, S., Elkis, Y., Elifantz, H., Koren, O., Ben-Hamo, R., Lerer-Goldshtein, T., Rahimi, R., Ben Horin, S., Nyska, A., Shpungin, S., et al. (2014). Reprogrammed and transmissible intestinal microbiota confer diminished susceptibility to induced colitis in TMF-/- mice. Proceedings of the National Academy of Sciences of the United States of America *111*, 4964-4969.

Bianconi, E., Piovesan, A., Facchin, F., Beraudi, A., Casadei, R., Frabetti, F., Vitale, L., Pelleri, M.C., Tassani, S., Piva, F., et al. (2013). An estimation of the number of cells in the human body. Annals of human biology *40*, 463-471.

Black, H.E. (1988). The effects of steroids upon the gastrointestinal tract. Toxicologic pathology *16*, 213-222.

Bolze, F., Rink, N., Brumm, H., Kuhn, R., Mocek, S., Schwarz, A.E., Kless, C., Biebermann, H., Wurst, W., Rozman, J., et al. (2011). Characterization of the melanocortin-4-receptor nonsense mutation W16X in vitro and in vivo. The pharmacogenomics journal *13*, 80-93.

Brignardello, J., Morales, P., Diaz, E., Romero, J., Brunser, O., and Gotteland, M. (2010). Pilot study: alterations of intestinal microbiota in obese humans are not associated with colonic inflammation or disturbances of barrier function. Alimentary pharmacology & therapeutics *32*, 1307-1314.

Bruckner-Kardoss, E., and Wostmann, B.S. (1978). Oxygen consumption of germfree and conventional mice. Laboratory animal science *28*, 282-286.

Caesar, R., Tremaroli, V., Kovatcheva-Datchary, P., Cani, P.D., and Backhed, F. (2015). Crosstalk between Gut Microbiota and Dietary Lipids Aggravates WAT Inflammation through TLR Signaling. Cell metabolism.

Cani, P.D., Amar, J., Iglesias, M.A., Poggi, M., Knauf, C., Bastelica, D., Neyrinck, A.M., Fava, F., Tuohy, K.M., Chabo, C., et al. (2007). Metabolic endotoxemia initiates obesity and insulin resistance. Diabetes *56*, 1761-1772.

Cani, P.D., Bibiloni, R., Knauf, C., Waget, A., Neyrinck, A.M., Delzenne, N.M., and Burcelin, R. (2008). Changes in gut microbiota control metabolic endotoxemia-induced inflammation in high-fat diet-induced obesity and diabetes in mice. Diabetes *57*, 1470-1481.

Caporaso, J.G., Lauber, C.L., Walters, W.A., Berg-Lyons, D., Lozupone, C.A., Turnbaugh, P.J., Fierer, N., and Knight, R. (2011). Global patterns of 16S rRNA diversity at a depth of millions of sequences per sample. Proceedings of the National Academy of Sciences of the United States of America *108 Suppl 1*, 4516-4522.

Chapman, K., Holmes, M., and Seckl, J. (2013). 11beta-hydroxysteroid dehydrogenases: intracellular gate-keepers of tissue glucocorticoid action. Physiological reviews *93*, 1139-1206.

Chen, J., Bittinger, K., Charlson, E.S., Hoffmann, C., Lewis, J., Wu, G.D., Collman, R.G., Bushman, F.D., and Li, H. (2012). Associating microbiome composition with environmental covariates using generalized UniFrac distances. Bioinformatics *28*, 2106-2113.

Chen, J.Q., Brown, T.R., and Russo, J. (2009). Regulation of energy metabolism pathways by estrogens and estrogenic chemicals and potential implications in obesity associated with increased exposure to endocrine disruptors. Biochimica et biophysica acta *1793*, 1128-1143.

Cooke, P.S., Heine, P.A., Taylor, J.A., and Lubahn, D.B. (2001). The role of estrogen and estrogen receptor-alpha in male adipose tissue. Molecular and cellular endocrinology *178*, 147-154.

Crawford, P.A., Crowley, J.R., Sambandam, N., Muegge, B.D., Costello, E.K., Hamady, M., Knight, R., and Gordon, J.I. (2009). Regulation of myocardial ketone body metabolism by the gut microbiota during nutrient deprivation. Proceedings of the National Academy of Sciences of the United States of America *106*, 11276-11281.

da-Silva, W.S., Ribich, S., Arrojo e Drigo, R., Castillo, M., Patti, M.E., and Bianco, A.C. (2011). The chemical chaperones tauroursodeoxycholic and 4-phenylbutyric acid accelerate thyroid hormone activation and energy expenditure. FEBS letters *585*, 539-544.

Damman, C.J., Miller, S.I., Surawicz, C.M., and Zisman, T.L. (2012). The microbiome and inflammatory bowel disease: is there a therapeutic role for fecal microbiota transplantation? The American journal of gastroenterology *107*, 1452-1459.

Daniel, H., Moghaddas Gholami, A., Berry, D., Desmarchelier, C., Hahne, H., Loh, G., Mondot, S., Lepage, P., Rothballer, M., Walker, A., et al. (2014). High-fat diet alters gut microbiota physiology in mice. The ISME journal *8*, 295-308.

David, L.A., Maurice, C.F., Carmody, R.N., Gootenberg, D.B., Button, J.E., Wolfe, B.E., Ling, A.V., Devlin, A.S., Varma, Y., Fischbach, M.A., et al. (2014). Diet rapidly and reproducibly alters the human gut microbiome. Nature *505*, 559-563.

De Filippo, C., Cavalieri, D., Di Paola, M., Ramazzotti, M., Poullet, J.B., Massart, S., Collini, S., Pieraccini, G., and Lionetti, P. (2010). Impact of diet in shaping gut microbiota revealed by a comparative study in children from Europe and rural Africa. Proceedings of the National Academy of Sciences of the United States of America *107*, 14691-14696.

de Vos, W.M. (2013). Fame and future of faecal transplantations--developing next-generation therapies with synthetic microbiomes. Microbial biotechnology *6*, 316-325.

de Wit, N., Derrien, M., Bosch-Vermeulen, H., Oosterink, E., Keshtkar, S., Duval, C., de Vogel-van den Bosch, J., Kleerebezem, M., Muller, M., and van der Meer, R. (2012). Saturated fat stimulates obesity and hepatic steatosis and affects gut microbiota composition by an enhanced overflow of dietary fat to the distal intestine. American journal of physiology. Gastrointestinal and liver physiology *303*, G589-599.

Dietschy, J.M., and Siperstein, M.D. (1965). Cholesterol synthesis by the gastrointestinal tract: localization and mechanisms of control. The Journal of clinical investigation *44*, 1311-1327.

Dimitriu, P.A., Boyce, G., Samarakoon, A., Hartmann, M., Johnson, P., and Mohn, W.W. (2013). Temporal stability of the mouse gut microbiota in relation to innate and adaptive immunity. Environmental microbiology reports *5*, 200-210.

Dubuc, P.U., and Willis, P.L. (1978). Age dependent effects of oxytetracycline in ob/ob mice. Diabetologia *14*, 129-133.

Duncan, S.H., Lobley, G.E., Holtrop, G., Ince, J., Johnstone, A.M., Louis, P., and Flint, H.J. (2008). Human colonic microbiota associated with diet, obesity and weight loss. International journal of obesity *32*, 1720-1724.

Edgar, R.C. (2010). Search and clustering orders of magnitude faster than BLAST. Bioinformatics *26*, 2460-2461.

Edgar, R.C. (2013). UPARSE: highly accurate OTU sequences from microbial amplicon reads. Nat Methods *10*, 996-998.

Edgar, R.C., Haas, B.J., Clemente, J.C., Quince, C., and Knight, R. (2011). UCHIME improves sensitivity and speed of chimera detection. Bioinformatics *27*, 2194-2200.

Eriksson, H., and Gustafsson, J.A. (1970). Steroids in germfree and conventional rats. Distribution and excretion of labelled pregnenolone and corticosterone in male and female rats. European journal of biochemistry / FEBS *15*, 132-139.

Eriksson, H., Gustafsson, J.A., and Sjovall, J. (1969). Steroids in germfree and conventional rats. Free steroids in faeces from conventional rats. European journal of biochemistry / FEBS *9*, 286-290.

Evans, J.M., Morris, L.S., and Marchesi, J.R. (2013). The gut microbiome: the role of a virtual organ in the endocrinology of the host. The Journal of endocrinology *218*, R37-47.

Even, P.C., and Nadkarni, N.A. (2012). Indirect calorimetry in laboratory mice and rats: principles, practical considerations, interpretation and perspectives. American journal of physiology. Regulatory, integrative and comparative physiology *303*, R459-476.

Everard, A., Lazarevic, V., Derrien, M., Girard, M., Muccioli, G.G., Neyrinck, A.M., Possemiers, S., Van Holle, A., Francois, P., de Vos, W.M., et al. (2011). Responses of gut microbiota and glucose and lipid metabolism to prebiotics in genetic obese and diet-induced leptin-resistant mice. Diabetes *60*, 2775-2786.

Fava, F., Gitau, R., Griffin, B.A., Gibson, G.R., Tuohy, K.M., and Lovegrove, J.A. (2013). The type and quantity of dietary fat and carbohydrate alter faecal microbiome and short-chain fatty acid excretion in a metabolic syndrome 'at-risk' population. International journal of obesity *37*, 216-223.

Fei, N., and Zhao, L. (2013). An opportunistic pathogen isolated from the gut of an obese human causes obesity in germfree mice. The ISME journal *7*, 880-884.

Festi, D., Schiumerini, R., Eusebi, L.H., Marasco, G., Taddia, M., and Colecchia, A. (2014). Gut microbiota and metabolic syndrome. World journal of gastroenterology : WJG *20*, 16079-16094.

Fleissner, C.K., Huebel, N., Abd El-Bary, M.M., Loh, G., Klaus, S., and Blaut, M. (2010). Absence of intestinal microbiota does not protect mice from diet-induced obesity. The British journal of nutrition *104*, 919-929.

Freier, T.A., Beitz, D.C., Li, L., and Hartman, P.A. (1994). Characterization of Eubacterium coprostanoligenes sp. nov., a cholesterol-reducing anaerobe. International journal of systematic bacteriology *44*, 137-142.

Fukuda, S., and Ohno, H. (2014). Gut microbiome and metabolic diseases. Seminars in immunopathology *36*, 103-114.

Furet, J.P., Kong, L.C., Tap, J., Poitou, C., Basdevant, A., Bouillot, J.L., Mariat, D., Corthier, G., Dore, J., Henegar, C., et al. (2010). Differential adaptation of human gut microbiota to bariatric surgery-induced weight loss: links with metabolic and low-grade inflammation markers. Diabetes *59*, 3049-3057.

Gao, Q., Mezei, G., Nie, Y., Rao, Y., Choi, C.S., Bechmann, I., Leranth, C., Toran-Allerand, D., Priest, C.A., Roberts, J.L., et al. (2007). Anorectic estrogen mimics leptin's effect on the rewiring of melanocortin cells and Stat3 signaling in obese animals. Nature medicine *13*, 89-94.

Gough, E., Shaikh, H., and Manges, A.R. (2011). Systematic review of intestinal microbiota transplantation (fecal bacteriotherapy) for recurrent Clostridium difficile infection. Clinical infectious diseases : an official publication of the Infectious Diseases Society of America *53*, 994-1002.

Grundy, S.M. (1978). Cholesterol metabolism in man. The Western journal of medicine *128*, 13-25.

Gustafsson, J.A. (1968). Steroids and germfree and conventional rats. 7. Identification of C19 and C21 steroids in faeces from conventional rats. European journal of biochemistry / FEBS *6*, 248-255.

Hansen, C.H., Nielsen, D.S., Kverka, M., Zakostelska, Z., Klimesova, K., Hudcovic, T., Tlaskalova-Hogenova, H., and Hansen, A.K. (2012). Patterns of early gut colonization shape future immune responses of the host. PloS one *7*, e34043.

Heine, P.A., Taylor, J.A., Iwamoto, G.A., Lubahn, D.B., and Cooke, P.S. (2000). Increased adipose tissue in male and female estrogen receptor-alpha knockout mice. Proceedings of the National Academy of Sciences of the United States of America *97*, 12729-12734.

Heldmaier, G. (1975). The influence of the social thermoregulation on the cold-adaptive growth of BAT in hairless and furred mice. Pflugers Archiv : European journal of physiology *355*, 261-266.

Henao-Mejia, J., Elinav, E., Jin, C., Hao, L., Mehal, W.Z., Strowig, T., Thaiss, C.A., Kau, A.L., Eisenbarth, S.C., Jurczak, M.J., et al. (2012). Inflammasome-mediated dysbiosis regulates progression of NAFLD and obesity. Nature *482*, 179-185.

Hildebrandt, M.A., Hoffmann, C., Sherrill-Mix, S.A., Keilbaugh, S.A., Hamady, M., Chen, Y.Y., Knight, R., Ahima, R.S., Bushman, F., and Wu, G.D. (2009). High-fat diet determines the composition of the murine gut microbiome independently of obesity. Gastroenterology *137*, 1716-1724 e1711-1712.

Himms-Hagen, J., and Villemure, C. (1992). Number of mice per cage influences uncoupling protein content of brown adipose tissue. Proceedings of the Society for Experimental Biology and Medicine. Society for Experimental Biology and Medicine *200*, 502-506.

Hooper, L.V., Littman, D.R., and Macpherson, A.J. (2012). Interactions between the microbiota and the immune system. Science *336*, 1268-1273.

Houten, S.M., Watanabe, M., and Auwerx, J. (2006). Endocrine functions of bile acids. The EMBO journal *25*, 1419-1425.

Hui, D.Y., Labonte, E.D., and Howles, P.N. (2008). Development and physiological regulation of intestinal lipid absorption. III. Intestinal transporters and cholesterol absorption. American journal of physiology. Gastrointestinal and liver physiology *294*, G839-843.

Huszar, D., Lynch, C.A., Fairchild-Huntress, V., Dunmore, J.H., Fang, Q., Berkemeier, L.R., Gu, W., Kesterson, R.A., Boston, B.A., Cone, R.D., et al. (1997). Targeted disruption of the melanocortin-4 receptor results in obesity in mice. Cell *88*, 131-141.

Jia, W., Li, H., Zhao, L., and Nicholson, J.K. (2008). Gut microbiota: a potential new territory for drug targeting. Nature reviews. Drug discovery *7*, 123-129.

Jost, L. (2007). Partitioning diversity into independent alpha and beta components. Ecology *88*, 2427-2439.

Jumpertz, R., Le, D.S., Turnbaugh, P.J., Trinidad, C., Bogardus, C., Gordon, J.I., and Krakoff, J. (2011). Energy-balance studies reveal associations between gut microbes, caloric load, and nutrient absorption in humans. The American journal of clinical nutrition *94*, 58-65.

Kabeerdoss, J., Devi, R.S., Mary, R.R., and Ramakrishna, B.S. (2012). Faecal microbiota composition in vegetarians: comparison with omnivores in a cohort of young women in southern India. The British journal of nutrition *108*, 953-957.

Karlsson, F., Tremaroli, V., Nielsen, J., and Backhed, F. (2013). Assessing the human gut microbiota in metabolic diseases. Diabetes *62*, 3341-3349.

Kelder, T., Stroeve, J.H., Bijlsma, S., Radonjic, M., and Roeselers, G. (2014). Correlation network analysis reveals relationships between diet-induced changes in human gut microbiota and metabolic health. Nutrition & diabetes *4*, e122.

Kir, S., Zhang, Y., Gerard, R.D., Kliewer, S.A., and Mangelsdorf, D.J. (2012). Nuclear receptors HNF4alpha and LRH-1 cooperate in regulating Cyp7a1 in vivo. The Journal of biological chemistry *287*, 41334-41341.

Kless, C., Muller, V.M., Schuppel, V.L., Lichtenegger, M., Rychlik, M., Daniel, H., Klingenspor, M., and Haller, D. (2015). Diet-induced obesity causes metabolic impairment independent of alterations in gut barrier integrity. Molecular nutrition & food research *59*, 968-978.

Klindworth, A., Pruesse, E., Schweer, T., Peplies, J., Quast, C., Horn, M., and Glockner, F.O. (2013). Evaluation of general 16S ribosomal RNA gene PCR primers for classical and next-generation sequencing-based diversity studies. Nucleic acids research *41*, e1.

Lagkouvardos, I., Klaring, K., Heinzmann, S.S., Platz, S., Scholz, B., Engel, K.H., Schmitt-Kopplin, P., Haller, D., Rohn, S., Skurk, T., et al. (2015). Gut metabolites and bacterial community networks during a pilot intervention study with flaxseeds in healthy adult men. Molecular nutrition & food research *59*, 1614-1628.

Lam, Y.Y., Ha, C.W., Campbell, C.R., Mitchell, A.J., Dinudom, A., Oscarsson, J., Cook, D.I., Hunt, N.H., Caterson, I.D., Holmes, A.J., et al. (2012). Increased gut permeability and microbiota change associate with mesenteric fat inflammation and metabolic dysfunction in diet-induced obese mice. PloS one *7*, e34233.

Lau, E., Carvalho, D., and Freitas, P. (2015). Gut Microbiota: Association with NAFLD and Metabolic Disturbances. BioMed research international *2015*, 979515.

Le Chatelier, E., Nielsen, T., Qin, J., Prifti, E., Hildebrand, F., Falony, G., Almeida, M., Arumugam, M., Batto, J.M., Kennedy, S., et al. (2013). Richness of human gut microbiome correlates with metabolic markers. Nature *500*, 541-546.

Le Roy, T., Llopis, M., Lepage, P., Bruneau, A., Rabot, S., Bevilacqua, C., Martin, P., Philippe, C., Walker, F., Bado, A., et al. (2013). Intestinal microbiota determines development of non-alcoholic fatty liver disease in mice. Gut *62*, 1787-1794.

Leibel, R.L., Rosenbaum, M., and Hirsch, J. (1995). Changes in energy expenditure resulting from altered body weight. The New England journal of medicine *332*, 621-628.

Leser, T.D., and Molbak, L. (2009). Better living through microbial action: the benefits of the mammalian gastrointestinal microbiota on the host. Environmental microbiology *11*, 2194-2206.

Levenson, S.M., Doft, F., Lev, M., and Kan, D. (1969). Influence of microorganisms on oxygen consumption, carbon dioxide production and colonic temperature of rats. The Journal of nutrition *97*, 542-552.

Ley, R.E., Backhed, F., Turnbaugh, P., Lozupone, C.A., Knight, R.D., and Gordon, J.I. (2005). Obesity alters gut microbial ecology. Proceedings of the National Academy of Sciences of the United States of America *102*, 11070-11075.

Louet, J.F., LeMay, C., and Mauvais-Jarvis, F. (2004). Antidiabetic actions of estrogen: insight from human and genetic mouse models. Current atherosclerosis reports *6*, 180-185.

Macia, L., Tan, J., Vieira, A.T., Leach, K., Stanley, D., Luong, S., Maruya, M., Ian McKenzie, C., Hijikata, A., Wong, C., et al. (2015). Metabolite-sensing receptors GPR43 and GPR109A facilitate dietary fibre-induced gut homeostasis through regulation of the inflammasome. Nature communications *6*, 6734.

Martinez-Augustin, O., and Sanchez de Medina, F. (2008). Intestinal bile acid physiology and pathophysiology. World journal of gastroenterology : WJG *14*, 5630-5640.

Membrez, M., Blancher, F., Jaquet, M., Bibiloni, R., Cani, P.D., Burcelin, R.G., Corthesy, I., Mace, K., and Chou, C.J. (2008). Gut microbiota modulation with norfloxacin and ampicillin enhances glucose tolerance in mice. FASEB journal : official publication of the Federation of American Societies for Experimental Biology *22*, 2416-2426.

Muccioli, G.G., Naslain, D., Backhed, F., Reigstad, C.S., Lambert, D.M., Delzenne, N.M., and Cani, P.D. (2010). The endocannabinoid system links gut microbiota to adipogenesis. Molecular systems biology *6*, 392.

Murphy, E.F., Cotter, P.D., Healy, S., Marques, T.M., O'Sullivan, O., Fouhy, F., Clarke, S.F., O'Toole, P.W., Quigley, E.M., Stanton, C., et al. (2010). Composition and energy harvesting capacity of the gut microbiota: relationship to diet, obesity and time in mouse models. Gut *59*, 1635-1642.

Nieuwdorp, M., Gilijamse, P.W., Pai, N., and Kaplan, L.M. (2014). Role of the microbiome in energy regulation and metabolism. Gastroenterology *146*, 1525-1533.

Ockenga, J., Valentini, L., Schuetz, T., Wohlgemuth, F., Glaeser, S., Omar, A., Kasim, E., duPlessis, D., Featherstone, K., Davis, J.R., et al. (2012). Plasma bile acids are associated with energy expenditure and thyroid function in humans. The Journal of clinical endocrinology and metabolism *97*, 535-542.

Packard, G.C., and Boardman, T.J. (1999). The use of percentages and size-specific indices to normalize physiological data for variation in body size: wasted time, wasted effort? Comparative Biochemistry and Physiology Part A *122*, 37-44.

Park, D.Y., Ahn, Y.T., Park, S.H., Huh, C.S., Yoo, S.R., Yu, R., Sung, M.K., McGregor, R.A., and Choi, M.S. (2013). Supplementation of Lactobacillus curvatus HY7601 and Lactobacillus plantarum KY1032 in diet-induced obese mice is associated with gut microbial changes and reduction in obesity. PloS one *8*, e59470.

Parks, B.W., Nam, E., Org, E., Kostem, E., Norheim, F., Hui, S.T., Pan, C., Civelek, M., Rau, C.D., Bennett, B.J., et al. (2013). Genetic control of obesity and gut microbiota composition in response to high-fat, high-sucrose diet in mice. Cell metabolism *17*, 141-152.

Patel, S.B. (2008). Plant sterols and stanols: their role in health and disease. Journal of clinical lipidology *2*, S11-19.

Pfeiffer, N., Desmarchelier, C., Blaut, M., Daniel, H., Haller, D., and Clavel, T. (2012). Acetatifactor muris gen. nov., sp. nov., a novel bacterium isolated from the intestine of an obese mouse. Archives of microbiology *194*, 901-907.

Plosch, T., Kruit, J.K., Bloks, V.W., Huijkman, N.C., Havinga, R., Duchateau, G.S., Lin, Y., and Kuipers, F. (2006). Reduction of cholesterol absorption by dietary plant sterols and stanols in mice is independent of the Abcg5/8 transporter. The Journal of nutrition *136*, 2135-2140.

Poutahidis, T., Kleinewietfeld, M., Smillie, C., Levkovich, T., Perrotta, A., Bhela, S., Varian, B.J., Ibrahim, Y.M., Lakritz, J.R., Kearney, S.M., et al. (2013). Microbial reprogramming inhibits Western diet-associated obesity. PloS one *8*, e68596.

Price, M.N., Dehal, P.S., and Arkin, A.P. (2010). FastTree 2--approximately maximum-likelihood trees for large alignments. PloS one *5*, e9490.

Rabot, S., Membrez, M., Bruneau, A., Gerard, P., Harach, T., Moser, M., Raymond, F., Mansourian, R., and Chou, C.J. (2010). Germ-free C57BL/6J mice are resistant to high-fat-diet-induced insulin resistance and have altered cholesterol metabolism. FASEB journal : official publication of the Federation of American Societies for Experimental Biology *24*, 4948-4959.

Ravussin, E., and Bogardus, C. (1989). Relationship of genetics, age, and physical fitness to daily energy expenditure and fuel utilization. The American journal of clinical nutrition *49*, 968-975.

Ridaura, V.K., Faith, J.J., Rey, F.E., Cheng, J., Duncan, A.E., Kau, A.L., Griffin, N.W., Lombard, V., Henrissat, B., Bain, J.R., et al. (2013). Gut microbiota from twins discordant for obesity modulate metabolism in mice. Science *341*, 1241214.

Ridlon, J.M., Kang, D.J., and Hylemon, P.B. (2006). Bile salt biotransformations by human intestinal bacteria. J Lipid Res *47*, 241-259.

Santacruz, A., Collado, M.C., Garcia-Valdes, L., Segura, M.T., Martin-Lagos, J.A., Anjos, T., Marti-Romero, M., Lopez, R.M., Florido, J., Campoy, C., et al. (2010). Gut microbiota composition is associated with body weight, weight gain and biochemical parameters in pregnant women. The British journal of nutrition *104*, 83-92.

Sayin, S.I., Wahlstrom, A., Felin, J., Jantti, S., Marschall, H.U., Bamberg, K., Angelin, B., Hyotylainen, T., Oresic, M., and Backhed, F. (2013). Gut microbiota regulates bile acid metabolism by reducing the levels of tauro-beta-muricholic acid, a naturally occurring FXR antagonist. Cell metabolism *17*, 225-235.

Schwiertz, A., Taras, D., Schafer, K., Beijer, S., Bos, N.A., Donus, C., and Hardt, P.D. (2010). Microbiota and SCFA in lean and overweight healthy subjects. Obesity *18*, 190-195.

Scott, K.P., Gratz, S.W., Sheridan, P.O., Flint, H.J., and Duncan, S.H. (2013). The influence of diet on the gut microbiota. Pharmacological research : the official journal of the Italian Pharmacological Society *69*, 52-60.

Seedorf, H., Griffin, N.W., Ridaura, V.K., Reyes, A., Cheng, J., Rey, F.E., Smith, M.I., Simon, G.M., Scheffrahn, R.H., Woebken, D., et al. (2014). Bacteria from diverse habitats colonize and compete in the mouse gut. Cell *159*, 253-266.

Sharpe, L.J., and Brown, A.J. (2013). Controlling cholesterol synthesis beyond 3-hydroxy-3-methylglutaryl-CoA reductase (HMGCR). The Journal of biological chemistry *288*, 18707-18715.

Smith, A.L., Mabus, S.L., Muir, C., and Woo, Y. (2005). Effects of housing density and cage floor space on three strains of young adult inbred mice. Comparative medicine *55*, 368-376.

Smith, K., McCoy, K.D., and Macpherson, A.J. (2007). Use of axenic animals in studying the adaptation of mammals to their commensal intestinal microbiota. Seminars in immunology *19*, 59-69.

Speakman, J.R. (2010). FTO effect on energy demand versus food intake. Nature *464*, E1; discussion E2.

Stecher, B., Chaffron, S., Kappeli, R., Hapfelmeier, S., Freedrich, S., Weber, T.C., Kirundi, J., Suar, M., McCoy, K.D., von Mering, C., et al. (2010). Like will to like: abundances of closely related species can predict susceptibility to intestinal colonization by pathogenic and commensal bacteria. PLoS pathogens *6*, e1000711.

Subramanian, S., Han, C.Y., Chiba, T., McMillen, T.S., Wang, S.A., Haw, A., 3rd, Kirk, E.A., O'Brien, K.D., and Chait, A. (2008). Dietary cholesterol worsens adipose tissue macrophage accumulation and atherosclerosis in obese LDL receptor-deficient mice. Arteriosclerosis, thrombosis, and vascular biology *28*, 685-691.

Taves, M.D., Gomez-Sanchez, C.E., and Soma, K.K. (2011). Extra-adrenal glucocorticoids and mineralocorticoids: evidence for local synthesis, regulation, and function. American journal of physiology. Endocrinology and metabolism *301*, E11-24.

Tremaroli, V., and Backhed, F. (2012). Functional interactions between the gut microbiota and host metabolism. Nature *489*, 242-249.

Tschöp, M.H., Speakman, J.R., Arch, J.R.S., Auwerx, J., Brüning, J.C., Chan, L., Eckel, R.H., Varese, R.V.J., Galgani, J.E., Hambly, C., et al. (2012). A guide to analysis of mouse metabolism. Nature Methods *9*, 57-63.

Turnbaugh, P.J., Hamady, M., Yatsunenko, T., Cantarel, B.L., Duncan, A., Ley, R.E., Sogin, M.L., Jones, W.J., Roe, B.A., Affourtit, J.P., et al. (2009). A core gut microbiome in obese and lean twins. Nature *457*, 480-484.

Turnbaugh, P.J., Ley, R.E., Mahowald, M.A., Magrini, V., Mardis, E.R., and Gordon, J.I. (2006). An obesity-associated gut microbiome with increased capacity for energy harvest. Nature *444*, 1027-1031.

Tziotis, D., Hertkorn, N., and Schmitt-Kopplin, P. (2011). Kendrick-analogous network visualisation of ion cyclotron resonance Fourier transform mass spectra: improved options for the assignment of elemental compositions and the classification of organic molecular complexity. European journal of mass spectrometry *17*, 415-421.

Untergasser, A., Cutcutache, I., Koressaar, T., Ye, J., Faircloth, B.C., Remm, M., and Rozen, S.G. (2012). Primer3--new capabilities and interfaces. Nucleic acids research *40*, e115.

van Olden, C., Groen, A.K., and Nieuwdorp, M. (2015). Role of Intestinal Microbiome in Lipid and Glucose Metabolism in Diabetes Mellitus. Clinical therapeutics *37*, 1172-1177.

Van Rooyen, D.M., Larter, C.Z., Haigh, W.G., Yeh, M.M., Ioannou, G., Kuver, R., Lee, S.P., Teoh, N.C., and Farrell, G.C. (2011). Hepatic free cholesterol accumulates in obese, diabetic mice and causes nonalcoholic steatohepatitis. Gastroenterology *141*, 1393-1403, 1403 e1391-1395.

Veiga, P., Juste, C., Lepercq, P., Saunier, K., Beguet, F., and Gerard, P. (2005). Correlation between faecal microbial community structure and cholesterol-to-coprostanol conversion in the human gut. FEMS microbiology letters *242*, 81-86.

Vijay-Kumar, M., and Gewirtz, A.T. (2012). Is predisposition to NAFLD and obesity communicable? Cell metabolism *15*, 419-420.

Vrieze, A., Van Nood, E., Holleman, F., Salojarvi, J., Kootte, R.S., Bartelsman, J.F., Dallinga-Thie, G.M., Ackermans, M.T., Serlie, M.J., Oozeer, R., et al. (2012). Transfer of intestinal microbiota from

lean donors increases insulin sensitivity in individuals with metabolic syndrome. Gastroenterology *143*, 913-916 e917.

Wang, Q., Garrity, G.M., Tiedje, J.M., and Cole, J.R. (2007). Naive Bayesian classifier for rapid assignment of rRNA sequences into the new bacterial taxonomy. Applied and environmental microbiology *73*, 5261-5267.

Watanabe, M., Horai, Y., Houten, S.M., Morimoto, K., Sugizaki, T., Arita, E., Mataki, C., Sato, H., Tanigawara, Y., Schoonjans, K., et al. (2011). Lowering bile acid pool size with a synthetic farnesoid X receptor (FXR) agonist induces obesity and diabetes through reduced energy expenditure. The Journal of biological chemistry *286*, 26913-26920.

Watanabe, M., Houten, S.M., Mataki, C., Christoffolete, M.A., Kim, B.W., Sato, H., Messaddeq, N., Harney, J.W., Ezaki, O., Kodama, T., et al. (2006). Bile acids induce energy expenditure by promoting intracellular thyroid hormone activation. Nature *439*, 484-489.

Wostmann, B.S. (1981). The germfree animal in nutritional studies. Annual review of nutrition *1*, 257-279.

Wostmann, B.S., Bruckner-Kardoss, E., and Pleasants, J.R. (1982). Oxygen consumption and thyroid hormones in germfree mice fed glucose-amino acid liquid diet. The Journal of nutrition *112*, 552-559.

Wostmann, B.S., Larkin, C., Moriarty, A., and Bruckner-Kardoss, E. (1983). Dietary intake, energy metabolism, and excretory losses of adult male germfree Wistar rats. Laboratory animal science *33*, 46-50.

Woting, A., Pfeiffer, N., Loh, G., Klaus, S., and Blaut, M. (2014). Clostridium ramosum promotes high-fat diet-induced obesity in gnotobiotic mouse models. mBio *5*, e01530-01514.

Wu, Y.Z., Abolhassani, M., Ollero, M., Dif, F., Uozumi, N., Lagranderie, M., Shimizu, T., Chignard, M., and Touqui, L. (2010). Cytosolic phospholipase A2alpha mediates Pseudomonas aeruginosa LPS-induced airway constriction of CFTR -/- mice. Respiratory research *11*, 49.

Xu, Y., Nedungadi, T.P., Zhu, L., Sobhani, N., Irani, B.G., Davis, K.E., Zhang, X., Zou, F., Gent, L.M., Hahner, L.D., et al. (2011). Distinct hypothalamic neurons mediate estrogenic effects on energy homeostasis and reproduction. Cell metabolism *14*, 453-465.

Yoo, S.R., Kim, Y.J., Park, D.Y., Jung, U.J., Jeon, S.M., Ahn, Y.T., Huh, C.S., McGregor, R., and Choi, M.S. (2013). Probiotics L. plantarum and L. curvatus in combination alter hepatic lipid metabolism and suppress diet-induced obesity. Obesity *21*, 2571-2578.

Yu, I.C., Lin, H.Y., Sparks, J.D., Yeh, S., and Chang, C. (2014). Androgen receptor roles in insulin resistance and obesity in males: the linkage of androgen-deprivation therapy to metabolic syndrome. Diabetes *63*, 3180-3188.

Zeng, H., Liu, J., Jackson, M.I., Zhao, F.Q., Yan, L., and Combs, G.F., Jr. (2013). Fatty liver accompanies an increase in lactobacillus species in the hind gut of C57BL/6 mice fed a high-fat diet. The Journal of nutrition *143*, 627-631.

Zhang, C., Zhang, M., Pang, X., Zhao, Y., Wang, L., and Zhao, L. (2012). Structural resilience of the gut microbiota in adult mice under high-fat dietary perturbations. The ISME journal *6*, 1848-1857.

Zhang, Y., Guo, K., LeBlanc, R.E., Loh, D., Schwartz, G.J., and Yu, Y.H. (2007). Increasing dietary leucine intake reduces diet-induced obesity and improves glucose and cholesterol metabolism in mice via multimechanisms. Diabetes *56*, 1647-1654.

Zimmer, J., Lange, B., Frick, J.S., Sauer, H., Zimmermann, K., Schwiertz, A., Rusch, K., Klosterhalfen, S., and Enck, P. (2012). A vegan or vegetarian diet substantially alters the human colonic faecal microbiota. European journal of clinical nutrition *66*, 53-60.

Zoetendal, E.G., and de Vos, W.M. (2014). Effect of diet on the intestinal microbiota and its activity. Current opinion in gastroenterology *30*, 189-195.

11 SUPPLEMENTARY DATA

TABLE S 1 LIST OF PRIMER SEQUENCES APPLIED IN GENE EXPRESSION ANALYSIS USING QRT-PCR.

Gene	Forward (5'-3')	Reverse (5'-3')	Product size (bp)	Reference
Abgc5	AGCTCTTCCAACACTTCGAC	TACGTTTCTATTTCCCGCTC	193	(This study)
Abcg8	GACCTGGTCCTTCTGATGAC	AGAGACTGTGCCTTCTCCAC	194	(This study)
Actb	AGAGGGAAATCGTGCGTGAC	CAATAGTGATGACCTGGCCGT	138	(Bolze et al., 2011)
Akr1d1	ATCGTCATTGTCGCACATAG	GGAATGACAACTATCCCTCG	176	(This study)
Cyp7a1	GCC TCT GAA GAA GTG AAT GG	TAA AAG TCA AAG GGT CTG GG	292	(This study)
Cyp27a1	TACACCAATGTGAATCTGGC	TAACCTCGTTTAAGGCATCC	238	(This study)
Dhcr7	TTCCAGGTGCTGCTTTATTC	CTGTGAATTTGCAGTCTTCG	359	(This study)
Eef2	ACCTGCCTGTCAATGAGTCC	CAGCATGTGGCAGTATCAGG	241	(This study)
Hmgcr	CCC TAA ATT TGA AGA GGA CG	GCC AGC AAT ACC CAG AAT	139	(This study)
Hmgcs	TGTGGTTCAGAAACTGATGG	TGTCTCCTGCAACTACCAGA	266	(This study)
Hprt1	CAGGCCAGACTTTGTTGGAT	TTGCGCTCATCTTAGGCTTT	147	(Wu et al., 2010)
Hsd11b1	TAGTGTCTCGCTGCCTTGAA	CAGAGTGGATGTCGTCATGG	186	(Designed in-house)
Hsp90	AGGAGGGTCAAGGAAGTGGT	TTTTTCTTGTCTTTGCCGCT	215	(Bolze et al., 2011)
Ldlr	CCATTTTGGAGGATGAGAAC	CTAGGCTGTGTGACCTTGTG	196	(This study)
Nr1h2	CACCATTGAGATCATGTTGC	GAAGTCGTCCTTGCTGTAGG	100	(This study)
Nr1h3	TGT TTC TCC TGA TTC TGC AA	TGA CTC CAA CCC TAT CCC T	142	(This study)
Nr1h4	GCA GGG AGA AAA CGG AAC	TCT GTA CAT GAC TGG TTG CC	174	(This study)
Srebf1	TGCAGTTTCTCTGTCAGCTC	GATTCCACCTTTCTGTGGTC	248	(Designed in-house)

TABLE S 2 LIST OF PRIMER SEQUENCES APPLIED FOR AMPLIFICATION OF 16S RRNA.

Primer	Sequence (5'-3')	Reference
515 HTS forward	GTG CCA GCM GCC GCG GTA-A	(Caporaso et al., 2011)
806 HTS reverse	GGA CTA CHV GGG TWT CTA AT	(Caporaso et al., 2011)
785 HTS reverse	GAC TAC HVG GGT ATC TAA TCC	(Klindworth et al., 2013)
515 forward	AAT GAT ACG GCG ACC ACC GAG ATC TAC ACT ATG GTA ATT GTG TGC CAG CMG CCG CGG TAA	(Caporaso et al., 2011)
806 reverse	CAA GCA GAA GAC GGC ATA CGA GAT barcode AGT CAG TCA GCC GGA CTA CHV GGG TWT CTA AT	(Caporaso et al., 2011)
341 forward	AAT GAT ACG GCG ACC ACC GAG ATC TAC ACT ATG GTA ATT GTC CTA CGG GNG GCW GCA G	(Klindworth et al., 2013)
785 reverse	CAA GCA GAA GAC GGC ATA CGA GAT barcode AGT CAG TCA GCC GACTA CHVGGGTAT CTAATCC	(Klindworth et al., 2013)

TABLE S 3 EXTERNAL AND INTERNAL STANDARDS USED FOR BILE ACID QUANTIFICATION BY MEANS OF UPLC-TOF/MS.

	Abbreviation	Molecular mass [M-H]-	Company	Order number
Chenodeoxycholic acid	CDCA	391.285383	Sigma	C9377-100MG
Cholic acid	CA	407.280298	Sigma	C1129-25G
Deoxycholic acid	DCA	391.285383	Sigma	D2510-10G
Glycochenodeoxycholate, sodium	GCDCA	448.306847	Sigma	G0759-100MG
Glycocholic acid, hydrate	GCA	464.301762	Sigma	G2878-100MG
Glycodeoxycholic acid, sodium	GDCA	448.306847	Calbiochem	361311-5GM
Glycoursodeoxycholic acid	GUDCA	448.306847	Sigma	06863-1G
Hyodeoxycholic acid	HDCA	391.285383	Sigma	H3878-5G
Lithocholic acid	LCA	375.290469	Sigma	L6250-10G
Taurochenodeoxycholate, sodium	TCDCA	498.289483	Sigma	T6260-100MG
Taurocholic acid, sodium hydrate	TCA	514.284397	Sigma	T4009-1G
Taurodeoxycholate, sodium hydrate	TDCA	498.289483	Sigma	T0875-1G
Taurolithocholate, sodium	TLCA	482.294568	Sigma	T7515-1G
Tauroursodeoxycholic acid, sodium	TUDCA	498.289483	Calbiochem	580549-1GM
Ursodeoxycholic acid	UDCA	391.285383	Sigma	U5127-1G
α-Muricholic acid	αMCA	407.280298	Steraloids	C1890-000
α-Tauromuricholic acid	αTMCA	514.284397	Steraloids	C1893-000
β-Muricholic acid	βMCA	407.280298	Steraloids	C1898-000
β-Tauromuricholic acid	βTMCA	514.284397	Steraloids	C1899-000
Ω-Muricholic acid	ΩMCA	407.280298	Steraloids	C1888-000
d^4-Cholic acid	d^4-DCA	411.304308	Sigma	D-2452
d^4-Deoxycholic acid	d^4-DCA	395.309393	CDN Isotopes	D-2941
d^5-Taurocholic acid	d^5-TCA	519.314684	Toronto research chemicals	NC0341860

TABLE S 4 LINEAR REGRESSION FORMULAS USED FOR DATA ADJUSTMENTS.

Experiment	Linear regression formula	Adjusted r^2, p-value
4.1.1 Figure 9	AKR/J Ctrl: FM [g] = -18.14 + 0,8187 * BM; AKR/J Exp: FM [g] = -17.93 + 0.789 * BM SWR/J Ctrl: FM [g] = -5.773 + 0.2979 * BM; SWR/J Exp: FM [g] = 2.92 - 0.0240 * BM	AKR/J Ctrl: 0.97, p < 0.001; AKR/J Exp: 0.84, p < 0.001; SWR/J Ctrl: 0.07, p = ns; SWR/J Exp: -0.09, p = ns
4.1.2 Table 13	Energy excretion$_{adj.}$ [kJ*d^{-1}] = 3.0878 + 0.0377 * Ein	0.18, p < 0.01
4.1.2 Table 13	HP$_{adj., 30°C, pa}$ [mW] = 75.9931 + 5.2458 * FM + 5.778 * LM	0.48, p < 0.001
4.1.2 Table 13	HP$_{adj., at rest, 22°C, ad-lib}$ [mW] = 130.092 + 12.599 * FM + 19.459 * LM	0.49, p < 0.001
4.1.2 Table 13	HP$_{adj., 22°C, ad-lib}$ [mW] = 67.1295 + 10.7812 * FM + 28.2232 * LM	0.38, p < 0.001
4.2.2 Table 15	Energy excretion$_{adj.}$ [kJ*d^{-1}] = 3.442 + 0.0356 * Ein	0.44, p < 0.001
4.2.2 Table 15	Energy resorption$_{adj}$ [kJ*d^{-1}] = 19.7765 – 1.0685 * FM + 3.9871 * LM	0.14, p < 0.05
4.2.2 Table 15	HP$_{adj., 30°C,pa}$ [mW] = 151.1926 + 4.4538 * FM + 3.1425 * LM	0.62, p < 0.001
4.2.2 Table 15	HP$_{adj., at rest, 22°C, ad-lib}$ [mW] = 303.6581 + 7.9923 * FM + 12.4168 * LM	0.57, p < 0.001
4.2.2 Table 15	HP$_{adj., 22°C, ad-lib}$ [mW] = 270.1721 + 5.4112 * FM + 20.2627 * LM	0.50, p < 0.001
4.3 Table 17	HP$_{adj., 30°C,pa}$ [mW] = -40.6719 + 1.4427 * FM + 11.8972 * LM	0.34, p < 0.05
4.3 Table 17	HP$_{adj., at rest, 22°C, ad-lib}$ [mW] = 31.5970 + 3.3776 * FM + 19.4026 * LM	0.32, p < 0.05
4.3 Table 17	HP$_{adj., 22°C, ad-lib}$ [mW] = -198.9478 + 5.8595 * FM + 34.0371 * LM	0.79, p < 0.001
4.4 Figure 18	HP$_{adj., 22°C, ad-lib}$ [mW] = 76.5196 + 7.4048 * FM + 24.9719 * LM	0.49, p < 0.001
4.4 Figure 18	HP$_{adj., 30°C,pa}$ [mW] = -18.851 + 3.2664 * FM + 11.072 * LM	0.44, p < 0.001
4.4 Figure 20	Fecal energy content $_{adj.}$ [kJ*g^{-1}] = 13.0443 + 0.0273 * Ein – 0.8356 * FP	0.32, p < 0.001
4.4 Figure 20	Fecal fat content $_{adj.}$ [%] = -0.0723 + 0.0261 * fat intake – 0.3704 * FP	0.52, p < 0.001
4.4 Figure 21	Energy resorption$_{adj.}$ [kJ*d^{-1}] = 41.1561 + 9.8037 * BM gain	0.43, p < 0.001

ADJ. – ADJUSTED. *AD-LIB – AD-LIBITUM*. BM – BODY MASS. E_{IN} – ENERGY INTAKE. FM – FAT MASS. FP – FECES PRODUCTION. HP – HEAT PRODUCTION. LM – LEAN MASS. PA – POST ABSORPTIVE.

TABLE S 5 CECAL METABOLITES AND RELATED KEGG METABOLIC PATHWAYS DIFFERENT BETWEEN PHFD- AND LHFD-FED GF MICE. Signal intensity of cecal m/z ratios (*10^4) and fold changes (FC) of fed and fasted GF and CV mice exposed to CD, pHFD or lHFD. Analysis was performed in the negative mode of ESI-FT-ICR/MS. CV CD: n = 10; CV pHFD: n = 10; CV lHFD: n = 10. GF CD: n = 10; GF pHFD: n = 10; GF lHFD: n = 10. Different letters indicate statistical significant interactions according to Welch's t-test between GF or CV mice fed lHFD and pHFD, respectively.

raw mass	KEGG cid	KEGG name	KEGG pathway	GF CD	GF pHFD	GF lHFD	CV CD	CV pHFD	CV lHFD	FC GF pHFD/ lHFD	FC GF pHFD/ CD	FC GF lHFD/ CD	FC CV pHFD/ lHFD	FC CV pHFD/ CD	FC CV lHFD/ CD	p GF pHFD/ lHFD	p CV pHFD/ lHFD
303.23297	C00219	Arachidonate	UFAB	6805	38635	13202	25583	16381	22460	2.9	5.7	1.9	0.7	0.6	0.9	8.7E-05	0.33
327.232905	C06429	DHA	UFAB	848	2360	942	5242	2953	3775	2.5	2.8	1.1	0.8	0.6	0.7	2.2E-03	0.33
329.248554	C16513	DPA	UFAB	898	1444	1001	376	531	322	1.4	1.6	1.1	1.6	1.4	0.9	3.1E-02	0.17
331.264275	C16527	DTA	UFAB	863	2302	1222	1799	1582	728	1.9	2.7	1.4	2.2	0.9	0.4	2.9E-03	0.07
303.23297	C00219	Arachidonate	AA metab	6805	38635	13202	25583	16381	22460	2.9	5.7	1.9	0.7	0.6	0.9	8.7E-05	0.33
367.212636	C05956	Prostaglandin G2	AA metab	10239	3012	4796	7186	4803	7102	0.6	0.3	0.5	0.7	0.7	1.0	2.6E-03	0.05
367.212636	C05962	6-Keto-prostaglandin E1	AA metab	10239	3012	4796	7186	4803	7102	0.6	0.3	0.5	0.7	0.7	1.0	2.6E-03	0.05
367.212636	C05964	11-Dehydro-thromboxane B2	AA metab	10239	3012	4796	7186	4803	7102	0.6	0.3	0.5	0.7	0.7	1.0	2.6E-03	0.05
337.23833	C14772	5,6-DHET	AA metab	1952	973	1708	2465	2419	2721	0.6	0.5	0.9	0.9	1.0	1.1	1.4E-03	0.52
337.23833	C14773	8,9-DHET	AA metab	1952	973	1708	2465	2419	2721	0.6	0.5	0.9	0.9	1.0	1.1	1.4E-03	0.52
337.23833	C14774	11,12-DHET	AA metab	1952	973	1708	2465	2419	2721	0.6	0.5	0.9	0.9	1.0	1.1	1.4E-03	0.52
337.23833	C14775	14,15-DHET	AA metab	1952	973	1708	2465	2419	2721	0.6	0.5	0.9	0.9	1.0	1.1	1.4E-03	0.52
285.186007	C00280	Androstenedione	SHBS	514	43	306	914	2256	439	0.1	0.1	0.6	5.1	2.5	0.5	7.7E-03	0.11
287.201672	C00535	Testosterone	SHBS	780	40	511	238	378	459	0.1	0.1	0.7	0.8	1.6	1.9	2.4E-04	0.57
287.201672	C00674	5α-Androstane-3,17-dione	SHB	780	40	511	238	378	459	0.1	0.1	0.7	0.8	1.6	1.9	2.4E-04	0.57
271.170365	C00951	Estradiol-17β	SHBS	753	20	418	532	301	278	0.0	0.0	0.6	1.1	0.6	0.5	3.8E-03	0.87
329.212246	C01176	17α-Hydroxyprogesterone	SHBS	1905	240	904	642	459	543	0.3	0.1	0.5	0.8	0.7	0.8	2.9E-03	0.58
287.201672	C01227	Dehydroepi-	SHBS	780	40	511	238	378	459	0.1	0.1	0.7	0.8	1.6	1.9	2.4E-04	0.57

raw mass	KEGG cid	KEGG name	KEGG pathway	GF CD	GF pHFD	GF lHFD	CV CD	CV pHFD	CV lHFD	FC GF pHFD/ lHFD	FC GF pHFD/ CD	FC GF lHFD/ CD	FC CV pHFD/ lHFD	FC CV pHFD/ CD	FC CV lHFD/ CD	p GF pHFD/ lHFD	p CV pHFD/ lHFD
		androsterone															
315.23292	C01953	Pregnenolone	SHBS	847	104	608	299	391	525	0.2	0.1	0.7	0.7	1.3	1.8	6.5E-04	0.55
345.207241	C02140	Corticosterone	SHBS	2979	461	1255	450	325	319	0.4	0.2	0.4	1.0	0.7	0.7	1.2E-03	0.86
271.170365	C02537	Estradiol-17α	SHBS	753	20	418	532	301	278	0.0	0.0	0.6	1.1	0.6	0.5	3.8E-03	0.87
329.212246	C03205	11-Deoxycorticosterone	SHBS	1905	240	904	642	459	543	0.3	0.1	0.5	0.8	0.7	0.8	2.9E-03	0.58
315.23292	C03681	5α-Pregnane-3,20-dione	SHBS	847	104	608	299	391	525	0.2	0.1	0.7	0.7	1.3	1.8	6.5E-04	0.55
329.212246	C03747	11α-Hydroxyprogesterone	SHBS	1905	240	904	642	459	543	0.3	0.1	0.5	0.8	0.7	0.8	2.9E-03	0.58
287.201672	C03772	5β-Androstane-3,17-dione	SHBS	780	40	511	238	378	459	0.1	0.1	0.7	0.8	1.6	1.9	2.4E-04	0.57
315.23292	C04042	20α-Hydroxy-4-pregnen-3-one	SHBS	847	104	608	299	391	525	0.2	0.1	0.7	0.7	1.3	1.8	6.5E-04	0.55
331.227882	C04518	17α,20α-Dihydroxypregn-4-en-3-one	SHBS	2556	436	1219	1209	838	889	0.4	0.2	0.5	0.9	0.7	0.7	1.6E-03	0.83
331.227882	C05138	17α-Hydroxy-pregnenolone	SHBS	2556	436	1219	1209	838	889	0.4	0.2	0.5	0.9	0.7	0.7	1.6E-03	0.83
299.165301	C05285	Adrenosterone	SHBS	565	45	331	109	204	216	0.1	0.1	0.6	0.9	1.9	2.0	2.9E-03	0.88
299.165301	C05297	19-Oxoandrost-4-ene-3,17-dione	SHBS	565	45	331	109	204	216	0.1	0.1	0.6	0.9	1.9	2.0	2.9E-03	0.88
299.165301	C05299	2-Methoxyestrone	SHBS	565	45	331	109	204	216	0.1	0.1	0.6	0.9	1.9	2.0	2.9E-03	0.88
365.23336	C05472	Urocortisol	SHBS	5615	7846	5064	13131	9259	11519	1.5	1.4	0.9	0.8	0.7	0.9	2.0E-03	0.43
347.222787	C05475	11β,21-Dihydroxy-5β-pregnane-3,20-dione	SHBS	3659	891	1693	2636	1549	1624	0.5	0.2	0.5	1.0	0.6	0.6	2.4E-03	0.68
349.238438	C05476	Tetrahydro-corticosterone	SHBS	2205	802	1318	2633	1713	1991	0.6	0.4	0.6	0.9	0.7	0.8	5.5E-03	0.19
345.207241	C05477	21-Hydroxy-5β-	SHBS	2979	461	1255	450	325	319	0.4	0.2	0.4	1.0	0.7	0.7	1.2E-03	0.86

raw mass	KEGG cid	KEGG name	KEGG pathway	GF CD	GF pHFD	GF lHFD	CV CD	CV pHFD	CV lHFD	FC GF pHFD/ lHFD	FC GF pHFD/ CD	FC GF lHFD/ CD	FC CV pHFD/ lHFD	FC CV pHFD/ CD	FC CV lHFD/ CD	p GF pHFD/ lHFD	p CV pHFD/ lHFD
		pregnane-3,11,20-trione															
347.222787	C05478	3α,21-Dihydroxy-5β-pregnane-11,20-dione	SHBS	3659	891	1693	2636	1549	1624	0.5	0.2	0.5	1.0	0.6	0.6	2.4E-03	0.68
315.232920	C05479	5β-Pregnane-3,20-dione	SHBS	847	104	608	299	391	525	0.2	0.1	0.7	0.7	1.3	1.8	6.5E-04	0.55
365.233360	C05481	Cortolone	SHBS	5615	7846	5064	13131	9259	11519	1.5	1.4	0.9	0.8	0.7	0.9	2.0E-03	0.43
349.238438	C05483	3α,20α,21-Trihydroxy-5β-pregnan-11-one	SHBS	2205	802	1318	2633	1713	1991	0.6	0.4	0.6	0.9	0.7	0.8	5.5E-03	0.19
331.227882	C05485	21-Hydroxy-pregnenolone	SHBS	2556	436	1219	1209	838	889	0.4	0.2	0.5	0.9	0.7	0.7	1.6E-03	0.83
347.222787	C05487	17α,21-Dihydroxy-pregnenolone	SHBS	3659	891	1693	2636	1549	1624	0.5	0.2	0.5	1.0	0.6	0.6	2.4E-03	0.68
345.207241	C05488	11-Deoxycortisol	SHBS	2979	461	1255	450	325	319	0.4	0.2	0.4	1.0	0.7	0.7	1.2E-03	0.86
343.191569	C05490	11-Dehydrocorticosterone	SHBS	1665	219	723	399	378	168	0.3	0.1	0.4	2.3	0.9	0.4	3.4E-03	0.21
345.207241	C05497	21-Deoxycortisol	SHBS	2979	461	1255	450	325	319	0.4	0.2	0.4	1.0	0.7	0.7	1.2E-03	0.86
329.212246	C05498	11β-Hydroxyprogesterone	SHBS	1905	240	904	642	459	543	0.3	0.1	0.5	0.8	0.7	0.8	2.9E-03	0.58
383.331984	C01164	7-Dehydrocholesterol	SBS	86	106	435	29	183	244	0.2	1.2	5.1	0.7	6.3	8.4	1.0E-02	0.75
383.331984	C01802	Desmosterol	SBS	86	106	435	29	183	244	0.2	1.2	5.1	0.7	6.3	8.4	1.0E-02	0.75
381.316352	C05107	7-Dehydrodesmosterol	SBS	55	20	191	0	75	128	0.1	0.4	3.5	0.6			1.5E-02	0.58
383.331984	C05437	Zymosterol	SBS	86	106	435	29	183	244	0.2	1.2	5.1	0.7	6.3	8.4	1.0E-02	0.75
383.331984	C05439	5α-Cholesta-7,24-dien-3β-ol	SBS	86	106	435	29	183	244	0.2	1.2	5.1	0.7	6.3	8.4	1.0E-02	0.75
383.331984	C05443	Vitamin D3	SBS	86	106	435	29	183	244	0.2	1.2	5.1	0.7	6.3	8.4	1.0E-02	0.75

raw mass	KEGG cid	KEGG name	KEGG pathway	GF CD	GF pHFD	GF lHFD	CV CD	CV pHFD	CV lHFD	FC GF pHFD/ lHFD	FC GF pHFD/ CD	FC GF lHFD/ CD	FC CV pHFD/ lHFD	FC CV pHFD/ CD	FC CV lHFD/ CD	p GF pHFD/ lHFD	p CV pHFD/ lHFD
439.394563	C08830	24-Methylenecycloartanol	SBS	0	173	701	0	157	391	0.2			0.4			7.4E-03	0.28

AA metab – arachidonic acid metabolism. CD – control diet. cid – collision-induced dissociation. CV – conventional. DHA – Docosahexaenoic acid. DHET – dihydoxyeisoatrienoic aicd. DPA – Docosapentaenoic acid. DTA – Docosatetraenoic acid. FC – fold change. GF – germfree. KEGG – Kyoto Encyclopedia of Genes and Genomes. lHFD – high-fat diet based on lard. p – p-value. pHFD – high-fat diet based on palm oil. SHBS – steroid hormone biosynthesis. SBS – steroid biosynthesis. UFAB – unsaturated fatty acid biosynthesis.

TABLE S 6 HEPATIC METABOLITES AND RELATED KEGG METABOLIC PATHWAYS DIFFERENT BETWEEN PHFD- AND LHFD-FED GF MICE. Signal intensity of hepatic m/z ratios (*10^4) and fold changes (FC) of GF and CV mice exposed to CD, pHFD or lHFD. Analysis was performed in the negative mode of ESI-FT-ICR/MS and with mice in the fed state at dissection. CV CD: n = 5; CV pHFD: n = 5; CV lHFD: n = 5. GF CD: n = 5; GF pHFD: n = 5; GF lHFD: n = 5. Different letters indicate statistical significant interactions according to Welch's t-test between GF or CV mice fed lHFD and pHFD, respectively.

raw mass	KEGG cid	KEGG name	KEGG pathway	GF CD	GF pHFD	GF lHFD	CV CD	CV pHFD	CV lHFD	FC GF pHFD/ lHFD	FC GF pHFD/ CD	FC GF lHFD/ CD	FC CV pHFD/ lHFD	FC CV pHFD/ CD	FC CV lHFD/ CD	p GF pHFD/ lHFD	p CV pHFD/ lHFD
279.232952	C01595	Linoleate	UFAB	33552	31264	16338	19464	30844	21624	1.9	0.9	0.5	1.4	1.6	1.1	0.02	0.29
311.295561	C06425	Icosanoic acid	UFAB	1369	1780	955	803	2099	1406	1.9	1.3	0.7	1.5	2.6	1.8	0.02	0.25
277.217292	C06426	(6Z,9Z,12Z)-Octadecatrienoic acid	UFAB	2329	2194	1141	1434	1845	1868	1.9	0.9	0.5	1.0	1.3	1.3	0.02	0.97
277.217292	C06427	(9Z,12Z,15Z)-Octadecatrienoic acid	UFAB	2329	2194	1141	1434	1845	1868	1.9	0.9	0.5	1.0	1.3	1.3	0.02	0.97
339.326852	C08281	Docosanoic acid	UFAB	627	743	392	569	955	744	1.9	1.2	0.6	1.3	1.7	1.3	0.00	0.38
367.358118	C08320	Tetracosanoic acid	UFAB	369	331	184	400	421	361	1.8	0.9	0.5	1.2	1.1	0.9	0.04	0.58
429.301073	C17337	7α-Hydroxy-3-oxo-4-cholestenoate	Primary BABS	48	372	42	0	48	104	8.9	7.8	0.9	0.5			0.00	0.51
363.217676	C05470	Tetrahydrocortisone	SHB	549	261	409	608	481	528	0.6	0.5	0.7	0.9	0.8	0.9	0.04	0.52
363.217676	C05471	11β,17α,21-Trihydroxy-5β-pregnane-3,20-dione	SHB	549	261	409	608	481	528	0.6	0.5	0.7	0.9	0.8	0.9	0.04	0.52
363.217676	C05474	3α,11β,21-Trihydroxy-20-oxo-5β-pregnan-18-al	SHB	549	261	409	608	481	528	0.6	0.5	0.7	0.9	0.8	0.9	0.04	0.52
363.217676	C05489	11β,17α,21-Trihydroxypregnenolone	SHB	549	261	409	608	481	528	0.6	0.5	0.7	0.9	0.8	0.9	0.04	0.52
465.249406	C11135	Androsterone glucuronide	SHB	800	0	314	102	0	62	0.0	0.0	0.4	0.0	0.0	0.6	0.02	0.37

raw mass	KEGG cid	KEGG name	KEGG pathway	GF CD	GF pHFD	GF lHFD	CV CD	CV pHFD	CV lHFD	FC GF pHFD/ lHFD	FC GF pHFD/ CD	FC GF lHFD/ CD	FC CV pHFD/ lHFD	FC CV pHFD/ CD	FC CV lHFD/ CD	p GF pHFD/ lHFD	p CV pHFD/ lHFD
465.249406	C11136	Etiocholan-3α-ol-17-one 3-glucuronide	SHB	800	0	314	102	0	62	0.0	0.0	0.4	0.0	0.0	0.6	0.02	0.37
365.196962	C05950	20-COOH-Leukotriene B4	AA metab	485	273	439	324	214	364	0.6	0.6	0.9	0.6	0.7	1.1	0.01	0.07
369.228254	C05961	6-Keto-prostaglandin F1α	AA metab	1232	467	879	774	374	637	0.5	0.4	0.7	0.6	0.5	0.8	0.00	0.08
369.228254	C05963	Thromboxane B2	AA metab	1232	467	879	774	374	637	0.5	0.4	0.7	0.6	0.5	0.8	0.00	0.08

AA metab – arachidonic acid metabolism. BABS – bile acid biosynthesis. CD – control diet. cid – collision-induced dissociation. CV – conventional. FC – fold change. GF – germfree. KEGG – Kyoto Encyclopedia of Genes and Genomes. lHFD – high-fat diet based on lard. p – p-value. pHFD – high-fat diet based on palm oil. SHB – steroid hormone biosynthesis. UFAB – unsaturated fatty acid biosynthesis.

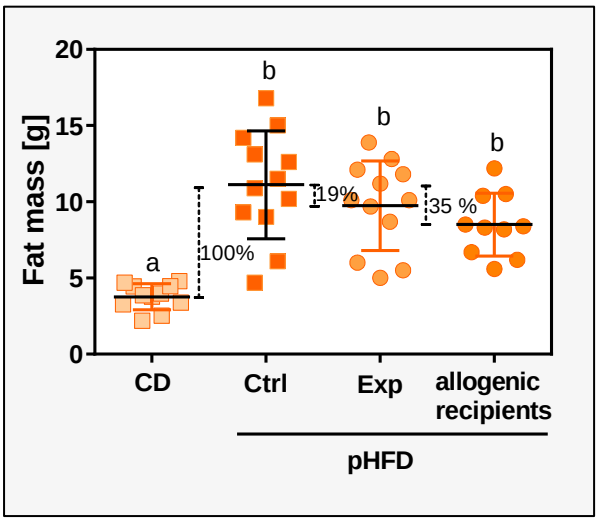

FIGURE S 1 COMPARISON OF TOTAL FAT MASS OF AKR/J MICE DUE TO CAGE SWAP AND MICROBIOTA TRANSPLANTATION. Fat mass of pHFD-fed AKR/J Ctrl, AKR/J Exp mice after cage swap or fecal transplantation of SWR/J microbiota related to that of CD-fed AKR/J mice. Percentages indicate reductions in fat mass induced by the respective treatment compared to pHFD Ctrl. AKR/J CD: n = 11; AKR/J Ctrl: n = 12; AKR/J Exp: n = 12; allogenic recipients: n = 10. Different letters indicate statistical significance. CD – Control diet. Ctrl – control. Exp – exposed. pHFD – palm oil-based high-fat diet.

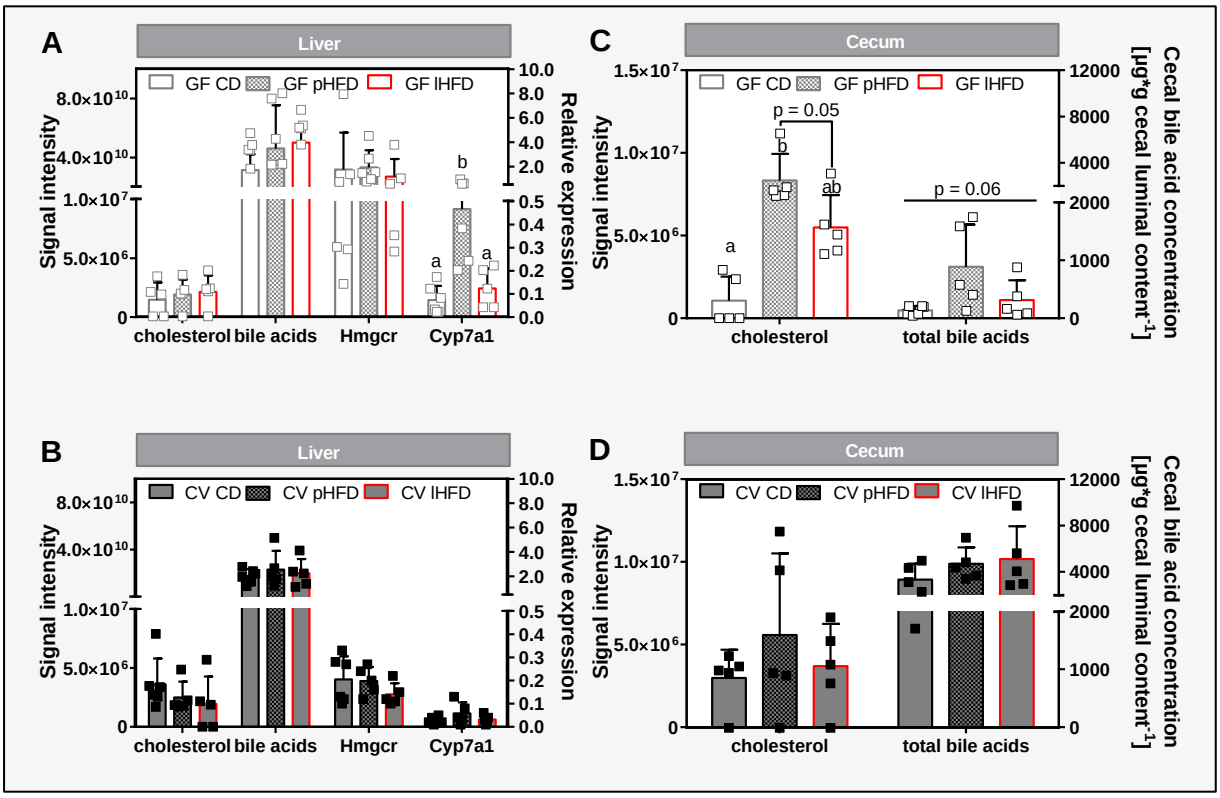

FIGURE S 2 HEPATIC AND CECAL CHOLESTEROL AS WELL AS BILE ACID LEVELS AND HEPATIC GENE EXPRESSION OF CD-, PHFD- AND LHFD-FED GF AND CV MICE. (A-B) Signal intensities of hepatic cholesterol and total bile acid levels as well as Hmgcr and Cyp7a1 gene expression of not fasted GF (A) and CV (B) mice. (C-D) Signal intensities of cecal cholesterol and total cecal bile acid concentration of not fasted GF (C) and CV mice (D). Different superscript letters indicate significance ($p < 0.05$). CV CD: n = 5; CV pHFD: n = 5; CV lHFD: n = 5. GF CD: n = 6; GF pHFD: n = 5; GF lHFD: n = 5. Data are shown as means + sd including single values. CD – control diet. CV – conventional. GF – germfree. lHFD/pHFD – lard-/palm oil-based high-fat diet.

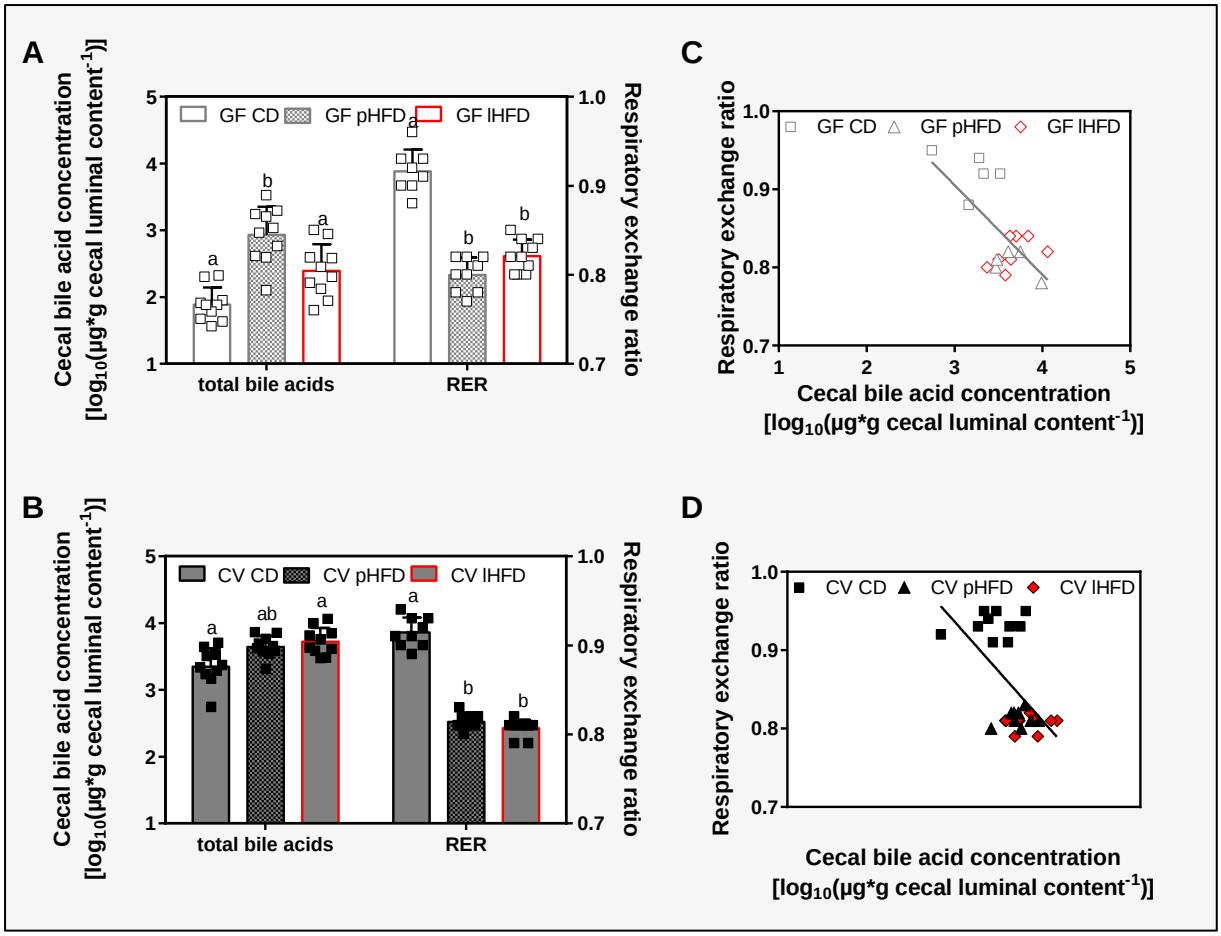

FIGURE S 3 TOTAL CECAL BILE ACID CONCENTRATION AND RESPIRATORY EXCHANGE RATIO (RER) IN CD-, PHFD- AND LHFD-FED GF (A, C) CV (B, D) MICE. (A-B) Data are shown as means + sd including dots representing single values. Different superscript letters indicate significance following post hoc ANOVA 1-way statistical analysis ($p < 0.05$). (C-D) Linear regression analysis between RER and cecal bile acid concentration of GF and CV mice. (C) $r^2 = 0.42$, $p < 0.01$. (D) $r^2 = 0.32$, $p < 0.01$. Data were measured at 22 °C. CV CD: n = 10; CV pHFD: n = 9; CV lHFD: n = 10; GF CD: n = 10; GF pHFD: n = 9; GF lHFD: n = 8. CD – control diet. CV – conventional. GF – germfree. lHFD/pHFD – lard-/palm oil-based high-fat diet.

LIST OF ABBREVIATIONS

A

AA metab	arachidonic acid metabolism
ABCG	ATP-binding cassette sub-family G member 5 and 8
Actb	β-actin
adj.	adjusted
ad-lib	*ad-libitum*
ANCOVA	analysis of covariance
ANOVA	analysis of variance
ASBT	apical sodium-dependent bile acid transporter

B

BA	bile acids
BABS	bile acid biosynthesis
bp	base pairs
BSEP	bile-salt export pump

C

CA	cholic acid
CD	control diet
CDCA	chenodeoxycholic acid
cDNA	complementary deoxyribonucleic acid
Chol	cholesterol
CO_2	carbon dioxide
Ctrl	control

CV	conventional
Cyp	cytochrome P450
Cyp11a1	cholesterol monooxygenase
Cyp11b1	11β-hydroxylase
Cyp11b2	aldosterone synthase
Cyp17	17α-hydroxylase
Cyp21	21-hydroxylase
Cyp7a1	cholesterol 7α-hydroxylase

D

d'NTP	deoxynucleotide triphosphate
DCA	deoxycholic acid
DHA	docosahexaenoic acid
DEPC	diethypyrocarbonate
DHCR24	Δ^{24}-sterol reductase
DHET	dihydroxyeicosatrienoic acid
DIO	diet-induced obesity
DMSO	dimethyl sulfoxide
DNA	deoxyribonucleic acid
DPA	docosapentaenoic acid
DTA	docosatetraenoic acid

E

E	energy
Eef2	eukaryotic elongation factor 2
E_{in}	energy intake
EGTA	ethylene tetraacetic acid

E_{out}	energy excretion
E_{res}	energy resorption
ESI-FT-ICR/MS	electron spray Fourier transform-ion cyclotron resonance mass spectrometry
eWAT	epididymal white adipose tissue
Exp	exposed

F

Fgf15	fibroblast growth factor 15
FT-IR	Fourier transform-infrared spectrometry
FXRα	farnesoid X receptor α
FELASA	Federation of European Laboratory Animal Science

G

GF	germfree
GCDCA	glycochenodeoxycholate
GCA	glycocholic acid
GDCA	glycodeoxycholic acid
GUDCA	glycoursodeoxycholic acid

H

HDCA	hyodeoxycholic acid
HFD	high-fat diet
HMG-CoA	β-hydroxyl-β-methyl glutarate Coenzyme A
HMGCR	HMG-CoA reductase
HMGCS	HMG-CoA synthase
HP	heat production
Hprt	hypoxanthine guanine phosphoribosyl transferase

HSD	hydroxysteroid dehydrogenase
Hsp90	heat shock protein 90
HTS	high-throughput sequencing

I

IBABP	ileal bile acid protein
iBAT	interscapular brown adipose tissue
iWAT	inguinal white adipose tissue

K

KEGG	Kyoto Enzyclopedia of Genes and Genomes
ki	knockin

L

LB	lysogeny broth
LCA	lithocholic acid
lHFD	lard-based high-fat diet
LRH-1	Liver Receptor Homolog-1

M

Mc4r	melanocortin-4 receptor
MCA	muricholic acid
MeV	Mutli Experiment Viewer
mRNA	messenger RNA

N

NTCP	Na^+/taurocholate cotransporting polypeptide transporter
ns	not significant

O

O_2	oxygen
OSTαβ	organic solute and steroid transporter αβ
OTU	operational taxonomic units

P

PAL	physical activity level
PBS	phosphate-buffered saline
PC	peptone and cysteine
PCoA	Principal Coordinate Analysis
PCR	polymerase chain reaction
pHFD	palm oil-based high-fat diet

Q

qRT-PCR	quantitative realtime-polymerase chain reaction

R

RER	respiratory exchange ratio
RNA	ribonucleic acid
rRNA	ribosomal ribonucleic acid
RXR	Retinoic X Receptor

S

SBS	steroid biosynthesis
SCFA	short-chain fatty acids
SH	steroid hormone
SHBS	steroid hormone biosynthesis

SHP	small hetereodimer partner
SM	squalene monooxygenase
SREBF1	Sterol regulatory element-binding factor 1
SR-B1	scavenger receptor class B1
StAR	steroidogenic acute regulatory protein

T

TCA	taurocholic acid
TCDCA	taurochenodeoxycholate
TDCA	taurodeoxycholate
TER	transepithelial resistance
TG	triglyceride
TLCA	taurolithocholate
TMCA	tauromuricholic acid
TNFα	tumor necrosis factor α
TOF/MS	time of flight mass spectrometry

U

UDCA	ursodeoxycholic acid
UFAB	unsaturated fatty acid biosynthesis
UPLC	Ultra performance liquid chromatography

V

v/v	volume per volume
vol-%	volume percent
vs.	versus

W

w/v	weight per volume
WCA	Wilkens-Chalgren anaerobe broth
wk	week
wt	wildtype

LIST OF FIGURES

LIST OF TABLES

LIST OF EQUATIONS

Equation 1: HP [mW] = (4.44 + 1.43 * RER) * $\dot{V}O_2$ [ml*h^{-1}] (Heldmaier, 1975)

Equation 2: Caloric value [J*g^{-1}] = $\frac{(W*\Delta T)-E_{thread}-(E_{combustion\ aid}*m_{combustion\ aid})}{m_{sample}}$

EE: energy equivalence value; ΔT: temperature rise by the combustion aid

Equation 3: E_{in} [kJ] = Food intake [g] * E_{food} [kJ*g^{-1}]

Equation 4: E_{out} [kJ] = Feces production [g] * E_{feces} [kJ*g^{-1}]

Equation 5: E_{res} [kJ] = E_{in} [kJ] - E_{out} [kJ]

Equation 6: Resorption efficiency [%] = $\frac{E_{res}\ [kJ]}{E_{in}\ [kJ]}$ * 100

Equation 7: Bacterial density [cell counts * g cecal content^{-1}] = S * K * V [v/v] * V [w/v]

S: total cell counts; K: chamber factor; V: dilution

Equation 8: DNA concentration [nM] = $\frac{\text{DNA concentration [ng/µl]} * 1{,}000{,}000}{549 * 660}$

ACKNOWLEDGMENTS

At this point, I would like to thank all the people that supported me during my time as a PhD student and those who contributed to the project.

Special thanks go to Prof. Martin Klingenspor who gave me the opportunity to re-start another and promising PhD project at his chair. His friendly and open-minded nature enabled fruitful discussions and solutions. He gave me plenty of rope to establish and execute own ideas. My sincere gratitude comes from his encouragement to take part in skill-enhancing programs as well as international congresses and to assure important co-operations.

As this project was part of the ZIEL Graduate School 'Intestinal Microbiome' and as an enclosed PhD member of the Research Training Group 1482, I would like to thank especially Prof. Dirk Haller as the head of both programs and all associated members. Special thanks go to Thomas Clavel, PhD, as my second supervisor and leader of the ZIEL Junior Group. He was very helpful in establishing experimental strategies within my topic and he was further involved in data processing of 16S rRNA sequencing and thesis correction.

Besides strong co-operations with Prof. Haller's chair of 'Biofunctionality', we co-operated with the chair of 'Physiology', the chair of 'General Food Technology' and the institute of 'Molecular BioGeoChemistry' at the Helmholtz Center Munich. I would therefore like to thank Prof. Daniel, Prof. Engel and Prof. Schmitt-Kopplin and their associates Valentina Luise Schüppel (Biofunctionality), Veronika Maria Müller (Physiology), Birgit Scholz (General Food Technology), and Alesia Walker (PhD, Molecular Biogeochemistry) for fruitful investigations and discussions.

I am much obliged to the whole working group for the friendliness, helpful troubleshooting as well as leisure activities. I would like to especially emphasize the nice working atmosphere in room 1.34 including Caroline Kless, Nadine Rink, Hui Wang as well as Florian Bolze, PhD, and all related

neighbors. Without the help of our in-house technical assistants Anika Zimmermann, Sabine Mocek, Philipp Strahsen, Melanie Klein, Caroline Ziegler and Sabrina Cabric this work would not have been realized. Many thanks go to our PhDs Florian Bolze and Tobias Fromme who were particularly engaged in topic discussions, creating ideas and thesis correction.

Last but not least I would like to express my biggest gratitude to my family, especially my husband Uli who encouraged me to tackle the PhD project and Shelley for linguistic affairs. But also as many thanks to my mother Ruth and my mother-in-law Inge who spent lots of time with babysitting little Maja and encouraged me in hard times. I have to acknowledge the easy-care of my sweetheart Maja – without which it would have been more difficult to finalize the thesis.

CURRICULUM VITAE

PERSONAL DATA

NAME	Raphaela Kübeck (birth name: Schurer)
ADDRESS	Rhododendronweg 7 / 80935 Munich / Germany
BIRTH DATE	03/12/1984
NATIONALITY	German
E-MAIL	raphaelakuebeck@gmail.com

EDUCATION & WORK EXPERIENCE

2/15 – to date **Parental leave**

02/12 – 1/15 **PhD Student, Chair in Molecular Nutritional Medicine, Technische Universität München (TUM), Germany**

Research topic: Experimental strategies to evaluate the gut microbiota-host-diet interaction in the regulation of energy balance supervised by Prof. Dr. rer. nat. Martin Klingenspor

10/14 – 04/14 **Supervisor of the Master's Thesis handed in by Christina Hoffmann, Chair in Molecular Nutritional Medicine, TUM, Germany**

Research topic: Impact of dietary fat quality on energy metabolism of germfree and conventional C57BL/6N mice

04/13 – 07/13 **Supervisor of the Bachelor's Thesis handed in by Simone Schwarz, Chair in Molecular Nutritional Medicine, TUM, Germany**

Research Topic: Einfluss verschiedener Diäten auf den Energiestoffwechsel und die Entstehung von Adipositas bei keimfreien und konventionellen Inzucht-Mausstämmen

01/11 – 11/11 **PhD Student, Chair in Molecular Nutrition, Kubus Research Center Dr. von Hauner'sches Kinderspital, Ludwig-Maximilians Universität München, Germany**

Research topic: Prenatal nutritive modulation of adipogenic programming in mouse offspring supervised by Prof. Dr. med. Regina Ensenauer

11/09 – 12/10 **Research Assistant, Chair in Preventive Pediatrics, TUM, Germany**

Research topics: Molecular effects of anabolic substances on primary human (cardio-) myocytes; Project management and coordination of human trials

03/09 – 09/09 **Master's Thesis at the Chair in Preventive Pediatrics, TUM, Germany (Grade: 1.0)**

Research topic: Effects of guanidinoacetate on human cardiomyocytes

10/07 – 09/09 **Master of Science in Nutritional Science, TUM, Germany (Grade: 1.3)**

04/07 – 09/07 **Bachelor's Thesis at the Else Kröner-Fresenius-Zentrum für Ernährungsmedizin, Freising, Germany (Grade: 1.3)**

Research topic: Different aspects in the regulation of the angiotensinogen promoter

10/04 – 09/07 **Bachelor of Science in Nutritional Science, TUM, Germany (Grade: 1.7)**

09/95 – 06/04 **Abitur, Gymnasium Ebingen, Albstadt (Grade: 1.8)**

SCIENTIFIC CONTRIBUTIONS

10/14 **2nd World Congress on Targeting Microbiota, Paris, France**

Poster presentation: Obesity resistance of germfree mice is dependent on the dietary fat source

10/14 **Beyond the Intestinal Microbiome, Herrenhäuser Konferenzen, Hannover, Germany**

01/14 **Nutrition Winterschool, Ylläs, Finland**

Oral presentation: Experimental strategies to evaluate the gut microbiota-host-diet interaction in energy balance regulation

09/13 **NuGo week, Freising, Germany**

Poster presentation: Cohousing of mice with different susceptibility to obesity influences energy balance

INTERNSHIPS

09/08 **Internship at the Chair in Preventive Pediatrics, TUM, Germany**

Research topic: Gene expression analysis of lymphocytes after creatine supplementation (Grade: 1.3)

02/08 **Internship at the Chair in Human Biology, TUM, Germany**

Research topic: Nerval control mechanisms in the intestine (Grade: 1.0)

08/06 **Internship at the Klinikum Berchtesgadener Land, Schönau am Königssee, Germany**

Topic: Nutritional advice

03/06 **Internship at the Dairy OMIRA, Rottweil, Germany**

Topic: Quality assurance in the laboratories of microbiology and chemistry

München, November 2015

Raphaela Kübeck

EIDESSTATTLICHE ERKLÄRUNG

Ich erkläre an Eides statt, dass ich die bei der Fakultät Wissenschaftszentrum Weihenstephan für Ernährung, Landnutzung und Umwelt (promotionsführenden Einrichtung) der TUM zur Promotionsprüfung vorgelegte Arbeit mit dem Titel:

Experimental strategies to evaluate the gut microbiota-host-diet interaction in the regulation of energy balance

am Lehrstuhl für Molekulare Ernährungsmedizin unter der Anleitung und Betreuung durch Prof. Dr. Martin Klingenspor ohne sonstige Hilfe erstellt und bei der Abfassung nur die gemäß § 6 Abs. 6 und 7 Satz 2 angegebenen Hilfsmittel benutzt habe.

Ich habe keine Organisation eingeschaltet, die gegen Entgelt Betreuerinnen und Betreuer für die Anfertigung von Dissertationen sucht, oder die mir obliegenden Pflichten hinsichtlich der Prüfungsleistungen für mich ganz oder teilweise erledigt.

Ich habe die Dissertation in dieser oder ähnlicher Form in keinem anderen Prüfungsverfahren als Prüfungsleistung vorgelegt.

Ich habe den angestrebten Doktorgrad noch nicht erworben und bin nicht in einem früheren Promotionsverfahren für den angestrebten Doktorgrad endgültig gescheitert.

Die öffentlich zugängliche Promotionsordnung der TUM ist mir bekannt, insbesondere habe ich die Bedeutung von § 28 (Nichtigkeit der Promotion) und § 29 (Entzug des Doktorgrades) zur Kenntnis genommen. Ich bin mir der Konsequenzen einer falschen Eidesstattlichen Erklärung bewusst.

Mit der Aufnahme meiner personenbezogenen Daten in die Alumni-Datei bei der TUM bin ich einverstanden

München, den ....

Unterschrift